

Mining and analysis of new viral potassium channel proteins

A structure and function study of new viral potassium channels from marine picoplankton and chlorella viruses



TECHNISCHE
UNIVERSITÄT
DARMSTADT

Vom Fachbereich Biologie der Technischen Universität Darmstadt

zur Erlangung des akademischen Grades

eines Doctorum rerum naturalium

genehmigte Dissertation von

Dipl.-Biol. Fenja Siotto

aus Frankfurt am Main

1. Referent: Prof. Dr. Gerhard Thiel

2. Referent: Prof. Dr. Adam Bertl

Eingereicht am: 20.10.2017

Mündliche Prüfung am: 18.12.2017

Darmstadt 2018

D17

So eine Arbeit wird eigentlich nie fertig, man muss sie für fertig erklären, wenn man nach der Zeit und den Umständen das Möglichste getan hat.

Johann Wolfgang von Goethe (1749-1832)

1. Table of content

1. ... Table of content	3
2. ... Summary	5
3. ... Zusammenfassung	7
4. ... Short general introduction (Chapter 1)	9
4.1. Ion channels	9
4.2. Potassium channels	9
4.3. Viral potassium channels	11
4.4. Mining of viral channels	15
4.4.1. Mining in fresh water samples	15
4.4.2. Internet mining	18
5. ... Methods	19
5.1. Sequences and algorithms	19
5.2. Virus isolation and subcloning	19
5.3. Patch-clamp	21
5.4. Bilayer	22
5.5. Calculations	24
5.6. Mutations und chimera PCR	24
5.7. Confocal laser scanning microscopy	25
6. ... Viruses encode for new hypothetical K ⁺ channels (Chapter 2)	26
6.1. Abstract	26
6.2. Introduction	26
6.3. Results and Discussion	29
6.3.1. Virus channels from in silico mining	29
6.3.2. New hypothetical virus channels isolated from fresh water samples	35
6.3.3. Kcv _{G^NL^D}	35
6.3.4. Kcv _{N^H}	36
7. ... New functional channels (Chapter 3)	38
7.1. Abstract	38
7.2. Introduction	39
7.3. Results and Discussion- Channels from salt water	40
7.3.1. Kmpv ₁ is a functional potassium channel	40
7.3.2. Filter mutant Kmpv ₁ S43T is not fully blocked by Ba ²⁺	43
7.3.3. Filter double-mutant Kmpv ₁ S43/44T is fully blocked by Ba ²⁺	44
7.3.4. Kbpv ₁ is a functional channel	45
7.3.5. Kmpv _{12T} shows a characteristic conductance in lipid bilayer	47
7.3.6. Kmpv _{PL1} :EGFP shows no characteristic conductance in HEK293 cells	50
7.3.7. Kmpv _{SP1} is an inward rectifying cationic channel	52
7.3.8. Kmpv _{SP1} S53F shows the same electrophysiological behavior as the wildtype	55
7.3.9. The transmembrane domains affect the selectivity of the chimera Kmpv _{SP1} /loop Kmpv ₁	57
7.3.10. Kolv ₄ show no characteristic conductance by over expression in HEK 293 cells	58
7.3.11. Kotv _{RT} is a functional potassium channel which shows a fast and voltage depended barium and cesium block	60
7.3.12. Kolpv ₂ shows no characteristic conductance when expressed in HEK293 cells	63
7.4. Results and Discussion - Channels from fresh water viruses	65

7.4.1.	Kcv _{NH} is a functional potassium channel	65
7.4.2.	Kcv _{G_NL_D} is a functional potassium channel from a hybrid virus	67
7.4.3.	Kcv _{MT325} generates K ⁺ conductance in HEK293 cells	68
7.5.	Channel sorting	70
8. ...	Main Discussion (Chapter 4)	73
9. ...	References	77
10. .	Appendix	83
11. .	Abbreviations	85
12. .	List of Figures	87
13. .	List of Tables	88
14. .	Ehrenwörtliche Erklärung	89
15. .	Own work	90
16. .	Curriculum vitae	92
17. .	Danksagung	94

2. Summary

Many viruses, which infect algae, code for small membrane proteins with the characteristics of potassium channels. The peculiarity of these channels is that they have a monomer size of less than 100 amino acids. The structural simplicity and functional robustness of these miniature channels makes viral K⁺ channels very good model systems for understanding the basic molecular architecture of potassium channels. To learn more about structure/function correlates in these simple channel proteins I tried to generate a library of channel sequences. For this purpose, I searched for channel orthologues in environmental water samples and DNA databases.

Here I present some interesting new viral potassium channels from salt and fresh water viruses. Structural prediction algorithms indicate that the new channels from salt water viruses have the canonical α -helix folds, which are typical for the pore module of all known K⁺ channels. However, structural prediction algorithms failed to identify the expected transmembrane domains flanking the potassium channel pores. The fact that electrophysiological measurements confirmed an activity of these channels suggests that the transmembrane organization of these proteins is achieved in a different manner than in other K⁺ channels.

The newly identified viral K⁺ channels have unique functional properties: Two genes encode proteins, Kmpv_{12T} and Kmpv₁, of only 78 or 79 amino acid per unit, respectively. These are the smallest known K⁺ channels and this small size is presumably close to the absolute minimal size for a K⁺ channel. Both could be identified as functional channels by a combination of heterologous expression and electrophysiological measurements. In addition to these extra small channels from *Micromonas* sp. viruses also the function of Kmpv_{sp1} was confirmed. This channel exhibits unlike all other viral channels a pronounced inward rectification and some permeability to Na⁺. Kbpv₁ from a *Bathycoccus* sp. virus and Kotv_{RT} from a *Ostreococcus* sp. virus could be identified as functional and selective potassium channels. Kotv_{RT} exhibits a steep voltage dependent Ba²⁺ and Cs⁺ block, which is similar to the Cs⁺ block of Kcv_{NTS}.

Two new channels were also isolated from fresh water *Chlorella* viruses. One of them, Kcv_{GLND} is from an evolutionarily interesting hybrid virus, which contains genes of SAG viruses and Pbi viruses. Kcv_{NH} is a channel from the Kcv_{ATCV-1} family, with interesting structure-function relations.

Some proteins like Kmpv_{12T} have a channel-like structure but fail to generate a conductance after expression in HEK293 cells. After investigating the cellular distribution of GFP-tagged proteins we found that all the channels, which were positively identified in HEK293 cells in patch clamp recordings, were sorted into the secretory pathway and presumably from there to the plasma membrane. The channels which failed to generate currents in the plasma membrane of HEK293 cells were on the other hand

predominantly sorted into the mitochondria or remained unsorted in the cytosol. When Kmpv_{12T} was synthesized as representative for the latter channels in vitro and reconstituted into planar lipid bilayers it also generated typical potassium channel activity. Collectively, the data show that the majority of newly identified viral K⁺ channels generated, in spite of non-canonical structural features such as a small size and an unusual transmembrane domain architecture, potassium channel function. Some of the new channels exhibit an unusual sorting to the mitochondria. The finding that some of these proteins generate channel activity in planar lipid bilayers suggests that also these proteins are functional K⁺ channels.

3. Zusammenfassung

Viele Viren die Algen als Wirt nutzen codieren für kleine Membranproteine mit den Eigenschaften von Kaliumkanälen. Das Besondere an diesen Kanälen ist, dass die Monomere aus weniger als 100 Aminosäuren bestehen. Durch die einfache Struktur und ihre funktionale Robustheit sind sie ein sehr gutes Modellsystem um die grundlegende molekulare Struktur von Kaliumkanälen zu verstehen. Um mehr über Struktur-/Funktionskorrelation in diesen einfachen Kanalproteinen zu erfahren, habe ich begonnen eine Bibliothek von Kanalsequenzen zu erstellen. Im Rahmen dessen habe ich Gewässerproben nach neuen Kanälen gescreent und in Datenbanken nach Orthologen gesucht.

Hier stelle ich nun einige interessante neue virale K^+ -Kanäle aus Salz- und Süßwasserviren vor. Algorithmen zu Strukturvorhersage zeigen, dass die neuen Kanäle aus Salzwasserviren die kanonischen α -Helixmotive aufweisen, die für das Porenmodul aller bekannten K^+ -Kanäle typisch sind. Allerdings wurden die erwarteten Transmembrandomänen, die die Kaliumkanalporen flankieren, von den Vorhersagealgorithmen nicht identifiziert. Die Tatsache, dass elektrophysiologische Messungen eine Aktivität dieser Kanäle bestätigten, deutet darauf hin, dass die Transmembranorganisation dieser Proteine in anderer Weise als in den bekannten K^+ -Kanälen erreicht wird.

Die neu gefundenen viralen K^+ -Kanäle haben einzigartige funktionelle Eigenschaften: Zwei der Gene kodieren für Proteine, $Kmpv_{12T}$ und $Kmpv_1$, die nur 78 bzw. 79 Aminosäuren pro Untereinheit groß sind. Dies sind die kleinsten bekannten Kaliumkanäle und vermutlich nahe am kleinstmöglichen Kaliumkanal. Beide konnten als funktionelle Kanäle durch eine Kombination von heterologer Expression und elektrophysiologischen Messungen nachgewiesen werden. Neben diesen besonders kleinen Kanälen von *Micromonas* sp. Viren konnte auch die Funktion von $Kmpv_{sp1}$ bestätigt werden. Dieser Kanal zeigt im Gegensatz zu allen anderen Viruskanälen eine ausgeprägte Einwärtsgleichrichtung und eine gewisse Leitfähigkeit für Na^+ . $Kbpv_1$ von einem *Bathycoccus* sp. Virus und $Kotv_{RT}$ aus einem *Ostreococcus* sp. Virus konnten ebenfalls als selektive Kaliumkanäle nachgewiesen werden. $Kotv_{RT}$ zeigt einen steilen spannungsabhängigen Ba^{2+} - und Cs^+ -Block, der ähnlich dem Cs^+ -Block von Kcv_{NTS} ist.

Zwei weitere neue Kanäle wurden aus Süßwasser-*Chlorella*-Viren isoliert. Einer von ihnen ist Kcv_{GLND} . Dieser stammt aus einem evolutionär interessanten Hybridvirus, der Gene von SAG-Viren und Pbi-Viren enthält. Kcv_{NH} ist ein Kanal aus der Kcv_{ATCV-1} -Familie mit interessanten Struktur-Funktions-Beziehungen.

Einige Proteine wie $Kmpv_{12T}$ haben eine kanalartige Struktur, aber dennoch keine Leitfähigkeit nach Expression in HEK293-Zellen gezeigt. Nach der Untersuchung der zellulären Verteilung von GFP-markierten Proteinen haben wir festgestellt, dass alle Kanäle die in HEK293-Zellen durch Patch-Clamp-Messungen positiv identifiziert wurden, in den sekretorischen Weg und von dort vermutlich zur

Plasmamembran transportiert wurden. Die Kanäle, die keine Ströme in der Plasmamembran von HEK293-Zellen gezeigt haben, wurden hingegen überwiegend in die Mitochondrien sortiert oder unsortiert im Cytosol belassen. Repräsentativ für die zu letzte genannten Kanäle wurde Kmpv_{12T} *in vitro* synthetisiert und in planaren Lipidbilyer rekonstituiert. Hier erzeugte er auch eine typische Kaliumkanalaktivität. Gemeinsam zeigen die Daten, dass die Mehrheit der neu identifizierten viralen K⁺-Kanäle trotz nicht-kanonischer Strukturmerkmale, sowie einer geringen Größe und einer ungewöhnlichen Transmembran-Domänenarchitektur Kaliumkanal-Funktion zeigen. Einige der neuen Kanäle zeigen eine ungewöhnliche Sortierung in die Mitochondrien. Die Kanalaktivität bei den planaren Lipidbilayer Versuchen deuten darauf hin, dass einige dieser Proteine funktionelle K⁺-Kanäle sind.

4. Short general introduction (Chapter 1)

4.1. Ion channels

Ion transport across cell membranes is catalyzed by membrane proteins like carriers, pumps and ion channels. Transport through ion channels is passive, which means it proceeds along an electrochemical gradient without consumption of energy. The special structure of channels allows a fast transport across the cell membranes, that can be nearly as fast as the diffusion rate of ions in water (Hille, 2001). This makes a rapid cell communication like an electrical stimulation of neurons possible (Hille, 2001). In this context, ion channels are essential for fundamental physiological processes including the heartbeat, sensorial perception or muscle contraction. Because of this prominent function of ion channels in human physiology it is no surprise that a malfunction can cause serious diseases. The understanding of the relevance of these so called channelopathies has been rapidly growing over the last decades (Ashcroft, 2006). Hence the interest in finding substances, which could control the behavior of channels and the understanding of their structure and function correlates is really high (Minor, 2007).

4.2. Potassium channels

Potassium channels are selective for potassium ions and play an important role in all aspects of physiology (Hille, 2001). They are divided into different groups according to their structure. All K^+ channels share a highly conserved structural element of two transmembrane domains (TM), which are connected via a pore domain (Fig. 1).

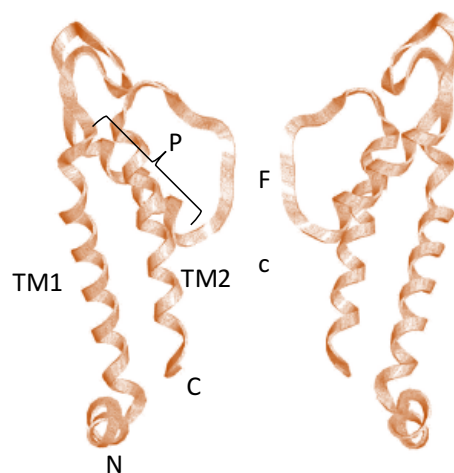


Fig. 1: Structural model of Kcv_{PBCV-1}. Shown are two of four subunits of a K^+ channel in a side view with the N- and C-terminus at the cytosolic side and the transmembrane domains (TM1 and TM2), the pore-helix (P), filter (F) and cavity (c) (modified from (Grunwald *et al.*, 2009)).

All Potassium channels known so far have a common amino acid sequence -TXXTXGY/FG-, which is termed the "signature sequence" of a K^+ channel (Heginbotham *et al.*, 1994). A functional channel is in most cases a tetramer, which is built of monomers with 2 or 6 TMDs. Also dimers in which each monomer contains 4 or 8 TMD are known (Fig. 2) (Thiel *et al.*, 2011). The subunits assemble in such a way that they form a central water filled pore (MacKinnon, 1991). These pores have three regions: the filter region with the selectiv filter (Jan and Jan, 1992; Miller, 1992) containing the signature sequence, the cavity and the pore helix (Fig. 1) (Sansom *et al.*, 2002). A structural model of a typical K^+ channel pore with all the aforementioned structural elements is shown in Fig. 1.

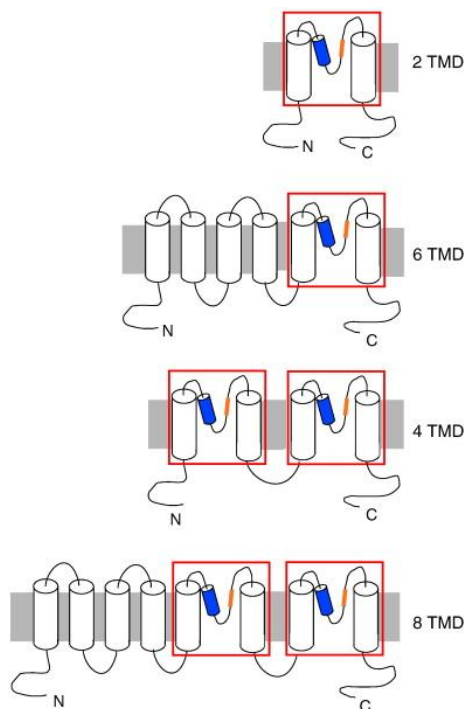


Fig. 2: Subunits of different potassium channel types. A functional channel has four monomers with either two or six transmembrane domains. An alternative assembly is a dimer from monomers with four or eight transmembrane domains. Red box: Pore module of the channels, blue: pore helix, orange: selectivity filter. Picture is from (Thiel *et al.*, 2011).

To enter the channel pore, the potassium ions need to lose their hydration shells. The carbonyl groups of the channel pore are arranged in such a way that they imitate the water shell of a K^+ ion. In this way, the protein substitutes the hydration of the ion. The ion can as a result strip of the water shell without the use of energy (Fig. 3). The carbonyl matrix of the filter is too wide for the smaller sodium ion, which prevents an efficient transport of Na^+ across K^+ channels (MacKinnon, 2004), which explains the selectivity for potassium ions over sodium ions.

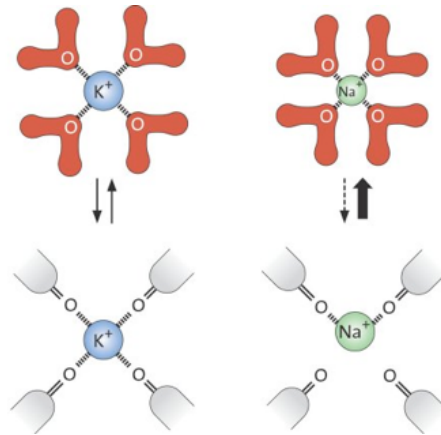


Fig. 3: Selectivity of potassium channels. To enter the channel pore, the potassium ion needs to lose its hydration shell. The carbonyl groups of the channel pore have the same radius as the hydration shell of the potassium ion. The smaller sodium ion can't be fully stabilized, so the entering into the channel is energetically unfavorable (from http://nobelprize.org/nobel_prizes/chemistry/laureates/2003/chempub4bhigh.jpg).

Another important property of channels is the gating. It describes the stochastic opening and closing of a channel, i.e. the fluctuation between open and closed states of a channel protein (Neher and Sakmann, 1976). Channel gating is accompanied by a conformation change of the channel protein, this can be influenced by chemical factors like ligands, but also by physical parameters like membrane voltage (Hille, 2001). The exact mechanism of channel gating is not yet fully understood. One hypothesis focuses on a hydrophobic gate at the entry into the channel on the cytosolic side (Aryal *et al.*, 2015). In the crystal structure of the KcsA channel it was found that the inner transmembrane domains overlap (Thompson *et al.*, 2008). This so called "bundle crossing" forms a barrier for ion flux into or out of the cavity. Since this barrier was opened up in the crystal structure of the MthK, which was presumably crystallized in the open state, it was assumed that a dynamic switching between bundle crossing and opening could present a gate in K^+ channels (Jiang *et al.*, 2002; Perozo *et al.*, 1999). In addition to the bundle crossing also the selectivity filter is discussed as a gate. Gating by the filter is presumably involved in fast gating (Kiss *et al.*, 1999; Schroeder and Hansen, 2007).

4.3. Viral potassium channels

Some viruses have genes that code for small ion channels (Nieva *et al.*, 2012). They are either involved in viral entry, viral replication or viral exit from the host (Hsu *et al.*, 2004; Nieva *et al.*, 2012; Thiel *et al.*, 2010). While most of these viral channels have no similarity to channels from eukaryotes, the channel proteins from *Chlorella* viruses have all the structural hallmarks of potassium channels from pro- and eukaryotes (Fig. 4). The peculiar feature of these viral encoded channels is, that they are truly minimal. The monomers which form these channels, are less than 100 amino acids short. In the case of the prototype virus PBCV-1 it was shown that this virus needs the channels for the infection of their host

cells (Romani *et al.*, 2013).

In the focus of this work are potassium channels from viruses, which are infecting fresh water *Chlorella* algae, and from viruses having picoplankton from the sea water as a host. The past decade has shown that the small viral K⁺ channels are very good model systems for understanding basic structure/function relations of K⁺ channels. This model character is favored by the fact that they are very small, but still functional (Fig. 4). In spite of their small size they still have the same overall architecture of the pore modules of all complex K⁺ channels from higher organisms. One explanation for this fact is that the viral potassium channels are presumably the ancestors of all potassium channels (Thiel *et al.*, 2013).

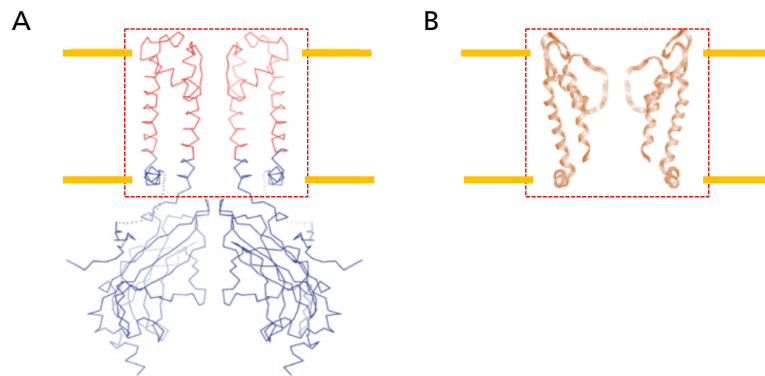


Fig. 4: Small virus channels are a good model system. Small virus channels exhibit a robust function and have the same pore structure of large complex channels. The Kir channel (A) modified from (Nishida *et al.*, 2007). Kcv_{PBCV-1} Channel (B) modified from (Grunwald *et al.*, 2009) and (Tayefeh *et al.*, 2009). Red colored boxes mark the structural domain of Kir channels, which correspond to Kcv_{PBCV-1}. The location of the membrane is shown schematically in yellow.

In addition to their small size, viral K⁺ channels are a promising model system for understanding structure/function correlates in potassium channel proteins: 1) Kcv-type channels have many functional and pharmacological properties, which are similar to those of more complex K⁺ channels in animal and plant cells (Tayefeh *et al.*, 2009; Thiel *et al.*, 2011). 2) Unlike the crystallized bacterial channels (e.g. KcsA) Kcv type channels and their mutants are easy to express in various heterologous systems and to reconstitute in lipid bilayers (Gebhardt *et al.*, 2011; Thiel *et al.*, 2011). 3) Molecular modeling of Kcv revealed that its architecture is similar to crystallized bacterial channels. The similarity includes the presence and position of the pore module elements and also the transmembrane domains (Tayefeh *et al.*, 2009). All these features allow an interpretation of structure/function correlates derived from Kcv in the wider context of K⁺ channel structure as such. An example for this is the identification of a Ba²⁺ binding site in the filter of Kcv and a demonstration that the same binding site is also present in complex Kir channels (Chatelain *et al.*, 2009).

The conventional strategy to uncover structure/function dependencies in K⁺ channel is to use structural predictions or multiple alignments to identify key amino acids, which might be important for function. The significance of these amino acids is then tested for function in combination with site-directed mutagenesis. This approach was very successful to uncover many essential amino acid positions in K⁺ channels and their role in channel function. But the strategy is limited: 1) Only the function of single amino acids within a protein can be analyzed with this approach; higher-order effects between multiple and dispersed amino acids are not accessible by single site mutations. 2) The identification of key amino acids in multiple alignments is biased by non-conservative amino acid exchanges; conservative exchanges such as Val versus Leu, which turned out to be relevant for function (Bichet *et al.*, 2004; Kang *et al.*, 2004), are unlikely to be detected with this approach. 3) Also, the rational approach is biased by our view on how the protein might work. For example, it was for a long time believed in the case K⁺ channels that the outer transmembrane helix of the channel pore has no relevance for protein function. More recent studies, which were based on model free assumptions, however revealed a functional importance of this domain in the channel molecule (Bichet *et al.*, 2004; Kang *et al.*, 2004). This clearly prompts for additional unbiased investigations.

One main aim of this work was to find new Kcv-type channels in environmental samples. Natural habitats provide an enormous source of genetic variability. The approach that we had used so far for identification of different K⁺ channel genes was biased. It depended entirely on the extraction of K⁺ channel genes from viruses, which were first isolated and then characterized (Kang *et al.*, 2004). However, these viruses represent only a tiny fraction of the unbiased genetic diversity of viruses present in natural habitats. Recent estimates of the concentration of viruses or viral DNA in natural habitats suggested that coastal waters, for example, can contain as much as 10⁸ viral particles/ml (Bergh *et al.*, 1989; Suttle *et al.*, 1991). Using a metagenomic approach, Breitbart and coworkers (Breitbart *et al.*, 2002) examined the variability of these viral communities. They found that 200 liters of seawater contain as many as 5000 different viruses. Notably, all of the viruses in these studies were new species. A finding, which shows our current imperfect sampling of genetic variability. In fact, many of the underrepresented viruses might have never been noticed without this metagenomic analysis. Further studies revealed that viruses are widely dispersed throughout the world's oceans. Local environmental conditions enrich for certain viral types through selective pressure; hence it must be expected that an already diverse viral community within one habitat is even more diversified due to prevailing environmental conditions (Angly *et al.*, 2006).

Up to now, the viral concentration in fresh water was not studied in the same detail, yet. There is no reason to believe that the numbers are much smaller. It has already been detected in the particular case of *Chlorella* viruses that these can occur with titers as high as 10⁵ plaque forming units (PFU)/ml in

natural habitats (Van Etten, 2003). Within one lake 4 different virus species were discovered, which is an impressive diversity, considering that this analysis was restricted to this viral subspecies alone. Therefore, viral DNA from natural habitats must provide a very rich source of K⁺ genes with the degree of variability and proven selective advantage that is desirable for structure/function analysis.

In this study, we were interested in the channels from viruses infecting *Chlorella*, which are unicellular green algae. These *Chlorella* species live as endosymbionts in *Paramecium bursaria*, *Hydra viridis* or *Acanthocystis turfacea* in fresh water habitats. In the symbiotic state, they are resistant to virus infection. For research purposes, they can fortunately be cultivated independent of the symbiont in the laboratory (Van Etten *et al.*, 1983a; Van Etten *et al.*, 1983b).

The chloroviruses, which infect algae, are host specific. Because of their host specificity and distinct sequence similarities, the channels could be divided into four groups: channels from NC64 virus, channels from Pbi virus, channels from *Hydra* virus and channels from SAG 3.83 virus (Tab.1) (Thiel *et al.*, 2013; Yamada *et al.*, 2006). The chloroviruses are large icosahedral viruses with a size around 200 nm and a genome size of >300 kbp. They are dsDNA viruses and have an internal lipid membrane (Van Etten and Dunigan, 2012).

Tab.1: Overview of *Chlorella* viruses and their hosts.

Virus Family	Type	Host	Symbiotic with
NC64A virus	PBCV-1	<i>Chlorella variabilis</i>	<i>Paramecium bursaria</i>
Pbi virus	CVA-1	<i>Micractinium conductrix</i>	<i>Paramecium bursaria</i>
Hydra virus	HVCV-1	<i>Chlorella</i>	<i>Hydra viridis</i>
SAG 3.83 virus	ATCV-1	<i>Chlorella heliozoae</i>	<i>Acanthocystis turfacea</i>

In addition to the viral channels from fresh water habitats, the present study also considers recently detected dsDNA viruses, which belong to the same family of phycodnaviruses, but which infect marine picoplankton. Full sequencing of these viruses revealed that they are also encoding for K⁺ channel-like proteins.

The phytoplankton is responsible for about half of the photosynthetic activity on the planet (Field *et al.*, 1998). The species *Micromonas*, *Bathycoccus* and *Ostreococcus*, which are the hosts of the aforementioned viruses, belong to the class *Prasinophyceae*. They are the dominant photosynthetic species in the marine habitat and therefore of great ecological and geochemical importance (Moreau *et*

al., 2010). *Micromonas* has a long flagellum apart from that it is a naked cell, the other two genera are immobile. The *Ostreococcus* species is also naked and the smallest known eukaryote (Derelle *et al.*, 2006). But, *Bathycoccus* cells are covered with scales (Moreau *et al.*, 2012). Their small genome consists of 15 Mb and 19 chromosomes.

The phytoplankton has an important role, it is the basis of the food chain and its population is controlled by viruses (Derelle *et al.*, 2008). Viruses can generate significant mortality in the populations and so they are involved in the termination of the algal blooms and shape the evolution and the biodiversity of the phytoplankton (Bellec *et al.*, 2009; Schroeder *et al.*, 2003).

4.4. Mining of viral channels

For structure/function studies it is helpful to have as many sequences as possible of functional channels. Every additional sequence contains a lot of information. It offers an extensive basis to identify detailed structural/function correlations. There are different ways to get more sequences which can build a functional channel. 1) To employ directed evolution methods, which means to create a library of randomized sequences and test them for function (Minor, 2009). This is a good way to screen possible functional sequence variations of a protein. 2) To search for new channels in environmental samples. In this case the evolution already sorted for the best functional sequence. 3) To search in internet databases for existing channel sequences. Of course, also these sequences are eventually from environmental samples. For the present project, we used the last two strategies for obtaining new channel sequences.

4.4.1. Mining in fresh water samples

The search for new channels with degenerated primers is simple and cheap. The 34 listed water samples (Tab. 2) were screened during this work. But this method has its limits also. We were lucky that the Kcv channels have conserved sequences at the beginning and end of the coding sequence, otherwise this method would have not been successful. Another point is that one cannot be completely sure that the sequence in the primer binding areas are definitely right. It is possible that the primer introduced a mutation into the sequence.

A final shortcoming of this strategy is that it only allows the detection of similar sequences. Completely different new channels will not be picked up with this method.

Isolation of the Kcv_{GND} channel is a good example for the limits of the method. The *Chlorella* virus, which was collected in a water sample from Greenland, turned out to be a hybrid virus. This means that it infects *Chlorella* SAG but contains in its genome also some genes which are typical for Pbi *Chlorella* viruses. The gene for the Kcv_{GND} channel is one of these examples. It has a high similarity to the channel

sequence from *Chlorella* Pbi viruses. This channel would have not been detected with the degenerated primers based on the sequences of channels, which are typical for viruses infecting *Chlorella* SAG. The experiments confirmed that the *Chlorella* SAG cultures were infected by a virus from this water sample. But the channel was not detected by PCR using degenerated primers of the respective virus. The mystery was solved when the entire genome of the virus from the Greenland water sample was sequenced by the Van Etten laboratory (Nebraska/USA). An annotation of the sequence showed that this virus contains mostly genes, which are typical for *Chlorella* SAG viruses, but also about 10% genes, which are similar to those from *Chlorella* Pbi viruses.

Tab.2: List of tested water samples. All results belong to screenings with SAG-degenerated Primers. *Only exception is the Kcv_{GND}, which leads to no result with this screening method, but was found from the van Etten Lab during a whole virus genome sequencing.

Sample #	Country	State/location	Sample source	Results
1	Finland	Hervantajärvi	siltasten lahti	Kcv _{NTS}
2	Finland	Nationalparli Nunksio	Haukkalampi	x
3	USA	New Jersey	Teich in Morris Plains	x
4	USA	New Jersey, Sparta	Lake Mohawk	x
5	USA	Vermont	Echo-Lake	x
6	USA	New Hampshire	Lake Winnepesaukee	Kcv _{NH}
7	USA	Maine	Moosehedd Lake (Lily Bay)	x
8	Portugal	Porto	City pond	x
9	Norway	Preikestolen Camping		x
10	Norway	Hemsedal	Hodnetjedne	x
11	Germany	Allgäu	Prinz-Luitpold-Haus	x
12	New Zealand	Süd Insel	Lake Tekapo	Kcv _{ATCV-1} A16T
13	New Zealand	North Island	Tauposee	x
14	Germany	Schleswig-Holstein	drainage ditch Stellau	x
15	Germany	Schleswig-Holstein	Feldmark at Kellinghusen (Iron)	x
16	Germany	Schleswig-Holstein	Störkathener Heide „Hoch Moor“	x

17	Iceland			x
18	Germany	Föhr	large pond	x
19	Germany	Föhr	small pond	x
20	Greenland		Hundesø lake (slightly salty)	x
21	Greenland		See im Ole-Tal	x
22	Greenland		Lake Sisimiut Campingground	*Kcv _{GNDL}
23	Greenland		Lake Ilulissat Campingground	x
24	Germany	Mecklenburg Vorpommern	Labussee	x
25	Germany	Mecklenburg Vorpommern	Canower See	x
26	Germany	Mecklenburg Vorpommern	kleiner Pälitzsee	x
27	Germany	Mecklenburg Vorpommern	Ellenbogensee	Kcv _{NTS} with silent mutation
28	Germany	Mecklenburg Vorpommern	Priepertsee	x
29	Germany	Mecklenburg Vorpommern	Woblitzsee	x
30	Italy		Lago di Mizzano	x
31	Italy		Pieve salti	Kcv _{ATCV-1} with silent mutation
32	Italy		Pieve Sprenna	x
33	Italy		Lago di Corbara	x
34	Italy		Lago Balsena	x

4.4.2. Internet mining

Screening of internet databases for channel sequences is a fast method for finding new genes. Inspired by this approach we searched in the National Center for Biotechnology database (<http://www.ncbi.nlm.nih.gov>) for viral proteins, which are annotated as K⁺ channels. Potassium channels are easy to identify because of their highly conserved signature-sequence (Heginbotham *et al.*, 1994).

Using this database searches, we found a list of putative channels candidates, which are listed in Tab. 3. This list includes some entirely new channels from viruses, which infect algae from salt water.

Tab. 3: Results of internet mining. Gene accession numbers, viral source of genes, nomenclature of putative K⁺ channels, protein accession numbers and protein sizes.

Gene accession number of virus genom	From virus	Name of putative K ⁺ channel	Protein accession number	Number of amino acids
HM004429	<i>Micromonas</i> sp. RCC1109 virus MpV1	Kmpv ₁	YP_004062056	79
HQ632826	<i>Micromonas pusilla</i> virus 12T	Kmpv _{12T}	YP_007676152	78
JF974320	<i>Micromonas pusilla</i> virus SP1	Kmpv _{SP1}	AET84893	86
HQ633072	<i>Micromonas pusilla</i> virus PL1	Kmpv _{PL1}	AET43568	85
HM004432	<i>Bathycoccus</i> sp. RCC1105 virus BpV1	Kbpv ₁	YP_004061440	83
JF974316	<i>Ostreococcus lucimarinus</i> virus OIV4	Kolv ₄	AET84496	102
JN225873	<i>Ostreococcus tauri</i> virus RT-2011	Kotv _{RT}	AFC34969	104
HQ704803	Organic Lake phycodnavirus 2	Kolpv ₂	ADX06223	105

5. Methods

5.1. Sequences and algorithms

Sequences of putative K⁺ channels were obtained from The National Center for Biotechnology database (<http://www.ncbi.nlm.nih.gov>). Sequence alignments were performed with the T-Coffee algorithm at <http://www.phylogeny.fr>. The phylogenetic tree was calculated with the maximal likelihood algorithm implemented on the same platform. The location of transmembrane domains was predicted by the following algorithms:

- (1) TMHMM (<http://www.cbs.dtu.dk/services/TMHMM-2.0>)
- (2) TMPred (http://www.ch.embnet.org/software/TMPRED_form.html)
- (3) DAS ([http://www.sbc.su.se/\\$miklos/DAS](http://www.sbc.su.se/$miklos/DAS))
- (4) SPLIT (<http://split.pmfst.hr/split/4>)
- (5) HMMTOP (<http://www.enzim.hu/hmmtop>)
- (6) SOSUI (<http://harrier.nagahama-i-bio.ac.jp/sosui>)
- (7) MPEx (<http://blanco.bio.mol.uci.edu/mpex>)
- (8) MEMSAT (<http://www.sacs.ucsf.edu/cgi-bin/memsat.py>)
- (9) PSIPREDV2.3 (<http://bioinf.cs.ucl.ac.uk/psipred>)
- (10) MINNOU (<http://minnou.cchmc.org>)
- (11) The α -helical folds were predicted with the Jpred algorithm (<http://www.comp.bio.dundee.ac.uk/www-jpred>) (Cole *et al.*, 2008).

5.2. Virus isolation and subcloning

The work flow for mining of new channel sequences is shown in Fig. 5. Fresh water samples were first filtered with a 0.45 μ m filter to separate the viruses from dust and bacteria. The filtered water was used to inoculate the pure SAG 3.83 cultures. These algae are a common host of viruses. To obtain single viruses we performed a plaque test (Van Etten *et al.*, 1983a; Van Etten *et al.*, 1983b). Single plaques

were picked and used to infect fresh alga cultures. The infected cultures were used as template for a PCR with degenerated primers: (SAG-forward (with a XhoI-restriction-site underlined): 5' TATCTCGAGATGTTGCTGCTTMTTCATA 3' and reverse (with a EcoRI-restriction-site underlined): 5' TATGAATTCYTACCACGGRAAYGTGAA 3'. A, T, G, C stand for the normal nucleotides; other letters are used when more than one kind could exist at the position (IUPAC): A = adenine, C = cytosine, G = guanine, T = thymine, R = G or A (purine), Y = T or C (pyrimidine), M = A C (amino). As template for the primers we used the known SAG 3.83 channel sequences (appendix). For the PCR the *Pfu*-Polymerase (Thermo Fisher Scientific, Waltham, USA) was used.

The new sequences were cloned into the pEGFP-N2 vector (Clontech-Takara Bio Europe, Saint-Germain-en-Laye, France) at the restriction sites XhoI and EcoRI with the downstream enhanced green fluorescent protein (EGFP). The sequencing was done by Eurofins Genomics (Ebersberg, Germany). The *fast Digest Restriction Enzymes* from Thermo Fisher Scientific (Waltham, USA) were used for digestion and the T4-Ligase from Thermo Fisher Scientific (Waltham, USA) for the ligation.

For multiplying the plasmids DH5 α *e.coli* were transformed by heat shock. For plasmid preparation the *Zyppy Plasmid Miniprep Kit* (Thermo Fisher Scientific, Waltham, USA) was used.

After cloning into a vector and sequencing, we were able to test the new channels in regard to their function via the patch-clamp-technique in HEK293 cells (Fig. 5).

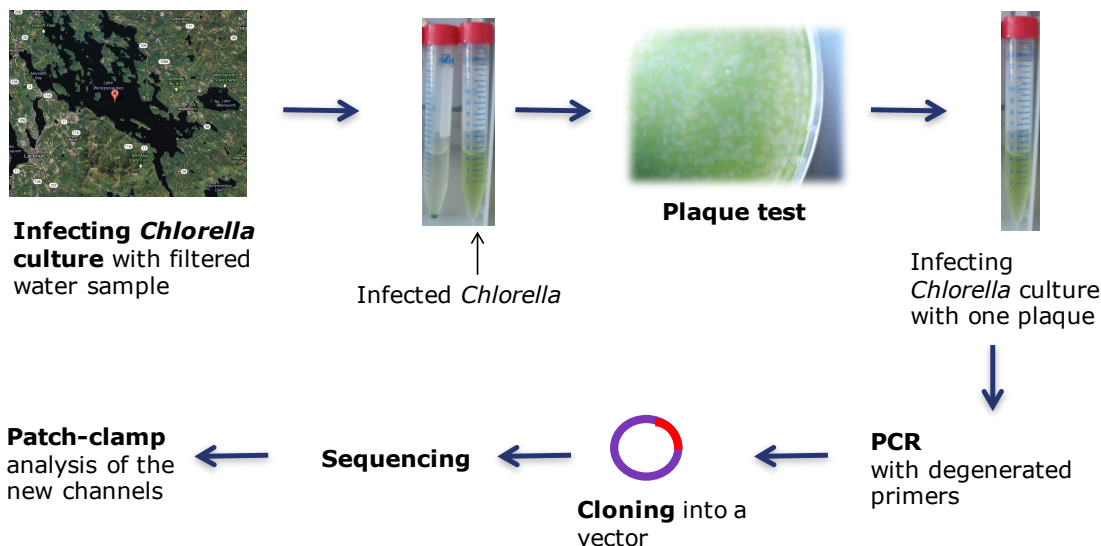


Fig. 5: Schematic work flow of channel mining in environmental samples.

The DNA sequences from Internet mining were synthesized by Eurofins Genomics (Ebersberg, Germany) or Genewiz (New York, USA). Gene synthesis and cloning into pEGFP-N2 of Kmpv₁, Kbpv₂, Kmpv_{12T} and

Kmpv_{PL1} were done by Eurofins Genomics (Ebersberg, Germany). Kmpv_{SP1}, Kolv₄, Kotv_{RT} and Kolpv₂ were synthesized and cloned into pEGFP-N2 by Genewiz (New York, USA). All channel genes were cloned into the XhoI- and EcoRI-restriction sites.

5.3. Patch-clamp

The electrical properties of the putative viral channels in HEK293 cells were recorded as reported previously (Moroni *et al.*, 2002). The HEK293 cells were cultured in DMEM/F12 (Merck Millipore, Darmstadt, Germany) with 10% FCS (Sigma-Aldrich, St. Louis, USA) and 1% Penicillin/Strptomycin (Sigma-Aldrich, St. Louis, USA), at 37°C and 4-5% CO₂.

Currents were recorded with an EPC-9 patch-clamp amplifier (HEKA, Lambrecht, Germany) and analyzed with Patchmaster and Fitmaster Software (HEKA, Lambrecht, Germany). The figures and further analysis were made with IGOR Pro 6 (Wavemetrics, Tigard, USA) and Excel (Microsoft, Redmond, USA). The currents were measured at room temperature in a standard medium (contents are listed in Tab. 4)

Tab. 4: Used patch-clamp solutions.

Pipette solution	130 mM potassium-D-gluconic acid
	10 mM NaCl
	5 mM HEPES
	5 mM EGTA
	0.1 mM guanosine triphosphate (GTP)
	0.1 mM CaCl ₂
	2 mM MgCl ₂
	5 mM phosphocreatine (Na salt)
	2 mM adenosine triphosphate (Na salt, pH 7.4)

50 mM KCl bathsolution

50 mM KCl

1.8 mM CaCl₂1 mM MgCl₂

5 mM 4-(2-hydroxyethyl)-1-piperazineethanesulfonic acid (HEPES, pH 7.4)

50 mM NaCl bathsolution

50 mM NaCl

1.8 mM CaCl₂1 mM MgCl₂

5 mM 4-(2-hydroxyethyl)-1-piperazineethanesulfonic acid (HEPES, pH 7.4)

In order to characterize the pharmacological properties of the channels either 10 mM BaCl₂ or 10 mM CsCl was added to the K⁺ containing media in order to block channel activity. The osmolarity of all solutions was adjusted with mannitol to 330 mOsmol. The osmolarity was measured with an osmometer (Gonotec, Berlin, Germany)

All constructs were transiently expressed, in HEK293 cells (human embryonic kidney 293 cell) (Graham *et al.*, 1977), as fusion proteins with EGFP on the C-terminus using the non-lipid based transfection reagent GeneJuice (Merck Millipore, Darmstadt, Germany).

Recordings were performed in whole-cell configuration.

5.4. Bilayer

The Kmpv_{12T} and Kmpv_{SP1} gene were cloned into the pEXP5-CT/TOPOs-vector. The protein was then synthesized cell-free with the MembraneMax™ HN Protein Expression Kit (Invitrogen by Thermo Fisher Scientific, Waltham, USA) following the manufacturer's instructions. For protein expression in its native form, a stop-codon was inserted right before the gene of a 6xHis-tag. The DNA template was incubated with the synthesis reaction mix (MembraneMax™ HN reagent carrying a poly-His-tag, ribosomes, T7 RNA polymerase and energy renewal system) for 35 min at 37°C (1000 rpm). The feeding buffer was added and the reaction was incubated for 1 h 45 min at 37°C (1000 rpm). After expression, the protein was loaded on a Ni-NTA column, which was equilibrated with an equilibration buffer 500mM NaCl, 30 mM HEPES, 10% glycerin (all from AppliChem ITW Reagents, Darmstadt, Germany), pH 7.5.

Unspecific binding was removed by washing the column with 20 mM imidazole twice (Sigma-Aldrich, St. Louis, USA). The protein was then eluted with 250 mM imidazole in seven fractions at 100 μ l. After elution, the protein was used directly in the planar lipid bilayer (Braun *et al.*, 2014). Planar lipid bilayer experiments were done with a vertical bilayer setup (Ionovation GmbH, Osnabrück, Germany) as described previously (Braun *et al.*, 2014). A 1% hexadecane solution (Merck KGaA, Darmstadt, Germany) in n-hexane (Carl ROTH, Karlsruhe, Germany) was used for pretreating the Teflon foil (Dielectric Corporation, Menomonee Falls, USA). The hexadecane solution (ca. 0.5 μ l) was pipetted onto the hole (100 μ m diameter) in the Teflon foil with a bent Hamilton syringe (Hamilton Company, Reno, Nevada, USA) until the solvent evaporated. The experimental solution contained 100 mM KCl and was buffered to pH 7.0 with 10 mM HEPES/KOH. As a lipid, we used 1,2-diphytanoyl-sn-glycero-3-phosphocholine (DPhPC) (from Avanti Polar Lipids, Alabaster, USA) at a concentration of 15 mg/ml in n-pentane (Merck KGaA, Darmstadt, Germany).

5.5. Calculations

Because of a large variability in the data the geometrical mean was used in the data analysis. Because the measured currents at negative voltages varied much more towards large negative currents than small currents the standard deviation would have resulted in error bars, which reach into the positive current range. This does not reflect the measured currents, which are all negative. For this reason, we use the geometrical mean, which represents the data in a more realistic way. For the reversal potential, the arithmetical mean was used.

$$\frac{1}{n} \sum_{i=1}^n I_i = \text{arithmetical mean}$$

$$\sqrt[n]{\prod_{i=1}^n I_i} = \text{geometrical mean}$$

n= variables for natural numbers

i= series of natural numbers

∏=Pi (product of a sequence of terms)

∑=sigma (sum)

√=root

l=values

5.6. Mutations und chimera PCR

Mutations were made with the *QuickChange* Site-directed Mutagenesis method (Stratagene, Agilent, Santa Clara, USA) (Braman *et al.*, 1996). All primers were synthesized by Eurofins GmbH (Ebersberg, Germany). The used *Pfu*-Polymerase (2.5 U/μl) was from Thermo Fisher Scientific (Waltham, USA).

The Chimera-PCR was made with 3 separated PCR steps. In the first and second PCR, the gene fragments which should be fused later were amplified. In order to allow fusion of the two gene fragments, in the third PCR reaction, one of the two gene fragments had an overhanging primer, which is complementary to the second gene fragment (appendix). The *Phusion* Polymerase (Thermo Fisher Scientific, Waltham, USA) was used for the PCR's.

All Enzymes were used as described by the manufacturer.

5.7. Confocal laser scanning microscopy

The sorting of proteins is affected by signal sequences coded on the protein. To verify the location of the channel-proteins in the cell we used Confocal Laser Scanning Microscopy (CLSM). This was important, because fusion to EGFP can result in sorting into different membranes of the cell (von Charpui *et al.*, 2015).

After changing the cell culture medium against PBS the cell cultures were treated with MitoTracker (Thermo Fischer Scientific, Waltham, USA) in order to label the mitochondria (Balss *et al.*, 2008). The MitoTracker was used in a final concentration of 25 nM and cell were incubated for 5 min. After incubation, the cells were washed again with PBS. The Leica TCS SP microscope (Leica, Wetzlar, Germany) was used for all localization studies. Images were obtained with an HCX PL APO 40.0x1.25 OIL UV objective and the following settings: Used laser for excitation were Argon Laser

(488 nm) and Krypton Laser (568 nm); excitation max. and emission max. of EGFP: 488 nm/509 nm and MitoTracker ®Red CMXRos (Thermo Fisher, Waltham, USA) 579 nm/599 nm.

The following programs were used for the evaluation of images: ImageJ (<https://imagej.net/Downloads>), Leica Confocal Software (Leica, Wetzlar, Germany).

6. Viruses encode for new hypothetical K⁺ channels (Chapter 2)

6.1. Abstract

The large genomes of phycodnaviruses encode many gene products, like small K⁺ channels, with homologs in prokaryotes and eukaryotes. Screening water samples for K⁺ channels revealed their abundance in viruses from fresh water habitats. Recent sequencing of viruses from marine algae or from salt water in Antarctica revealed sequences with the predicted characteristics of K⁺ channels, but with some unexpected features. Here we have a closer look at the sequences of ten new hypothetical channel proteins. Two genes encode either 78 or 79 amino acid proteins, which are the smallest known K⁺ channels. Also of interest is an unusual sequence in the canonical α -helices in K⁺ channels. Structural prediction algorithms indicate that the new channels from salt water have the conserved α -helix folds, but the algorithms failed to identify the expected transmembrane domains flanking the K⁺ channel pores. Further, a channel sequence of a hybrid virus was examined.

6.2. Introduction

It has been mentioned in the general introduction that several viruses have genes which encode for proteins with ion channel activity (Fischer and Sansom, 2002; Nieva *et al.*, 2012; Wang *et al.*, 2011). Depending on the virus, these channels are either involved in viral entry, viral replication or viral exit from the host (Hsu *et al.*, 2004; Nieva *et al.*, 2012; Thiel *et al.*, 2010). Bioinformatics analyses of these viral encoded channels have not revealed any obvious sequence similarities to channel proteins from cellular organisms (Fischer and Sansom, 2002). One exception are viruses in the family of the *Phycodnaviridae*, which code for proteins with the structural and functional hallmarks of K⁺ channels (Plugge *et al.*, 2000; Thiel *et al.*, 2011). The prototype K⁺ channel Kcv is coded by chlorovirus PBCV-1 (Kcv_{PBCV-1}) (Plugge *et al.*, 2000) and like its prokaryotic and eukaryotic homologs, it is functional as a tetramer (Pagliuca *et al.*, 2007; Shim *et al.*, 2007). Each Kcv monomer has two transmembrane domains (TMDs), which are linked by a pore helix (Tayefeh *et al.*, 2009). The pore helix contains a motif of 8 amino acids, which is the signature sequence for all K⁺ channels (Heginbotham *et al.*, 1994). Assembly of four Kcv monomers creates a central pore with a selectivity filter that allows passage of K⁺ across the membrane (Tayefeh *et al.*, 2009). The major difference between Kcv_{PBCV-1} and K⁺ channels from other organisms is the small size of the monomers, which is only 94 amino acids (Plugge *et al.*, 2000); Kcv_{PBCV-1} basically consists of the pore module present in all K⁺ channels (Thiel *et al.*, 2011). However, in spite of its small size the Kcv_{PBCV-1} channel has all the functional hallmarks of more complex K⁺ channels when expressed in heterologous systems, including selectivity for K⁺ and sensitivity to many of the known K⁺

channel blockers (Thiel *et al.*, 2011).

After discovering Kcv_{PBCV-1} , it was realized that K^+ channel encoding genes are common in members of the *Phycodnaviridae* family. K^+ channel sequences have been detected in more than 80 phycodnaviruses (Gazzarrini *et al.*, 2006; Hamacher *et al.*, 2012; Kang *et al.*, 2004) (Thiel and Van Etten, unpublished data). From an evolutionary point of view it is interesting that K^+ channel coding sequences are found in members representing four genera in the *Phycodnaviridae*. These viruses infect different algal hosts. Three of these viruses replicate in species of unicellular green algae from fresh water habitats, *Chlorella variabilis*, *Chlorella heliozoae*, and *Micractinium conductrix* (Fitzgerald *et al.*, 2007; Jeanniard *et al.*, 2013). Collectively these viruses are called chloroviruses. A fourth virus, EsV-1, also encodes a K^+ channel protein named Kesv. EsV-1 infects the marine filamentous brown alga *Ectocarpus siliculosus*. EsV-1 is distantly related to the viruses that infect fresh water green algae (Van Etten *et al.*, 2002). Several studies have established that the Kcv channels are located in the internal membrane of the chloroviruses (Frohns *et al.*, 2006; Romani *et al.*, 2013) and that they serve an important role in the early steps of infection and DNA ejection into the host (Greiner *et al.*, 2009; Neupartl *et al.*, 2008). The biological role of the K^+ channel in the marine EsV-1 is unknown but presumably it is different from that in the chloroviruses. The reason for this assumption is that chloroviruses have a lytic life cycle while EsV-1 is lysogenic (Delaroque *et al.*, 1999; Van Etten *et al.*, 2002). Also the energetic barrier for ejecting viral DNA into the host, which is lowered by Kcv activity in the fresh water algae (Neupartl *et al.*, 2008; Thiel *et al.*, 2010), is not relevant in the marine habitat because virus EsV-1 infects the *sporophytes* of the host cells, which lack a cell wall and hence have no turgor pressure (Delaroque *et al.*, 1999).

Although, the K^+ channels from phycodnaviruses are similar, they exhibit significant structural and functional diversity. An obvious structural difference is their monomer size, which ranges from 124 amino acids in the Kesv channel from virus EsV-1 (Balss *et al.*, 2008) to 82 amino acids in viruses, which infect *Chlorella heliozoae* (Gazzarrini *et al.*, 2009). These size differences are mostly due to the presence or absence of cytoplasmic domains and an extracellular turret domain in the channels (Thiel *et al.*, 2010). Diversity also exists in the functional properties of the channels when they are expressed in heterologous systems. For example, Kcv_{PBCV-1} has a lower open probability than the corresponding channel from chlorovirus ATCV-1, Kcv_{ATCV-1} . Also, Kcv_{PBCV-1} conducts Rb^+ better than K^+ whereas the situation is reversed in Kcv_{ATCV-1} (Gazzarrini *et al.*, 2009). In addition to their functional differences the K^+ channels are sorted differently. The chlorovirus encoded Kcv channels are sorted into the secretory pathway and finally targeted to the plasmamembrane in either HEK293 cells or in yeast, the Kesv channel from EsV-1 is targeted to the mitochondria (Balss *et al.*, 2008).

Another interesting question is the origin and the evolution of the viral K^+ channel proteins. The fact

that all K⁺ channels from cellular organisms contain a pore, which resembles the viral K⁺ channels, is consistent with the traditional assumption that viruses are ‘pick pockets’ (Moreira and Lopez-Garcia, 2009) and acquire their genes from their host via molecular piracy. However, this traditional view on the evolution of viral K⁺ channels has been challenged recently. Comparative analysis of the Kcv channels from different chloroviruses and from virus EsV-1 with those coded by the two host cells found no evidence of co-evolution between the viruses and their hosts (Hamacher *et al.*, 2012). Instead, a phylogenetic analysis indicated that the viral channels form, in spite of their structural and host diversities, a defined clade; i.e., the viral channels are clearly separated from their host K⁺ channels and from K⁺ channels from other cellular organisms (Thiel *et al.*, 2013). This analysis clearly argues against the hypothesis that viruses have acquired their K⁺ channels from their current hosts. This conclusion is further supported by a bioinformatics analysis of 41 chloroviruses with one of their hosts. The results of this study did not find any evidence to indicate a major transfer of genes from the host to the chloroviruses. For a few genes the results even indicated a flow of genes in the opposite direction, i.e., from virus to host (Jeanniard *et al.*, 2013).

In the context of the question about the origin of viral K⁺ channels, recent sequencing projects of viruses infecting marine unicellular algae (Derelle *et al.*, 2008; Derelle *et al.*, 2006; Moreau *et al.*, 2010) and metagenomic sequencing of an organic lake in Antarctica (Yau *et al.*, 2011; Zhou *et al.*, 2013) revealed open reading frames that were annotated as K⁺ channels. Furthermore, in the context of the minimal size required for a functional K⁺ channel, two of the newly detected putative K⁺ channels have a monomer size of 78 and 79 amino acids, which is even smaller than the 82 amino acids Kcv_{ATCV-1} channel (Gazzarrini *et al.*, 2009). Here we report a detailed structural and functional examination of three of the new putative K⁺ channel proteins, as well as their phylogenetic relationships. The results revealed considerable variability among the viral K⁺ channels. A phylogenetic analysis indicated that the K⁺ channels from the fresh water viruses are clearly separated from those from the marine/salt water habitats. These results support the notion of a long evolutionary history for the viral K⁺ channels.

6.3. Results and Discussion

6.3.1. Virus channels from in silico mining

Fig. 6A shows an alignment of eight newly detected putative K⁺ channel sequences from viruses infecting algae. Seven of the viruses with K⁺ channel-like sequences infect small unicellular algae, which are the main components of the so-called picoplankton community. Their hosts, *Micromonas*, *Bathycoccus* and *Osterococcus* species, belong to the class of *Prasinophyceae* within the *Chlorophyta*, these algae are ecologically important because they are often the dominant photosynthetic species in marine habitats. Four of the viruses (MpV12T, MpVSP1, MpV1, MpvPL1) infect *Micromonas pusilla*. Two viruses BpV1 and BpV2 infect *Bathycoccus* species. The sequence of the putative K⁺ channel protein from these two viruses are identical. Two additional viruses (OIV4, ORT) infect *Osterococcus* species. The name of the gene products in Fig. 6A is composed of K for K⁺ channel, and the virus, which encodes the sequence, e.g., mpv stands for *M. pusilla* virus, the index specifies the virus isolate. Thus Kmpv_{12T} is the K⁺ channel from *M. pusilla* virus isolate 12T. Finally, a K⁺ channel-like sequence was detected in a metagenomic sequencing project of viral genomes in an organic lake in Antarctica (Yau *et al.*, 2011). In this case, neither the host nor the virus encoding the K⁺ channel from the organic lake phycodnavirus 2, Kolpv₂, is known. Information on the gene accession numbers, on the source of the genes and on the protein nomenclature are summarized in Tab. 3. The sequences reveal some structural hallmarks of K⁺ channels (Fig. 6). All the predicted proteins contain a consensus or a consensus-like sequence of K⁺ channels (Heginbotham *et al.*, 1994) including, either a GYG or GFG motif in the core of the selectivity filter. However, the second Thr in the consensus sequence is not conserved in all of the channels. Worth noting is that four of the eight sequences have a Ser instead of the canonical Thr in the consensus sequence prior to the GY/FG motive. This same amino acid substitution is present in the selectivity filter of the viral Kesv channel (Bals *et al.*, 2008). Even though this amino acid substitution is conservative, previous studies established that replacement of this canonical Thr with Ser resulted in a drastic reduction in the sensitivity of the channels to Ba²⁺ in Kcv_{PBCV-1} and Kir channels (Chatelain *et al.*, 2009). Even more unusual is the Kolpv₂ sequence, which has a Leu in this position. Structure/function analyses of K⁺ channels have shown that they require a pair of aromatic amino acids upstream of the filter, which act as a cuff and keep the pore in the correct diameter for K⁺ passage (Doyle *et al.*, 1998). The alignment in Fig. 6A indicates that these obligatory aromatic amino acids are present in all 8 proteins.

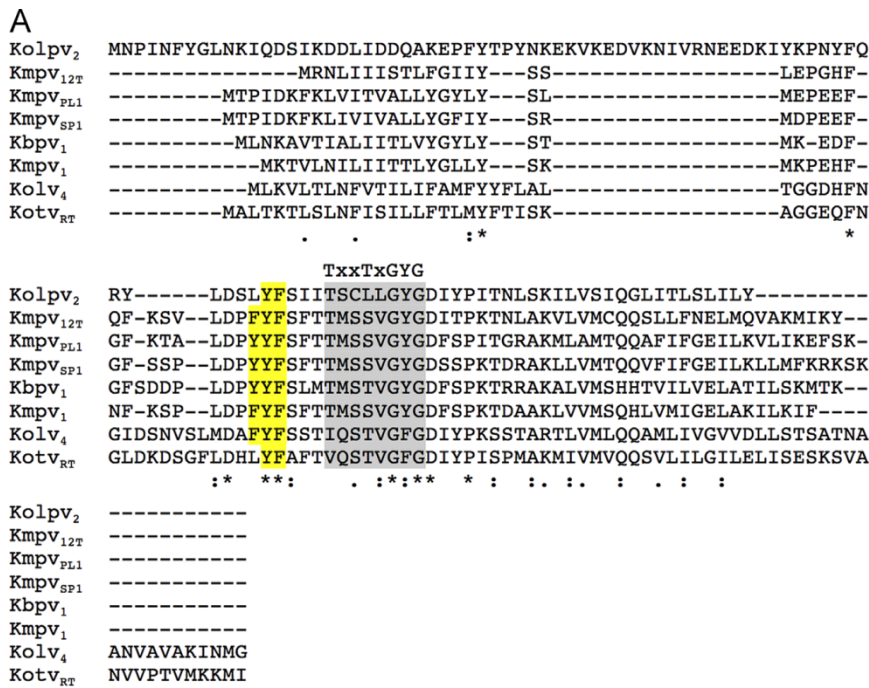


Fig. 6. Alignment of putative viral K^+ channel sequences from a salt water lake in Antarctica (Kolpv₂) and marine water viruses (remaining sequences). (A) The consensus sequence for K^+ channel filters are indicated in gray and the aromatic amino acids upstream of the filter are shown in yellow. The consensus sequence of the K^+ channel filter region is shown on top of the sequences. * mark the amino acids which are identical in all sequences, : mark the conserved and . mark the semi-conserved amino acids. (B) Schematic architecture of channels sequences including reference channel Kcv_{PBCV-1} (1) and putative K^+ channels Kolpv₂ (2) Kmpv_{12T} (3) Kmpv_{PL1} (4) Kmpv_{SP1} (5) Kbpv₁ (6) Kmpv₁ (7) Kolv₄ (8) Kotv_{RT} (9). The predicted position of the α -helices is shown in orange, the filter with GYG or GFG is in blue. The α -helices in the Kcv_{PBCV-1} channel form the outer TMD (TMD1) the inner TMD (TMD2) and the pore helix (PH) of typical K^+ channels. The predicted position of the α -helices was predicted with Jpred (Cole *et al.*, 2008).

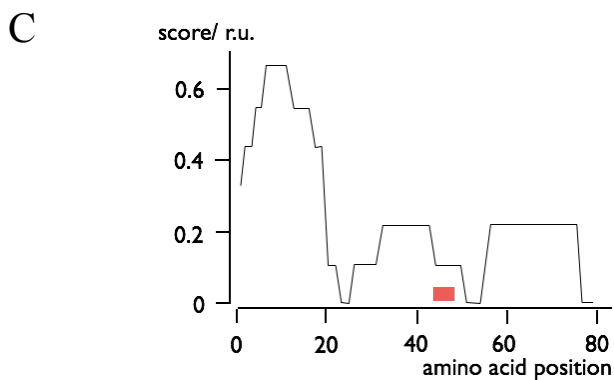
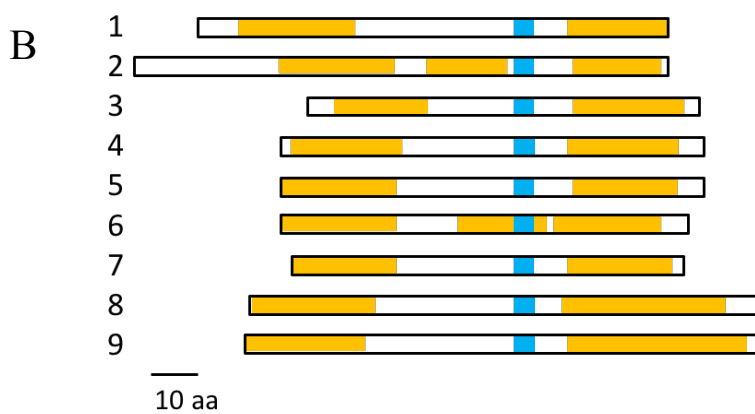
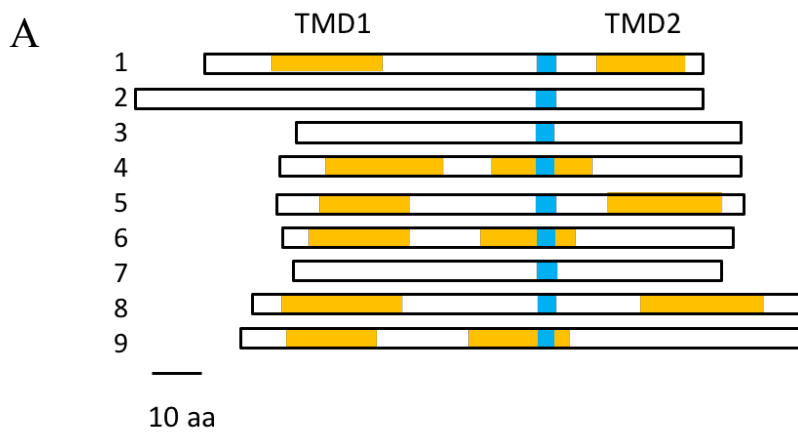


Fig. 7: Prediction algorithms fail to detect an expected K^+ channel Transmembrane Domains in some of the viral sequences. Schematic architecture of channels sequences including reference channel $Kcv_{PB_{CV-1}}$ (1) and putative K^+ channels Kolpv2 (2) Kmpv12T (3) KmpvPL1 (4) KmpvSP1 (5) Kbpv1 (6) Kmpv1 (7) Kolv4 (8) KotvRT (9). The predicted position of the TMDs are shown in orange, the filter with GYG or GFG is in blue. The position of the TMDs was predicted with the TMHMM (A) or MINNOU (B) algorithms. (C) Consensus for prediction of TMDs in channel Kmpv1. The plot was calculated as mean value from predictions with 10 different algorithms (see material and methods 5.1 algorithm (1) - (10)). An amino acid was assigned the value 1 when it was predicted as part of a transmembrane domain and 0 if it was not. The y-axis shows the mean value from the predictions. The red bar indicates the location of the GYG motive in the filter.

A surprise arose from in silico analyses of possible TMDs in these new putative K^+ channel proteins. The

general architecture of a K⁺ channel requires one TMD downstream and one TMD upstream of the selectivity filter (Doyle *et al.*, 1998; Tayefeh *et al.*, 2009). However, one of the most established prediction programs for TMDs, the TMHMM 2.0 algorithm (Amico *et al.*, 2006), did not predict the expected second TMD in the Kmpv₁, Kmpv_{12T} and Kolpv₂ sequences (Fig. 7). In the Kmpv_{PL1}, Kbpv₁ and Kotv_{RT} sequences two TMDs were predicted, but the second TMD was in the wrong position, i.e., in the center of the selectivity filter (Figs.7 and 8), this hydrophobic domain probably represents the pore helix of the K⁺ channel proteins (Doyle *et al.*, 1998; Tayefeh *et al.*, 2009). In the two remaining viral channels, the algorithm predicts a protein architecture that is compatible with a K⁺ channel. Which means, they have two peripheral TMDs, which are connected by a stretch of hydrophobic amino acids, this stretch is in the correct position of the pore helix of K⁺ channel proteins.

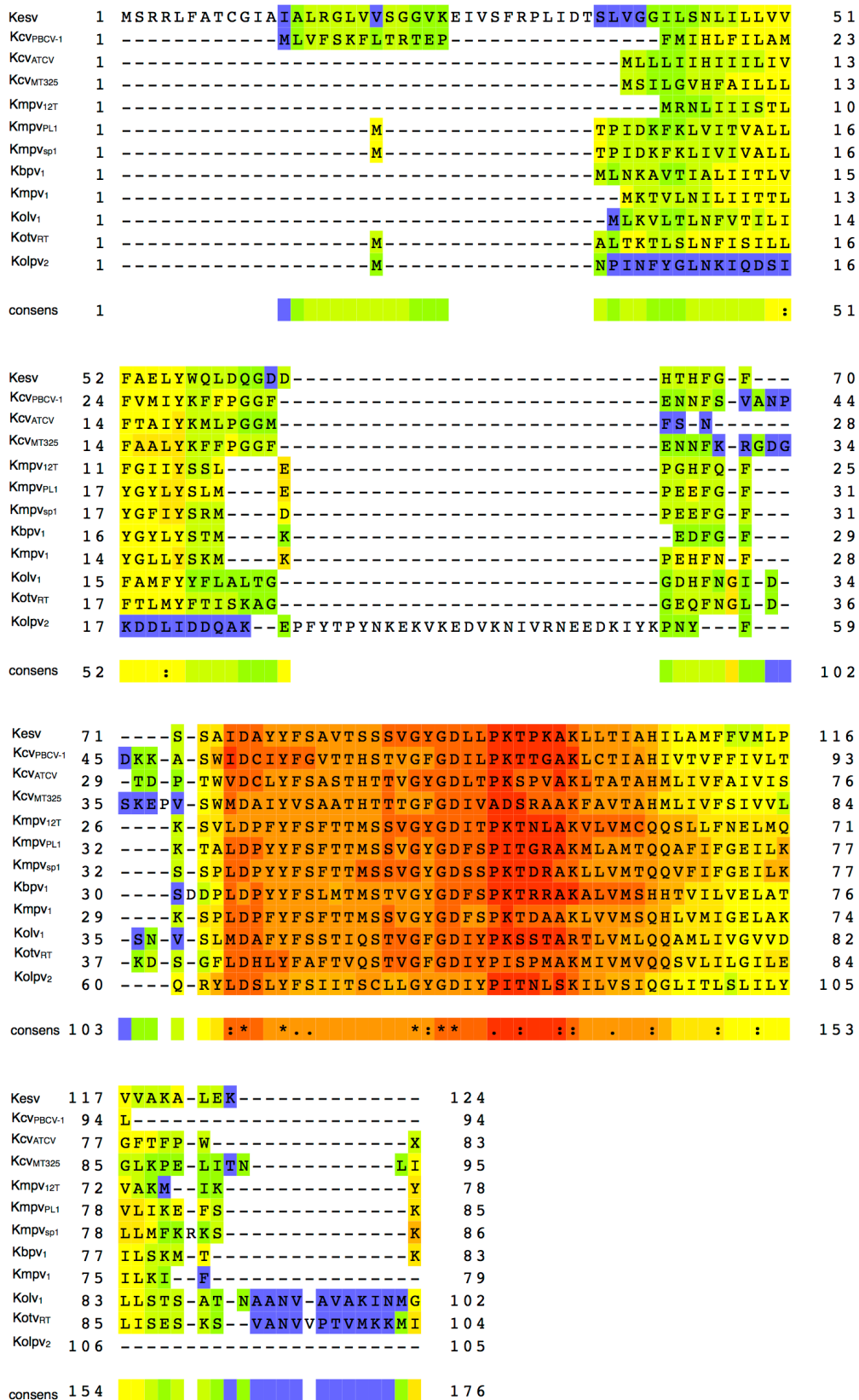


Fig. 8: Full multiple alignment of K⁺ channels from viruses with different origins. The alignment includes established K⁺ channels from chloroviruses (KCV_{PBCV-1}, KCV_{ATCV}, KCV_{MT325}) and from the *Ectocarpus siliculosus* virus (Kesv). The remaining sequences are K⁺ channels from viruses described in this thesis. Alignment was constructed with T-coffee software. The colors depict the degree of similarity from conserved (red) to not conserved (blue). * mark the amino acids which are identical in all sequences, : mark the conserved and . mark the semi-conserved amino acids.

Because of the ambiguous predictions of the TMDs in six viruses we selected the Kmpv₁ channel, e.g. a channel in which the aforementioned algorithm did not predict the expected TMDs and analyzed this protein with 10 different algorithms (see material and methods 5.1 (1) - (10)). Also in this analysis, many algorithms did not predict any TMD in the protein. A consensus prediction for Kmpv₁ from all the algorithms is shown in Fig. 7C. The data illustrate that a TMD downstream of the selectivity filter seem rather unlikely on the basis of structural predictions. In the 10 prediction platforms tested only one (Cao *et al.*, 2006) suggested for the Kmpv₁ channel TMDs in positions, which are in agreement with a canonical K⁺ channel structure (Fig. 7A). This analysis, which is based on the predicted solvent accessibility and secondary structure of each amino acid in a sequence (Cao *et al.*, 2006) appears to be the most suitable tool for the analysis of the apparent unusual structures of the viral proteins. The same tool was used for a scrutiny of all putative channel proteins. The data in Fig. 7A indicate that this prediction suggests for all sequences two TMDs one upstream and one downstream of the selectivity filter.

Because of the ambiguous predictions for TMDs, we also examined the proteins with respect to their predicted folds. The structure of a K⁺ channel requires two α -helices, which form the two TMDs and an α -helix upstream of the filter, which forms the pore helix (Doyle *et al.*, 1998; Tayefeh *et al.*, 2009). Analysis of known viral channels such as Kcv_{PBCV-1} with a structure prediction algorithm Jpred 3 revealed α -helices in the expected positions (Fig. 6B). Analyses of the new sequences indicated that all 8 proteins have an α -helix in the position of the Kcv_{PBCV-1} protein and a third helix in front of the pore helix. The results from this analysis indicate, that all the new putative K⁺ channel proteins have the potential to fold according to the architecture of a functional K⁺ channel the putative channels apparently have a high conservation for folding, but achieve this with different amino acid sequences.

6.3.2. New hypothetical virus channels isolated from fresh water samples

During this work, we found two new sequences with the hallmarks of potassium channels in environmental samples, named Kcv_{G_{NLD}} and Kcv_{NH}. In the following we will have a closer look at the sequences.

6.3.3. Kcv_{G_{NLD}}

An alignment of the Kcv_{G_{NLD}} (Kcv Greenland) with the two most similar channels Kcv_{cmv-1} and Kcv_{MT325} is shown in Fig. 9. The data show that Kcv_{G_{NLD}} shares a high degree of sequence identity with other viral proteins. These proteins, Kcv_{CMV1} and Kcv_{MT325}, were isolated from viruses, which infect *Chlorella* Pbi cells. It was previously shown that they function as K⁺ channels (Gazzarrini *et al.*, 2006). Kcv_{G_{NLD}} was obtained from a water sample from Greenland taken at Sisimiut Camping (N 66° 56.149" W 053° 37.541"). Viruses which were contained in this water sample were amplified by infecting cultures with potential host cells. The aforementioned channel was isolated from a virus, which infected and replicated in a *Chlorella* species, which lives as a symbiont in *Heliozoae* species. This is very surprising since all channels, which were so far isolated from *Heliozoae* exhibit the typical “ATCV-1-Typ” sequence. Kcv_{G_{NLD}} instead shows a high sequence identity with Kcv channels from Pbi viruses, which use *Micractinium conductrix* as a host. The van Etten laboratory (Lincoln, Nebraska) has sequenced the entire genome of the virus from which I isolated Kcv_{G_{NLD}} and found a mixture of typical gene sequences (Van Etten unpublished data). This suggests that the respective virus is a hybrid of the SAG virus and Pbi virus. This finding is very interesting from an evolutionary point of view. The virus could be an ancestor of the of SAG virus and the Pbi virus before they split up in two groups. Alternatively, the hybrid virus could also be a descendant of SAG and Pbi viruses.

```

KcvGNLD      MLRSIL -PHIIVFTFFVLYKFFPGGFEDSFKRGDGSRRKAT
Kvcvmv-1     M--SILGVHFALLLLFAALYKFFPGGFANFKRSDGSKPEVVS
KcvMT325     M--SILGVHFALLLLFAALYKFFPGGFENFKRGDGSKEPVS

cons         *  ***  * : : : * . . ***** : . *** . *** : . :

KcvGNLD      WMDCIYFATATHTTTGFGDVVPDNDAAARTAVTMHMLIVFAIV
Kvcvmv-1     WMDAIYVSAATHTTTGFGDIVADSRAAKFAVTAHMLIVFSIV
KcvMT325     WMDAIYVSAATHTTTGFGDIVADSRAAKFAVTAHMLIVFSIV

cons         *** . ** . : : ***** : * . * . ** : *** ***** : **

KcvGNLD      VLGIKL-----
Kvcvmv-1     VLGLKPELITNLYKIM
KcvMT325     VLGLKPELITNLI---

cons         *** . *

```

Fig. 9: Multiple alignment of conserved new K⁺ channels from viruses. The alignment includes the established K⁺ channels Kcv_{cmv-1} and Kcv_{MT325} from Pbi for comparison. Alignment was constructed with T-coffee software. The colors depict the degree of similarity from conserved (rose) to not conserved (blue). * mark the amino acids which are identical in all sequences, : mark the conserved and . mark the semi-conserved amino acids.

Kcv_{G_NL_D} is 89 aa long and has a shorter c-terminus than Kcv_{cmv-1} and Kcv_{MT325} (Fig. 10). Kcv_{G_NL_D} also shows the typical consensus sequence of K⁺ channels (Heginbotham *et al.*, 1994). It has a GFG motif, like the channels from Pbi viruses. The channels from SAG viruses in contrast typically have a GYG motif.

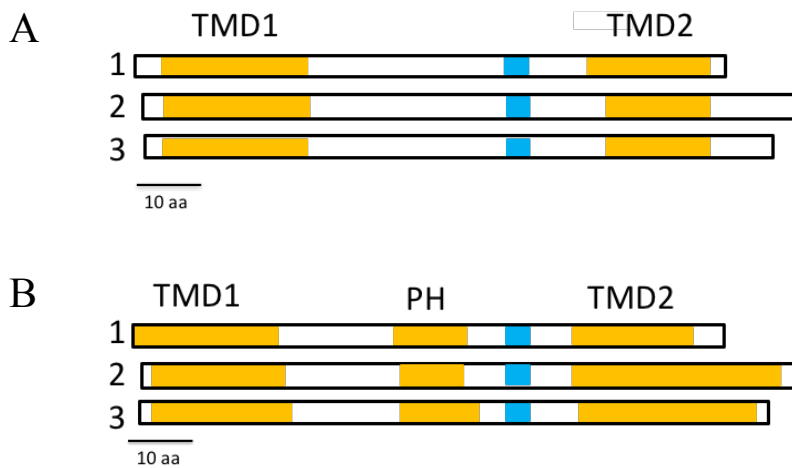


Fig. 10: Prediction algorithms detect expected K⁺ channel TMD and α -helices. Schematic architecture of channels sequences of putative Kcv_{G_NL_D} (1) and established K⁺ channels Kcv_{cmv-1} (2) and Kcv_{MT325} (3). The predicted position of the TMDs are shown in orange, the filter with GYG or GFG is in blue. The position of the TMDs was predicted with the TMHMM algorithm (A). The predicted position of the α -helices was predicted with Jpred (B) and is shown in orange, the filter with GYG or GFG is in blue.

The *in silico* analysis of possible TMDs in Kcv_{G_NL_D} with the TMHMM 2.0 algorithm (Amico *et al.*, 2006) predicts the expected TMD1 and TMD2 (Fig. 10 A). Also the Jpred 3 algorithm (Cole *et al.*, 2008) predicts α -helices including the pore helix in the expected positions (Fig. 10 B).

6.3.4. Kcv_{NH}

A further putative viral K⁺ channel Kcv_{NH} (Kcv New Hampshire) was found in a water sample from the Winnepesaukee lake in New Hampshire. It was isolated as described in 5.2 from *Chlorella* cells, which are symbionts of *Acanthocystis turfacea* in nature. The derived amino acid sequence shows, as expected, the typical highly conserved sequence of Kcv channels from SAG viruses (Fig. 11).

A Kcv_{NH} monomer is 82 aa long (Fig. 11) and shows the typical consensus sequence of K⁺ channels in the filter domain (Heginbotham *et al.*, 1994), like all other channels from SAG viruses it includes a GYG motif.

```

KcvATCV-1  MLLLIHIIILIVFTAIYKMLPGGMFSNTDPTWVDCLYF
KCVNTS     MLLLIHLSILVIFTAIYKMLPGGMFSNTDPTWVDCLYF
KcvS       MLLLIHVGILVFFTTVYKMLPGGMFSNTDPSWVDCLYF
KcvNH      MLLLIHICILVFFTTIVYKMLPGGMFSYADPSWVDCIYF

cons       ****:*:* :*:* :***** :*:*:**:*

KcvATCV-1  SASTHTTVGYGDLTPKSPVAKLTATAHMLIVFAIVISGF
KCVNTS     SASTHTTVGYGDLTPKSPVAKLTATAHMLIVFAIVISGF
KcvS       SASTHTTVGYGDLTPKSPVAKLVATAHMMIVFAIVVSSF
KcvNH      SASTHTTVGYGDLTPKSAVAKLTATAHMLIVFAIVVSSF

cons       *****.****.*****.*****:*.*

KcvATCV-1  TFPW
KCVNTS     TFPW
KcvS       TFPW
KcvNH      TFPW

cons       ****

```

Fig. 11: Alignment of highly conserved new K⁺ channels from SAG viruses. The alignment includes the established K⁺ channels Kcv_{NTS}, Kcv_S and Kcv_{ATCV-1} for comparison. Alignment was constructed with T-coffee software. The colors depict the degree of similarity from conserved (rose) to not conserved (blue). The whole sequence is conserved (rose). * mark the amino acids which are identical in all sequences, : mark the conserved and . mark the semi-conserved amino acids.

Kcv_S (Kcv Smith) shares the highest sequence similarity with Kcv_{NH}, both proteins differ in only 10 aa (Greiner, 2011). An *in silico* analysis of possible TMDs in Kcv_{NH} with the TMHMM 2.0 algorithm (Amico *et al.*, 2006) predicts the expected TMD1 and TMD2 (Fig. 12A). Also the Jpred 3 algorithm (Cole *et al.*, 2008) revealed α -helices including the pore helix in the expected positions (Fig. 12B).

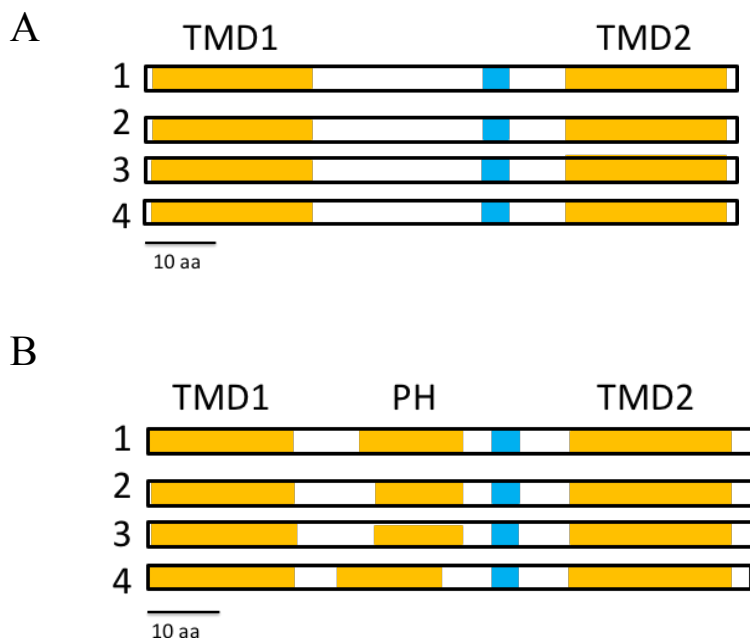


Fig. 12: Prediction algorithms detect expected K⁺ channel TMDs and α -helices. Schematic architecture of channels sequences of established KcvATCV-1 (1), KcvNTS (2), KcvS (3) and putative K⁺ channels KcvNH (4). The predicted position of the TMDs are shown in orange, the filter with GYG or GFG is in blue. The position of the TMDs was predicted with the TMHMM (A). The position of the α -helices was predicted with Jpred (B) and is shown in orange, the filter with GYG or GFG is in blue.

7. New functional channels (Chapter 3)

7.1. Abstract

Here I examine ten new hypothetical potassium channels. Two new Kcv channels were found in the context of fresh water sample screening. Eight were found by internet mining from *Micromonas* virus, *Bathyllococcus* virus, *Ostreococcus* virus (Derelle *et al.*, 2008; Moreau *et al.*, 2010) and from a metagenomics sequencing project of viral genomes in an organic lake in Antarctica (Yau *et al.*, 2011). Seven of the ten channels could be detected as functional potassium channels named Kmpv₁, Kmpv_{12T}, Kmpv_{SP1}, Kbpv₁, Kotv_{RT}, Kcv_{NH}, Kcv_{GnLD}. For Kolv₄, Kmpv_{PL1} and Kolpv₂ channel activity could so far not be supported by experiments.

Kmpv₁ with 79 amino acids per monomer shows a typical linear I/V-relationship and is sensitive to the canonical K⁺ channel blocker Ba²⁺, but even at a high concentration of 10 mM it is not fully blocked. The related channel Kmpv_{12T} is with 78 amino acids per monomer the smallest K⁺ channel known so far. We were not able to measure its activity in HEK293 cells. But after *in vitro* expression we were able to measure channel activity as protein in a bilayer system. Kmpv_{12T} shows a linear I/V-relationship in a buffer with potassium. An exchange of K⁺ for Na⁺ on one side of the membrane generated a strong shift of the reversal voltage indicating that this channel is highly selective for K⁺ over Na⁺. Another channel from a *Micromonas* virus, Kmpv_{SP1} surprisingly is not selective for potassium, it also conducts some sodium. The most interesting feature of this channel is that it exhibits in HEK293 cells an inherent inward rectification. The inward currents can be blocked completely with barium. All the results could be confirmed by functional reconstitution of the channel in planar lipid bilayers. Kbpv₁ from a *Bathyllococcus* virus, showed a linear I/V-relationship with a voltage sensitive inactivation at high negative voltages. Kbpv₁ was fully blocked by barium and selective for potassium. Kotv_{RT} from an *Ostreococcus* virus is a channel with an interesting sensitivity to blockers. In potassium buffer, it showed a linear I/V-relationship and was selective for potassium. Addition of 10 mM BaCl₂ or CsCl to the K⁺ buffer solution elicits in ~ 50% of the measurements a remarkable steep and voltage depended block.

The new Kcv channel Kcv_{GnLD} was found in a virus from a water sample from Sisimiut lake (Greenland). It is encoded by an interesting hybrid virus, which infects *Chlorella heliozoae*, but also has typical genes, from Pbi *Chlorella* viruses. Also, the channel has higher sequence identity and similar electrophysiological properties to of related channels from the Pbi *Chlorella* viruses. Kcv_{GnLD} shows a typical inactivation at high negative voltages, which is also evident in the channel Kcv_{MT325} from a Pbi *Chlorella* virus. In measurements in HEK293 cells and also in *Xenopus laevis* oocytes Kcv_{MT325} shows this typical inactivation (Gazzarrini *et al.*, 2006). Kcv_{GnLD} is selective for potassium and blocked by barium.

Kcv_{NH} was isolated from a water sample collected from the New Hampshire Winnepesaukee lake. The channel sequence was isolated from the sample by degenerated primers. It can be assigned to a virus which infects a *Chlorella heliozoae* species in the Winnepesaukee lake. The gene product has the highest sequence identity with Kcv_s and exhibits the same electrophysiological behavior as Kcv_s. It is blocked by barium and shows a moderate cesium block. It is selective for potassium over sodium.

In some initial mutation experiments we explored the opportunities, which the library of channel sequences offers for structure/function studies. One example, is an interesting chimera of Kmpv₁, which has only the transmembrane-domains of Kmpv_{SP1}, but shows the selectivity and gating behavior of Kmpv_{SP1}. This underscores the impact of the transmembrane domains on the filter and on gating.

7.2. Introduction

Potassium channels are proteins which transport K⁺ across the cell membranes (Hille, 2001). Potassium channels are highly selective for potassium, which is attributed to the selectivity filter with its highly conserved consensus sequence: TXXTXG/FG (Heginbotham *et al.*, 1994). Phycodnaviruses and most chloroviruses encode small K⁺ channels with homologs in prokaryotes and eukaryotes. In the following we tested the functional features of new channel proteins, which were obtained either from screening water samples or from mining data bases in the internet.

All channels were first analyzed with the structural prediction programs mentioned in the previous chapter 2. All sequences exhibit some structural hallmarks of K⁺ channels (Fig. 6A). They all have the consensus-like sequence of K⁺ channels with a GYG or GFG motif in the selectivity filter (Heginbotham *et al.*, 1994). The second Thr in the consensus sequence is not conserved in all the channels. Four channels have a Ser instead of the typical Thr in the consensus sequence. The same amino acid substitution is also present in the selectivity filter of the viral Kesv channel (Balss *et al.*, 2008). The respective amino acid substitution was examined in previous studies and it was established that the replacement of this canonical Thr with Ser resulted in a reduction in the sensitivity of the channels to Ba²⁺ (Chatelain *et al.*, 2009). For this reason, it was interesting to have a closer look at the Ba²⁺ sensitivity of these channels. The alignment in Fig. 6A shows that also the aromatic amino acids, which are essential for K⁺ channel function, are present in all 8 proteins (Doyle *et al.*, 1998). But the algorithms failed to identify the expected transmembrane domains in some channel sequences from salt water viruses (Fig. 7A). This prediction may indicate that these proteins are not able to intercalate into the membrane and are hence unable to function as ion channel. When the same sequences were analyzed with an algorithm, which predicts α -helixes, the expected folds were identified at the expected positions (Fig. 7b, 10b and 12b).

Because of these ambivalent structural predictions, it was essential to examine the function of the new proteins. All putative channels were therefore expressed in HEK293 cells and their function was tested by whole-cell patch-clamp recordings. The functional characterization included a test of selectivity and sensitivity to a block by barium.

7.3. Results and Discussion- Channels from salt water

7.3.1. Kmpv₁ is a functional potassium channel

To determine, if the new viral proteins from internet mining are functional K⁺ channels, we expressed them in HEK293 cells. The HEK293 cell expression system was successfully used previously to record currents from several other viral K⁺ channels (Braun *et al.*, 2014; Moroni *et al.*, 2002). Fig. 13A reports the typical currents of an untransfected HEK293 cell, which serves as a control. Voltage steps from -160 mV to +80 mV elicit only small currents in these cells. The current/voltage (I/V) relation was typically linear at voltages negative of ca. 0 mV. At more positive voltages a K⁺ outward rectifier contributes to the membrane conductance (Moroni *et al.*, 2002).

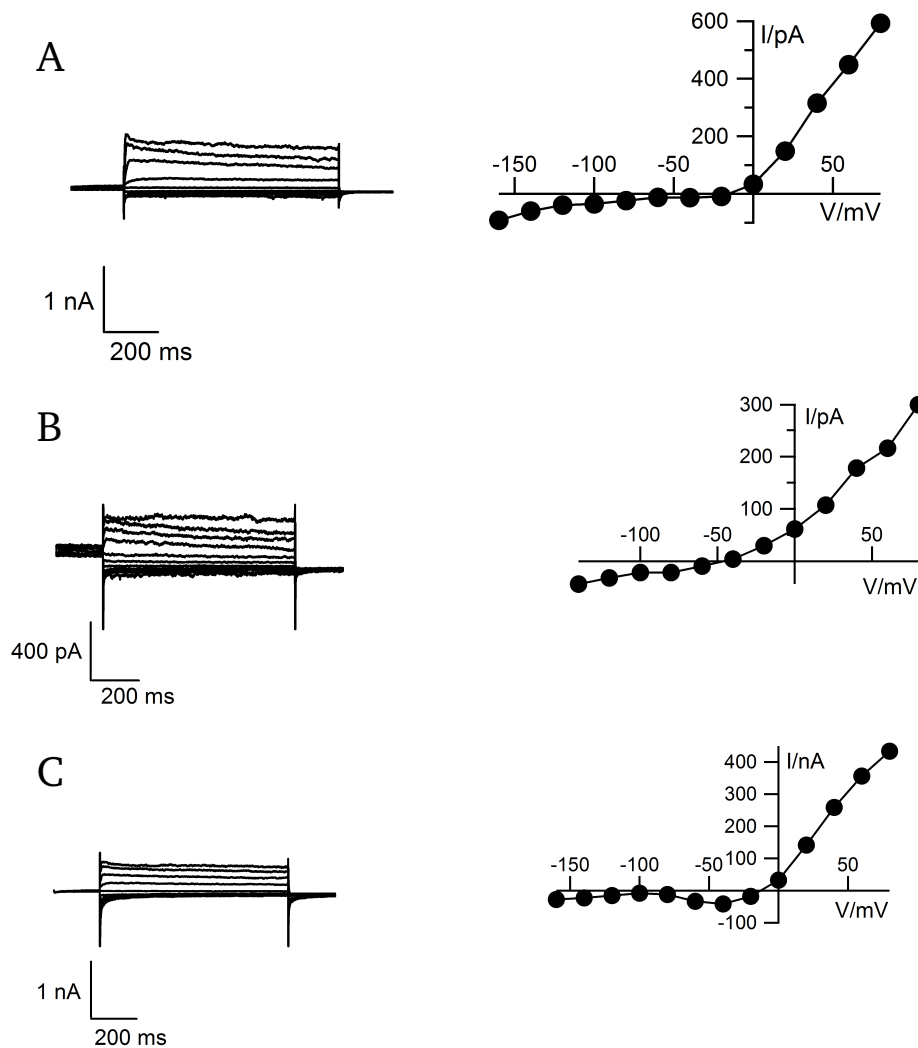


Fig. 13: HEK293 cells show very small endogenous currents. (A) Current responses (left) and I/V relationship (right) of a non-transfected HEK293 cell in 50 mM K⁺ bath solution to voltage steps from holding voltage (0 mV) to test voltages between -160 mV and +80 mV. Same experiments but with 50 mM Na⁺ bath solution (B) or 50 mM K⁺ + 10 mM Ba²⁺ bath solution (C).

Cells expressing a chimera of Kmpv₁ with a C-terminally linked EGFP (Kmpv₁;EGFP) had much larger currents (Fig. 14). The steady state I/V-relation was quasi linear over the tested window of clamp voltages. At a reference voltage of -100 mV, Kmpv₁ expressing cells exhibited a geometrical mean current of -0.7 nA (-0.5 nA; +0.3 nA; n=13). At the same voltage, the untransfected control cells had a geometrical mean current of only -34 pA (-98 pA; +25 pA; n=9). To verify that the channels are selective for K⁺, we performed the same experiments in a buffer in which the extracellular K⁺ was replaced with Na⁺. These cells had a lower inward current and a concomitant left shift of the reversal voltage (Fig. 14B).

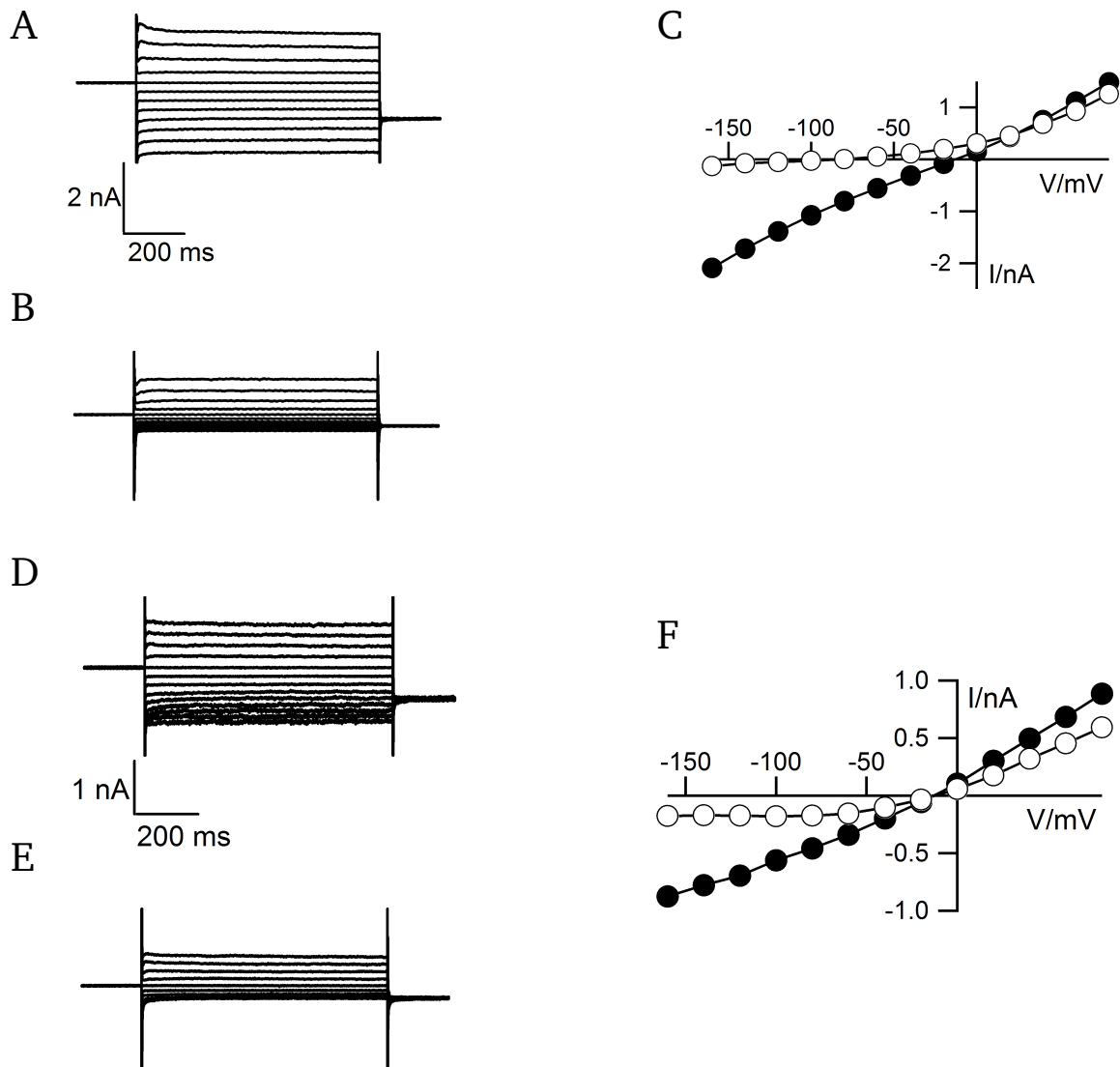


Fig. 14: Expression of Kmpv₁:EGFP generates K⁺ conductance in HEK293 cells. Current responses of a HEK293 cell expressing Kmpv₁:EGFP to voltage steps from holding voltage (0 mV) to test voltages between -160mV and +80 mV. Currents were recorded in buffer with 50 mM K⁺ (A) and 50 mM Na⁺ (B). (C) Corresponding steady state I/V relations from measurements in (A) (closed symbols) and (B) (open symbols). Data in (D) and (E) were measured as in (A) with HEK293 cells expressing Kmpv₁:EGFP. Currents were recorded in buffer with 50 mM K⁺ in the absence (D) and presence of 10 mM BaCl₂ (E). (F) Corresponding steady-state I/V relations from measurements in (D) (closed symbols) and (E) (open symbols).

These results are consistent with the view that Kmpv₁ is a functional and K⁺ selective channel. Having a mean negative shift of the reversal voltage by -53 mV for measurements with either K⁺ (n= 13) or Na⁺ (n= 8) in the bath medium, suggests according to the constant field model (Hille, 2001), that the channel is approximately 10 times more selective for K⁺ than Na⁺. This value is similar to the selectivity of other viral K⁺ channels in the same expression system (Moroni *et al.*, 2002). As a further test of typical K⁺ channel function, currents were recorded in a solution containing 50 mM K⁺, with and without 10

mM Ba^{2+} . A typical recording is shown in Fig. 14D–F. The HEK293 cells expressing $Kmpv_1$ had a large and quasi-linear conductance before Ba^{2+} addition. Addition of the channel blocker to the bath medium resulted in an inhibition of the current. As expected for a voltage-dependent block by Ba^{2+} , the inward current was more blocked than the outward current. It is interesting that this high concentration of Ba^{2+} did not completely inhibit the channel. Under the same conditions, the reference channel Kcv_{PBCV-1} was completely inhibited by Ba^{2+} (Chatelain *et al.*, 2009). As noted above, $Kmpv_1$ has a Ser at residue 44 in the selectivity filter sequence. Since substitution of Thr for Ser in this position lowers the sensitivity of a channel to Ba^{2+} block in other channels (Chatelain *et al.*, 2009), we speculate that the natural occurrence of Ser in this critical position renders the channel less sensitive to Ba^{2+} .

7.3.2. Filter mutant $Kmpv_1$ S43T is not fully blocked by Ba^{2+}

To test the importance of the Ser residues for Ba^{2+} -block, we made mutants of the $Kmpv_1$ channel. At first we changed only the position 43 into a Thr. $Kmpv_1$ S43T is like the wild type still not fully blocked (Fig. 15B).

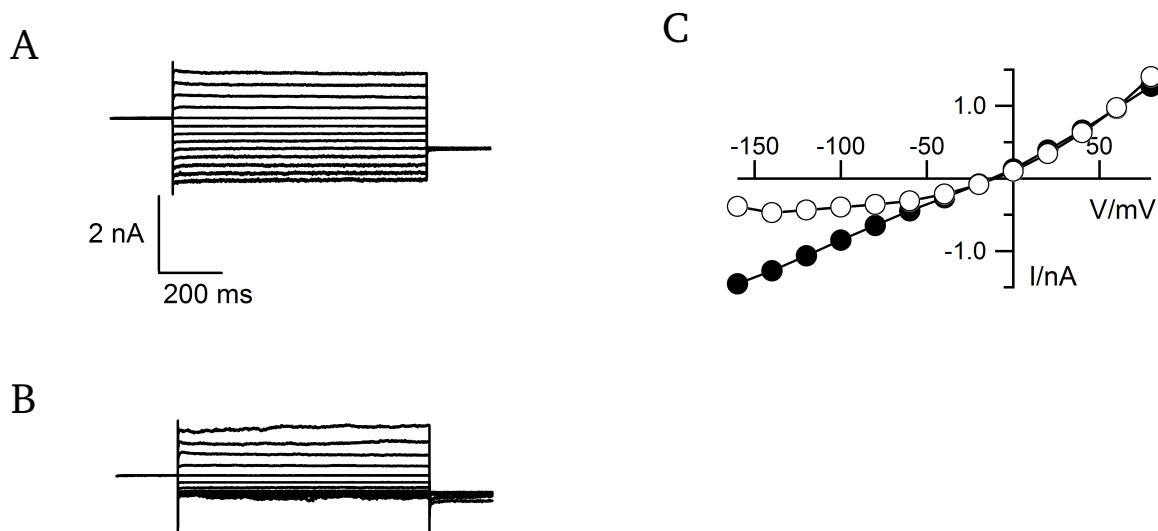


Fig. 15: $Kmpv_1$ S43T is not fully blocked by Ba^{2+} . Current responses of a HEK293 cell expressing $Kmpv_1$:EGFP S43T to voltage steps from holding voltage (0 mV) to test voltages between -160 mV and +80 mV. Currents were recorded in buffer with 50 mM K^+ in the absence (A) and presence of 10 mM $BaCl_2$ (B). (C) Corresponding steady state I/V relations from measurements in (A) (closed symbols) and (B) (open symbols).

$Kmpv_1$ S43T expressing cells showed a geometrical mean current in potassium buffer of -0.6 nA (-0.6 nA; +0.3 nA; n=12) at -100 mV. After addition of 10 mM Ba^{2+} the geometrical mean current was still

-0.2 nA (-0.3 nA; +0.1 nA; n=10) meaning that Ba²⁺ caused only in 57.5% ($\pm 8.5\%$; n=10) inhibition in the mutant. The wildtype Kmpv₁ had under the same conditions a geometrical mean current with 10 mM Ba²⁺ of -0.2 nA (- 0.2 nA; +0.8 nA; n=13). This translates into a block of around 71,3% of the channel by 10 mM Ba²⁺. The results of these experiments show, that one Thr in the filter domain is on the background of the Kmpv₁ channel not alone relevant for the sensitivity of the channel to Ba²⁺.

7.3.3. Filter double-mutant Kmpv₁ S43/44T is fully blocked by Ba²⁺

To further test the functional significance of Ser versus Thr in the filter domain of this channel I created the double mutant Kmpv₁ S43/44T. In this mutant all Ser, which may lower the Ba²⁺ sensitivity of the channel (Chatelain *et al.*, 2009), are mutated into Thr. Kmpv₁ S43/44T expressing cells exhibited in a potassium buffer a geometrical mean current of -0.8 nA (- 1.2 nA; +0.5 nA; n=10) (Fig. 16). With 10 mM Ba²⁺ the mean current was reduced to -38 pA (- 53 pA; +22 pA; n=10).

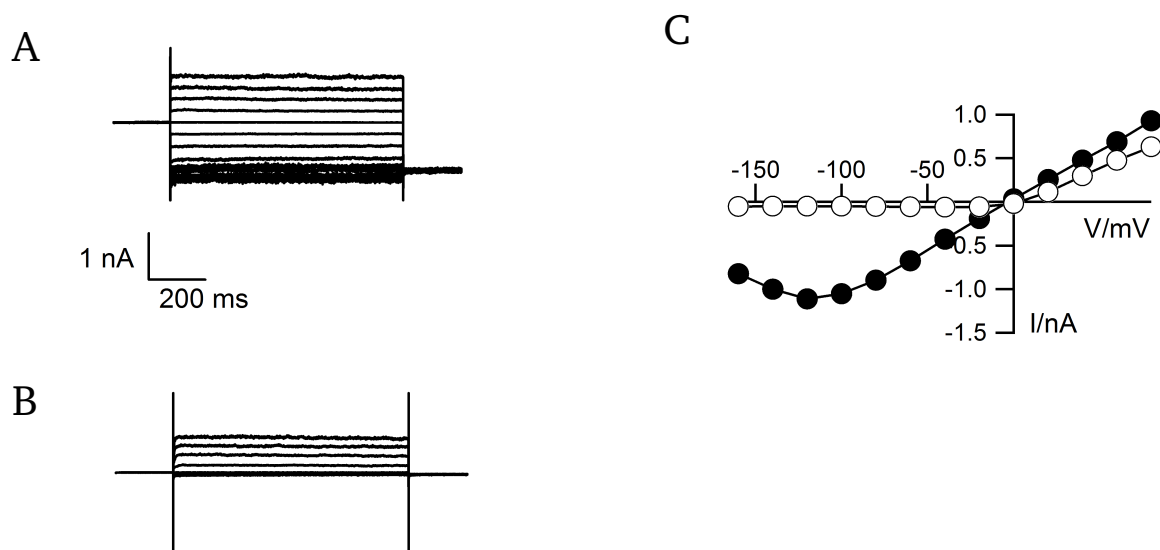


Fig. 16: Kmpv₁:EGFP S43/44T is fully blocked by Ba²⁺. Current responses of a HEK293 cell expressing Kmpv₁:EGFP S43/44T to voltage steps from holding voltage (0 mV) to test voltages between -160 mV and +80 mV. Currents were recorded in buffer with 50 mM K⁺ in the absence (A) and presence of 10 mM BaCl₂ (B). (C) Corresponding steady state I/V relations from measurements in (A) (closed symbols) and (B) (open symbols).

This means that the mutant channel was blocked by 93.8% ($\pm 5\%$; n=10) in the presence of 10 mM Ba²⁺ (Fig. 16 B). In the experiments in 7.3.2 only one Serin (Ser 43) was exchanged by Thr. In this case the experiments showed that 10 mM Ba²⁺ reduced the current by only 57.5% ($\pm 8.5\%$; n=10) under the same conditions. The results of these experiments confirm the relevance of the position 44 in the filter

for the barium block. They also highlight the importance of Thr for a high sensitivity to Ba²⁺ block in the filter of potassium channels.

The functional characterization of this newly discovered channel with its peculiar filter sequence gives a first indication on the opportunities, which are offered by the sampling of channel sequences from the environment or internet mining.

7.3.4. Kbpv₁ is a functional channel

Similar experiments were repeated with Kbpv₁ fused to EGFP (Kbpv₁:EGFP). This protein also generated a significant and quasi-linear increase in membrane conductance in HEK293 cells (Fig. 17A and C). Worth noting is a negative slope conductance of the I/V relation at negative voltages (Fig. 17C). This decrease in conductance at extreme voltages is a typical feature of Kcv type channels (Abenavoli *et al.*, 2009; Arrigoni *et al.*, 2013) and is probably due to a flickering block of the filter (Abenavoli *et al.*, 2009). At a reference voltage of -100 mV, Kbpv₁:EGFP expressing cells had a mean current of 2.9 nA (-3.4 nA; +1.6 nA; n= 8).

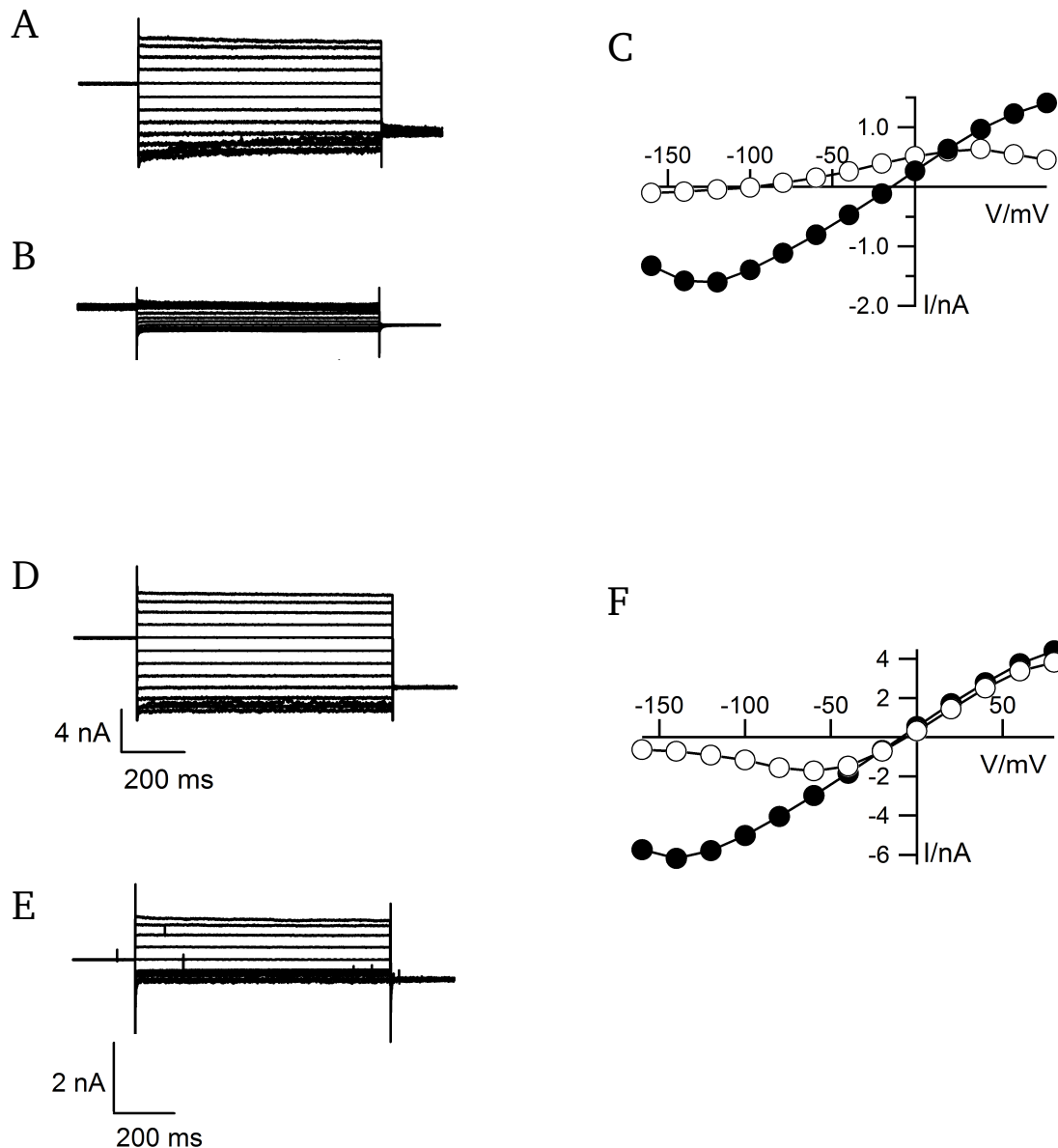


Fig. 17: Expression of Kbpv₁:EGFP creates a specific conductance in HEK293 cells. Current responses of a HEK293 cell expressing Kbpv₁:EGFP to voltage steps from holding voltage (0 mV) to test voltages between -160 mV and +80 mV. Currents were recorded in buffer with 50 mM K⁺ (A) and 50 mM Na⁺ (B). (C) Corresponding steady state I/V relations from measurements in (A) (closed symbols) and (B) (open symbols). Data in (D) and (E) were recorded as in (A) with HEK293 cells expressing Kbpv₁:EGFP. Currents were recorded in buffer with 50 mM K⁺ in the absence (D) and presence of 10 mM BaCl₂ (E). (F) Corresponding steady state I/V relations from measurements in (D) (closed symbols) and (E) (open symbols).

Also, the Kbpv₁ generated conductance is K⁺-selective. Exchange of K⁺ in the external bath solution for Na⁺ caused in the present example a 90 mV left shift of the reversal voltage (Fig. 17B and C). After changing K⁺ for Na⁺ in the bath medium in a total of 5 experiments, a left shift of the reversal potential by -63.5 mV (± 20 mV; n=5) was observed. These results imply an even higher selectivity for K⁺ over Na⁺ than in Kmpv₁. Collectively, these data indicate that Kbpv₁, which contains a K⁺ consensus sequence, generates K⁺ conductance in HEK293 cells. Further experiments established that Ba²⁺ (10mM) also

blocked Kbpv₁ conductance (Fig. 17D and E). Like Kmpv₁, the block was voltage dependent but not complete (Fig. 17 E and F). Ba²⁺ caused at -100 mV a 82 % (±6%; n=3) block of the Kbpv₁ conductance. This result is surprising because Kbpv₁ has a canonical Thr and not a Ser in the critical position in the selectivity filter (Fig. 7A). The results of these experiments indicate that Ba²⁺ sensitivity is not determined by a single amino acid but by additional structural elements in the filter domain.

7.3.5. Kmpv_{12T} shows a characteristic conductance in lipid bilayer

We also tested the potential channel function of the smallest protein, Kmpv_{12T}, by expressing it in HEK293 cells. Unlike in the experiments with Kmpv₁, and Kbpv₁, cells transfected with Kmpv_{12T} rarely exhibited a conductance that was appreciably different from untransfected control cells (Fig. 18/19). At a reference voltage of -100 mV, Kmpv_{12T} expressing cells showed a geometrical mean current of -76 pA (-253 pA; +58 pA; n=6). At the same voltage the untransfected control cells had a geometrical mean current of -34 pA (-98 pA; +25 pA; n=9).

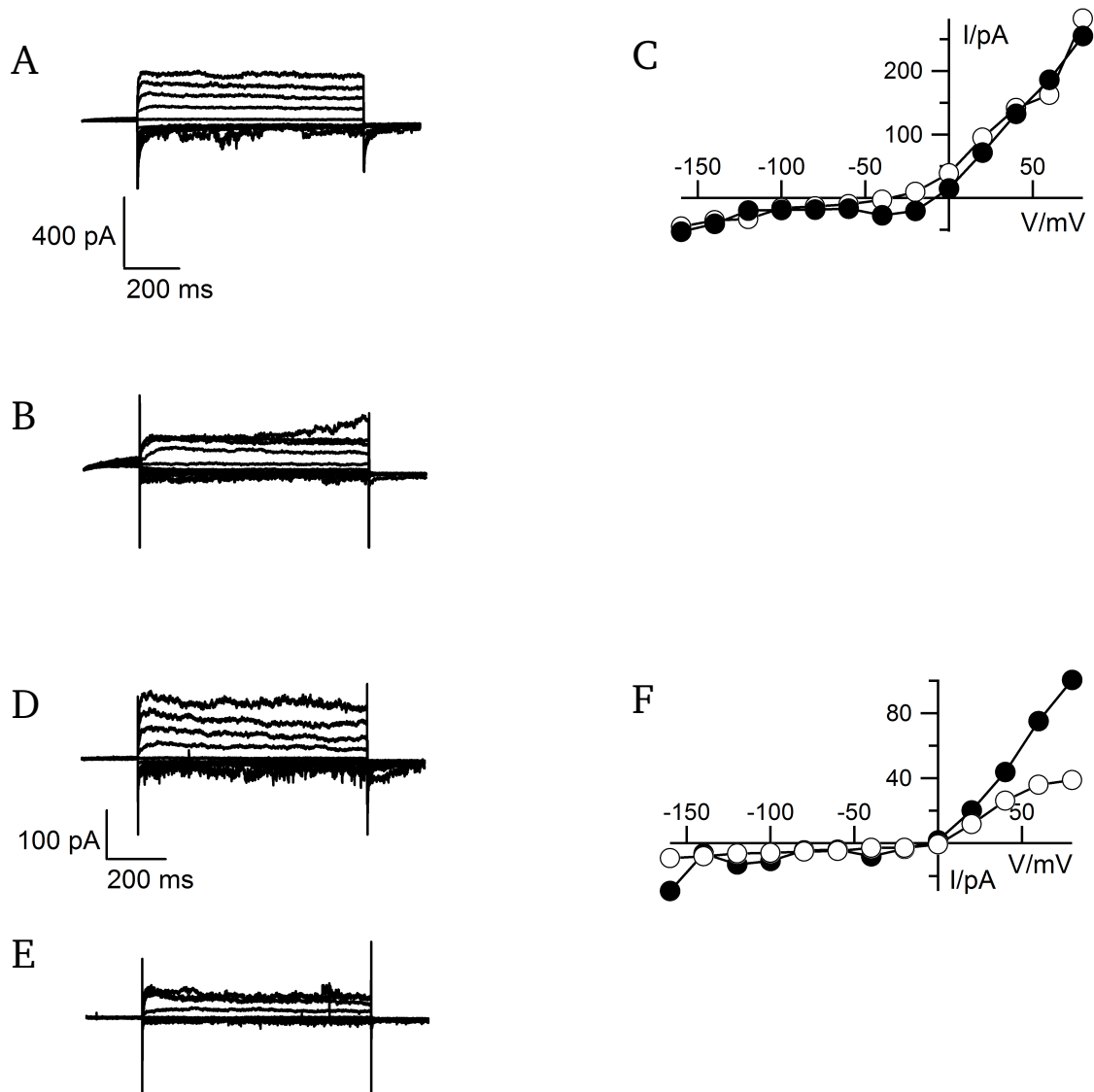


Fig. 18: Expression of Kmpv_{12T}:EGFP shows no specific conductance in HEK293 cells. Current responses of a HEK293 cell expressing Kmpv_{12T}:EGFP to voltage steps from holding voltage (0 mV) to test voltages between -160 mV and +80 mV. Currents were recorded in buffer with 50 mM K⁺ (A) and 50 mM Na⁺ (B). (C) Corresponding steady state I/V relations from measurements in (A) (closed symbols) and (B) (open symbols). Data in (D) and (E) were obtained as in (A) with HEK293 cells expressing Kmpv_{12T}:EGFP. Currents were recorded in buffer with 50 mM K⁺ in the absence (D) and presence of 10 mM BaCl₂ (E). (F) Corresponding steady state I/V relations from measurements in (D) (closed symbols) and (E) (open symbols).

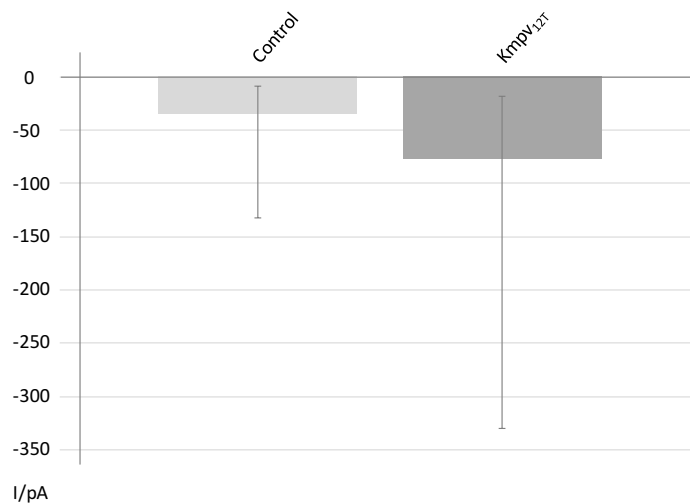


Fig. 19: Expression of Kmpv_{12T}:EGFP shows no specific conductance in HEK293 cells. At a reference voltage of -100 mV, Kmpv_{12T} expressing cells exhibit a geometrical mean current of -76 pA (-253 pA; +58 pA; n=6). At the same voltage, the untransfected control cells have a geometrical mean current of only -34 pA (-98 pA; +25 pA; n=9). Cells transfected with Kmpv_{12T} rarely exhibited a conductance that was significantly different from untransfected control cells.

Since these results were not convincing enough to establish a channel function of Kmpv_{12T}:EGFP, we synthesized the protein *in vitro* and reconstituted it in planar lipid bilayer. This procedure was used previously to measure channel function of small viral proteins (Braun *et al.*, 2014). When the recombinant Kmpv_{12T} protein was tested in a synthetic DPhPC membrane, channel fluctuations were routinely detected (Fig. 20 A and B). These channel fluctuations only occurred after adding the protein, hence the results were not due to contamination or unspecific membrane pores. Channel fluctuations and the corresponding I/V relation for a recording of channel activity in a solution with symmetrical 100 mM KCl are reported in Fig. 20A and B. From the linear slope of the I/V relation we estimate a conductance of 42 pS (n=5). This value is smaller than the viral K⁺ channels studied previously (Braun *et al.*, 2014; Pagliuca *et al.*, 2007). Kmpv_{12T} is highly selective for potassium. With 100 mM KCl in the cis and 100 mM NaCl in the trans chamber it shows a left shift of the I/V relation with no obvious reversal potential. This suggests a very high selectivity of K⁺ over Na⁺ (Fig. 20B)

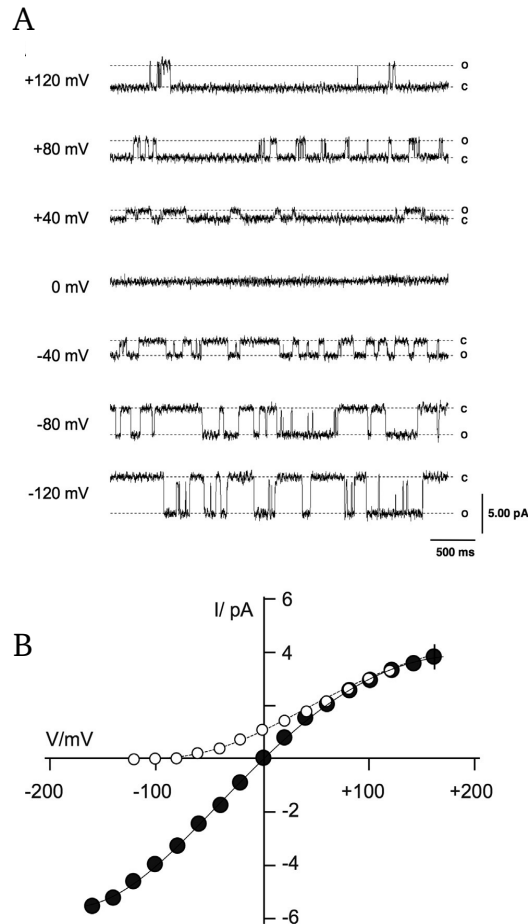


Fig. 20: Kmpv_{12T} protein is a canonical K⁺ channel. Functional reconstitution of Kmpv_{12T} protein results in single channel fluctuations. The open and closed levels of the channel at clamp voltages given on the left are indicated by o and c, respectively. (B) Mean unitary single channel conductance as a function of clamp voltage with 100 mM symmetrical KCl (solid circles) and with 100 mM KCl in cis and 100 mM NaCl in trans chamber (open circles). Data are the means of 5 measurements. Membrane potential are referred to the cis compartment. The protein was added into the trans compartment.

7.3.6. Kmpv_{PL1}:EGFP shows no characteristic conductance in HEK293 cells

As another putative channel protein from a *Micromonas* virus we tested was Kmpv_{PL1}:EGFP. Like the Kmpv_{12T} the conductance rarely differs from the untransfected HEK293 cells (Fig. 22). At a reference voltage of -100 mV, Kmpv_{PL1} expressing cells exhibited a geometrical mean current of -10.1 pA (-22.2 pA; +6.96 pA; n=11). At the same voltage the untransfected control cells had a geometrical mean current of only -34 pA (-98 pA; +25 pA; n=9) (Fig. 22A). Also, sodium ions are not conducted by Kmpv_{PL1} (Fig. 21B). The little left shift of -20 mV (± 12 mV; n=3) is generated by endogenous HEK293 cell channels. Also the current reduction of 57% ($\pm 17\%$; n=3) in the presence of Ba²⁺ in the buffer can be assigned to a block of endogenous channels.

The results of these experiments suggest that Kmpv_{PL1} generates no functional channel in the plasma membrane of HEK293 cells. This was surprising, because the protein has a high degree of sequence identity to Kmpv_{SP1}.

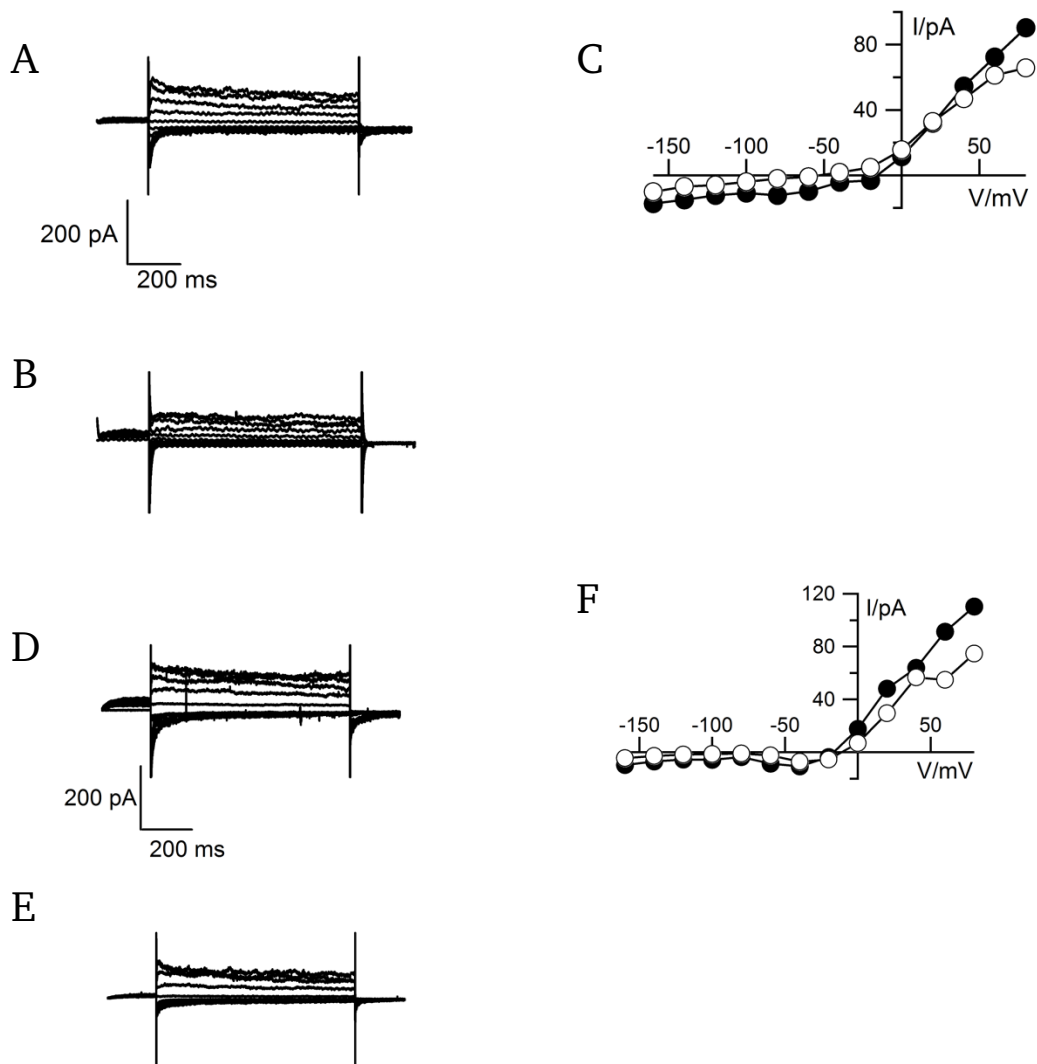


Fig. 21: Expression of $Kmpv_{PL1}:EGFP$ shows no specific conductance in HEK293 cells. Current responses of a HEK293 cell expressing $Kmpv_{PL1}:EGFP$ to voltage steps from holding voltage (0 mV) to test voltages between -160 mV and +80 mV. Currents were recorded in buffer with 50 mM K^+ (A) and 50 mM Na^+ (B). (C) Corresponding steady state I/V relations from measurements in (A) (closed symbols) and (B) (open symbols). Data in (D) and (E) were measured as in (A) with HEK293 cells expressing $Kmpv_{PL1}:EGFP$. Currents were recorded in buffer with 50 mM K^+ in the absence (D) and presence of 10 mM $BaCl_2$ (E). (F) Corresponding steady state I/V relations from measurements in (D) (closed symbols) and (E) (open symbols).

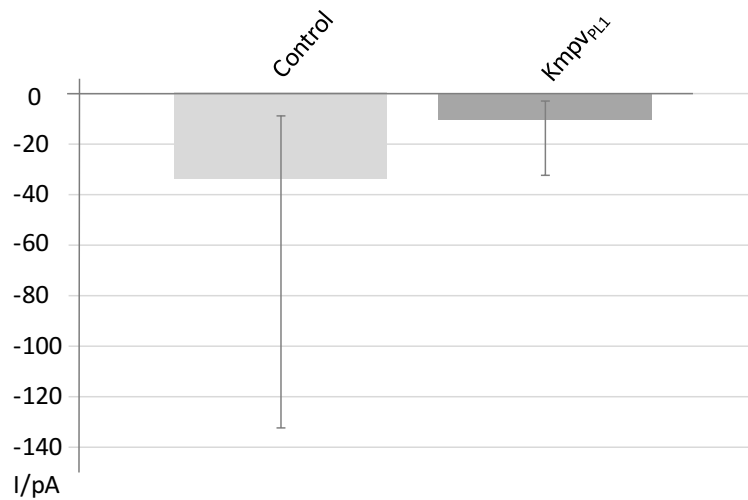


Fig. 22: Expression of Kmpv_{PL1}:EGFP shows no specific conductance in HEK293 cells. At a reference voltage of -100 mV, Kmpv_{PL1} expressing cells exhibit a geometrical mean current of -10.1 pA (-22.2 pA; +6.96 pA; n=11). At the same voltage the untransfected control cells have a geometrical mean current of only -34 pA (-98 pA; +25 pA; n=9). Cells transfected with Kmpv_{PL1} rarely exhibited a conductance that was significantly different from untransfected control cells.

7.3.7. Kmpv_{SP1} is an inward rectifying cationic channel

Cells expressing Kmpv_{SP1}:EGFP had much larger currents (Fig. 23) than the untransfected control HEK293 cells (Fig. 13). The steady state I/V relationship and the current response (Fig. 23A and C) showed a large inward current of K⁺ ions and nearly no outward current. At a reference voltage of -100 mV, Kmpv_{SP1} expressing cells exhibit a geometrical mean current of -0.8 nA (-0.8 nA; +0.4; n=25). At the same voltage the untransfected control cells had a geometrical mean current of only -34 pA (-98 pA; +25 pA; n=9). To test whether the channels are selective for K⁺, we performed the same experiments as in Fig. 17A and B in a buffer where extracellular K⁺ was replaced by Na⁺. In a Na⁺ containing buffer the cells had a lower inward current and a concomitant left shift of the reversal voltage (Fig. 23A and B). By changing K⁺ for Na⁺ in the buffer the reversal voltage shifted negative by -58.8 mV (± 22 mV; n=3). From the shift of the reversal voltage we can estimate that Kmpv_{SP1} is 10 times more selective for K⁺ than for Na⁺.

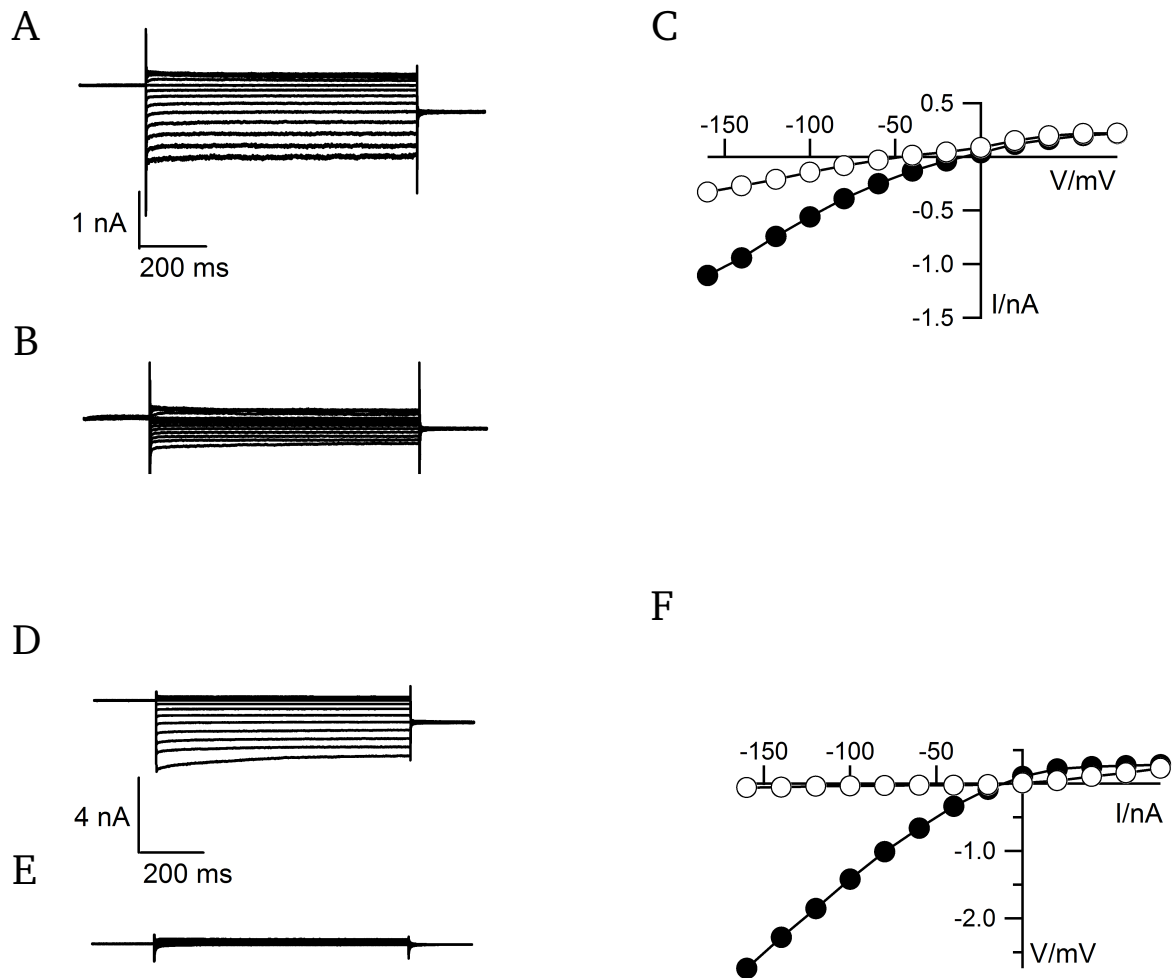


Fig. 23: Expression of $Kmpv_{SP1}:EGFP$ generates K^+ conductance in HEK293 cells. Current responses of a HEK293 cell expressing $Kmpv_{SP1}:EGFP$ to voltage steps from holding voltage (0 mV) to test voltages between -160 mV and +80 mV. Currents were recorded in buffer with 50 mM K^+ (A) and 50 mM Na^+ (B). (C) Corresponding steady state I/V relations from measurements in (A) (closed symbols) and (B) (open symbols). Data in (D) and (E) measured as in (A) with HEK293 cells expressing $Kmpv_{SP1}:EGFP$. Currents were recorded in buffer with 50 mM K^+ in the absence (D) and presence of 10 mM $BaCl_2$ (E). (F) Corresponding steady state I/V relations from measurements in (D) (closed symbols) and (E) (open symbols).

It is important to note that the I/V relation of the $Kmpv_{SP1}$ channel in a Na^+ buffer is different from all the other channels. Even though the reversal voltage shifts negative, indicating a low selectivity of the channel for Na^+ , $Kmpv_{SP1}$ still generates a substantial inward current. At the reference voltage of -100 mV we measured in a Na^+ buffer a geometrical mean current of -0.04 nA (-0.04 nA; +0.02 nA; n=15). This inward current in a Na^+ solution was much higher than in other channels (e.g. Fig. 14C). Worth noting is also that the Na^+ inward current exhibits the same rectification properties of the K^+ current. (Fig. 23B). With these features $Kmpv_{SP1}$ shows functional properties, which are not explained by the constant field theory (Hille, 2001). The data suggest that the channel is more permeable to K^+ than to

Na⁺, but still allows Na⁺ inward current in a voltage dependent manner. The mechanism, which is underlying this process is not known and not investigated further here.

Like the other channels also Kmpv_{SP1} was measured in the absence and presence of 10 mM Ba²⁺. The data in Fig. 23E show that the Kmpv_{SP1} generated conductance is blocked by 93.4% (± 5 %; n=3) by 10 mM Ba²⁺ in the medium (Fig. 23E).

To get more information on this interesting channel and the unique inward rectification we synthesized the protein in vitro and reconstituted it in planar lipid bilayers. The Kmpv_{SP1} protein was tested in a synthetic DPhPC membrane with a symmetrical solution of 100 mM KCl (Fig. 23A).

The data in Fig. 23 show some typical single channel fluctuations from bilayer measurements. Channel openings can only be seen at negative voltages. This underscores an inherent inward rectification of the channel. The channel has at negative voltages a high open probability. The current trace recorded at -160 mV shows that channel flickers rapidly between a closed and an open state. Longer closed times are visited only rarely.

The channel protein showed at a reference voltage of -160 mV a mean current of -8.0 pA (± 0.4 pA; n=3) and at +160 mV a mean current of -0.3 pA (± 0.03 pA; n=3). Thus, the inward rectifier characteristics of Kmpv_{SP1} could be confirmed by the bilayer measurements. All the well-known viral potassium channels like Kcv_{PBCV-1}, Kcv_{ATCV-1} or Kcv_{MT325} (Gazzarrini *et al.*, 2009; Gazzarrini *et al.*, 2006; Kang *et al.*, 2004) do not show such a rectification. Even the other *Micromonas* virus channels do not show a comparable behavior. Kmpv_{PL1} has the highest similarity to Kmpv_{SP1}, both channels differ in only 21 aa (Fig. 7). Unfortunately, we have no useful electrophysiological data of Kmpv_{PL1} to compare the two channels. (Fig. 21).

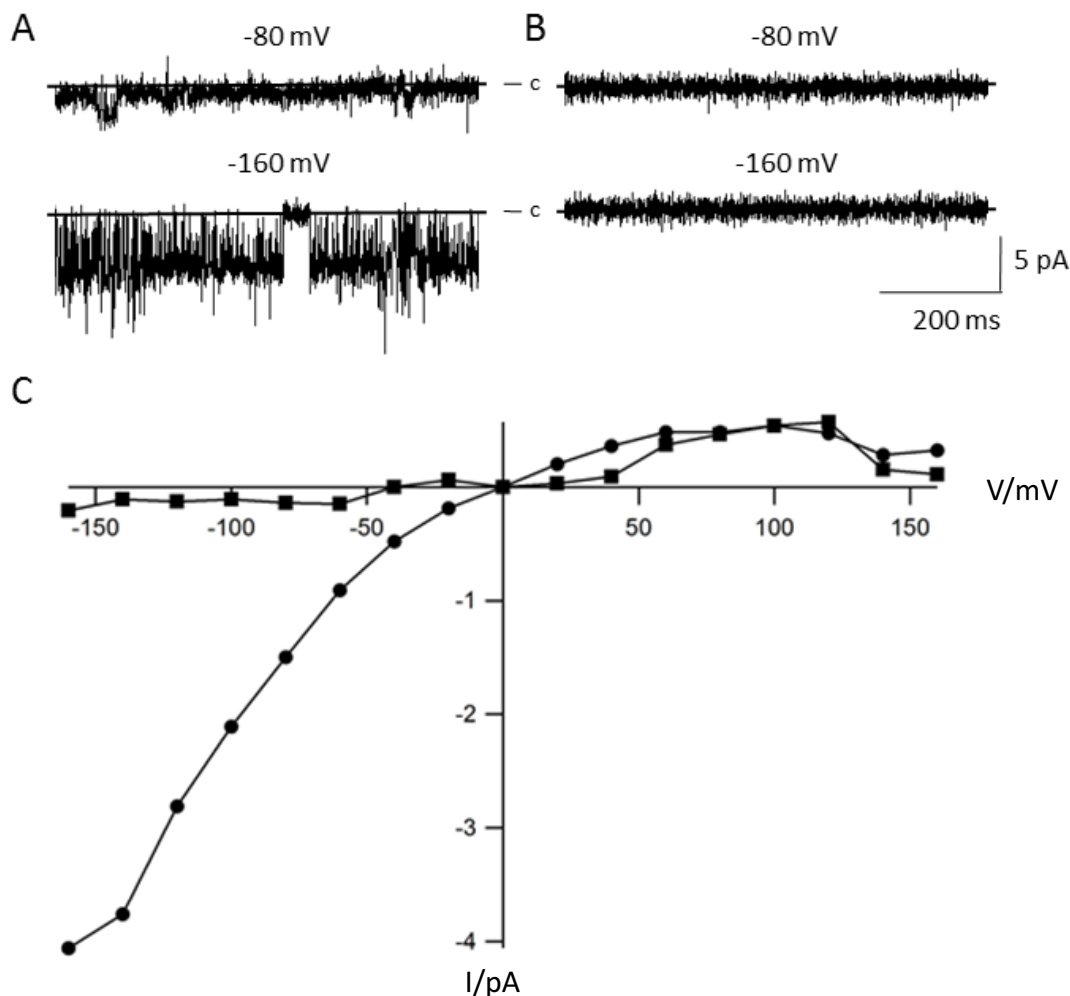


Fig. 24: Kmpv_{SP1} protein is a canonical K⁺ channel. (A) Functional reconstitution of Kmpv_{SP1} Protein results in single channel fluctuations. The closed levels of the channel are indicated by c. (B) A final concentration of 1 mM Ba²⁺ in a 100 mM K⁺ solution leads to a block of the channel current. (C) single channel conductance as a function of clamp voltage in solution with 100 mM symmetrical KCl (solid circles). Membrane potential are referred to the cis compartment. The protein was added into the *trans* compartment.

It has been mentioned before that the channel is vividly flickering at negative voltages. At these voltages, the channel is open most of the time (Fig. 24). To test if these noisy current traces are indeed generated by an active channel, the channel blocker Ba²⁺ was added at 1 mM to the bath medium on the trans side of the channel. This resulted in a robust block of the flickering currents (Fig. 24). The I/V relation of the channel taken in the absence and presence of Ba²⁺ recapitulate the experimental results obtained in HEK293 cells (compare Fig. 24C and 23F). In both cases Ba²⁺ caused an efficient block of Kmpv_{SP1} generated currents.

7.3.8. Kmpv_{SP1} S53F shows the same electrophysiological behavior as the wildtype

Kmpv₁ and Kmpv_{SP1} have a high sequence similarity (Fig. 8). Kmpv_{SP1} is only 7 amino acids longer than Kmpv₁ and they differ in only a few amino acids (Chapter 3). Both channels showed a potassium conductance, but Kmpv_{SP1} is not selective for potassium and it exhibits an inherent inward rectification.

Because of the functional differences between the two channels we had a closer look at the alignments of the various other viral potassium channels to identify special amino acids in the sequence of Kmpv_{SP1}. At first we concentrated on the filter region. The probability is high that the amino acids around the filter have an important impact on the role for the electrophysiological properties of the channels. It was conspicuous that Kmpv_{SP1} has a serin at the position 53. All other channels (Fig. 8) have a phenylalanin, leucin oder isoleucin at the respective position.

However, the mutant Kmpv_{SP1} S53F showed the same specific conductance like the wild-type channel (Fig. 25). Most importantly the mutant also exhibited a strong inward rectification. At a reference voltage of -100 mV, Kmpv_{SP1} S53F expressing cells exhibited a geometrical mean current of -0.6 nA (-0.3 nA; +0.2 nA; n=7). At the same voltage, the untransfected control cells had a geometrical mean current of only -34 pA (-98 pA; +25 pA; n=9). The wildtype Kmpv_{SP1} had a geometrical mean current of -0.75 nA (-0.81 nA; +0.4 nA; n=29).

A close inspection of the I/V relations further showed that the mutant also exhibited the non-canonical Na⁺ conductance. The I/V-relation was left shifted after replacing K⁺ for Na⁺, but the cells still showed a substantial inward Na⁺ current. At the reference voltage of -100 mV we had a geometrical mean current of -0.03 nA (-0.03 nA; +0.01 nA; n=4).

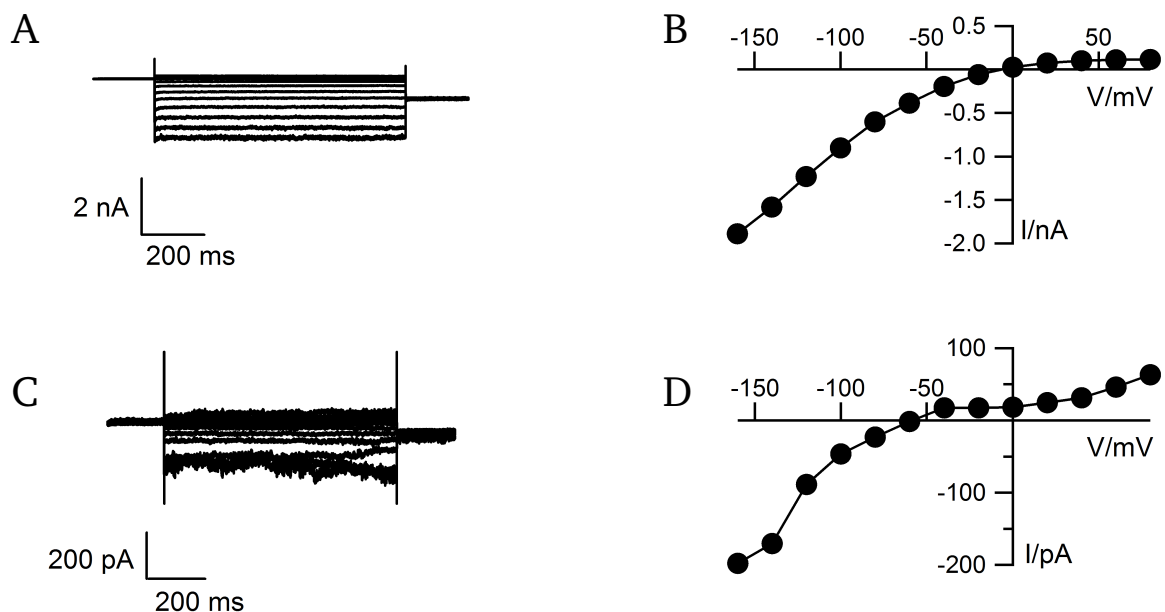


Fig. 25: Expression of Kmpv_{SP1}:EGFP S53F shows the same specific conductance in HEK293 cells as the wildtype. Current responses of a HEK293 cell expressing Kmpv_{SP1}:EGFP S53F to voltage steps from holding voltage (0 mV) to test voltages between -160 mV and +80 mV. Currents were recorded in buffer with 50 mM K⁺ (A) and 50 mM Na⁺ (C). (B) Corresponding steady state I/V relations from measurements in (A). (D) Corresponding steady state I/V relations from measurements in (C).

7.3.9. The transmembrane domains affect the selectivity of the chimera $Kmpv_{SP1}/loop\ Kmpv_1$

The functional properties of the mutant $Kmpv_{SP1}\ S53F$ are barely distinguishable from those of $Kmpv_{SP1}$. Thus, the question is why $Kmpv_1$ and $Kmpv_{SP1}$ have different electrophysiological properties. The filter is well known for his selectivity function (Heginbotham *et al.*, 1994), so we made a chimera of the filter from the selective channel $Kmpv_1$ and the TMD of $Kmpv_{SP1}$. We suspected that the chimera might function like $Kmpv_1$. A test of the chimera showed that it was active. This implies that the TMDs can be exchanged between channels without compromising function. A closer scrutiny of the chimera showed that its functions are like $Kmpv_{SP1}$. It exhibited a pronounced inward rectification and showed an appreciable Na^+ inward current. The important results of these experiments are that the TMDs affect the selectivity of the channel and gating (Fig. 26).

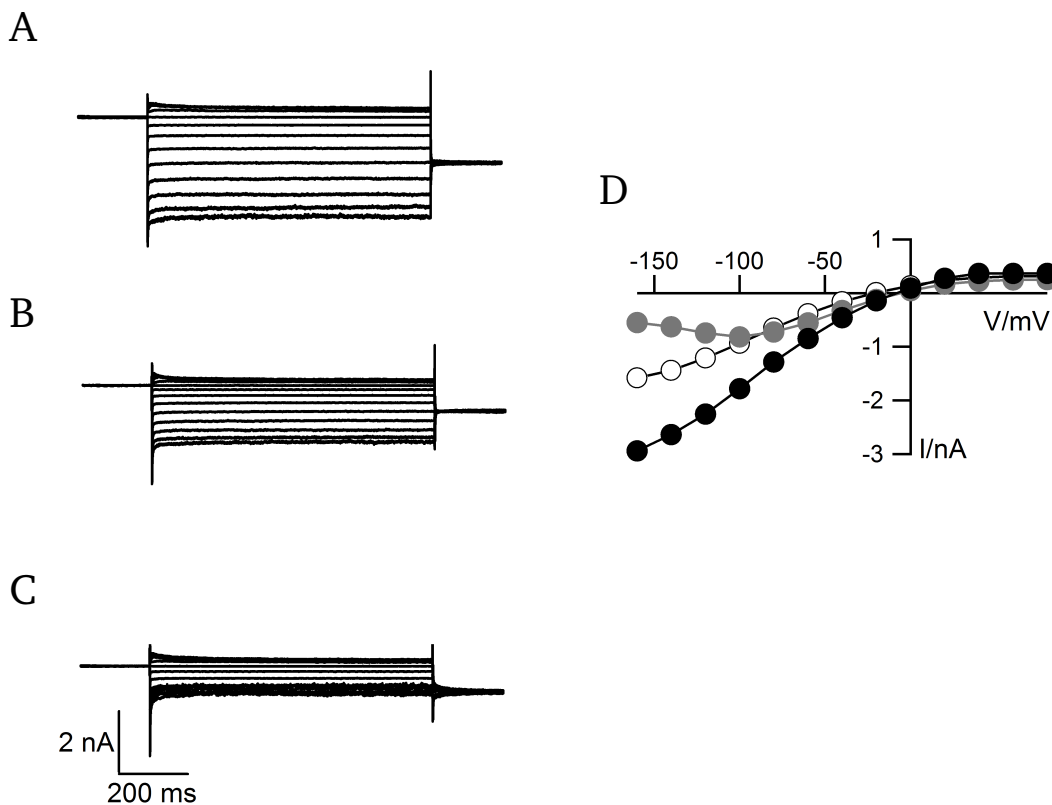


Fig. 26: Expression of the $Kmpv_{SP1}$:EGFP chimera shows the same specific conductance in HEK293 cells as the wildtype. Current responses of a HEK293 cell expressing $Kmpv_{SP1}$:EGFP chimera to voltage steps from holding voltage (0 mV) to test voltages between -160 mV and +80 mV. Currents were recorded in buffer with 50 mM K^+ (A) and 50 mM Na^+ (B). (C) Currents were recorded in buffer with 50 mM K^+ in the presence of 10 mM $BaCl_2$. (D) Corresponding steady state I/V relations from measurements in (A) (closed symbols), (B) (open symbols) and (C) (grey symbols).

At a reference voltage of -100 mV, the chimera expressing cells exhibited a geometrical mean current of -0.8 nA (-0.5 nA; +0.3 nA; n=9). At the same voltage, the untransfected control cells had a geometrical

mean current of only -34 pA (-98 pA; +25 pA; n=9). The wildtype Kmpv_{SP1} had a geometrical mean current of -0.75 nA (-0.81 nA; +0.4 nA; n=29). The mutant also showed an appreciable sodium inward conductance. At the reference voltage of -100 mV we had a geometrical mean current of -0.06 nA (-0.3 nA; +0.05 nA; n=14). The results from these experiments are very interesting. The general view in the literature is that selectivity and gating are mostly determined by the selectivity of a channel. The present results in contrast underscore that this is not necessarily the case.

The crystal structures of K⁺ channels show clearly that the ions are transported through the selectivity filter and this domain prefers the transport of K⁺ over Na⁺. On the basis of these structural data the influence of the TMD on selectivity and gating can only be an indirect one. A similar importance of the TMDs on channel function was already demonstrated in previous studies. In this case it was found that the transmembrane domains of a Kcv channel have an impact on Cs⁺ selectivity and therefore an indirect influence on the filter (Greiner, 2011; Kang *et al.*, 2004). It is reasonable to assume that the transmembrane domains have an overall impact on the location of the total protein in the membrane and define in this way the behavior of the protein.

7.3.10. Kolv₄ show no characteristic conductance by over expression in HEK 293 cells

Two other putative channel proteins were obtained from *Ostreococcus* viruses. HEK293 cells expressing Kolv₄:EGFP rarely exhibited a conductance, which was different from that of untransfected HEK293 cells (Fig. 13). The recordings in these cells were similar to those expressing Kmpv_{12T} and Kmpv_{PL1}.

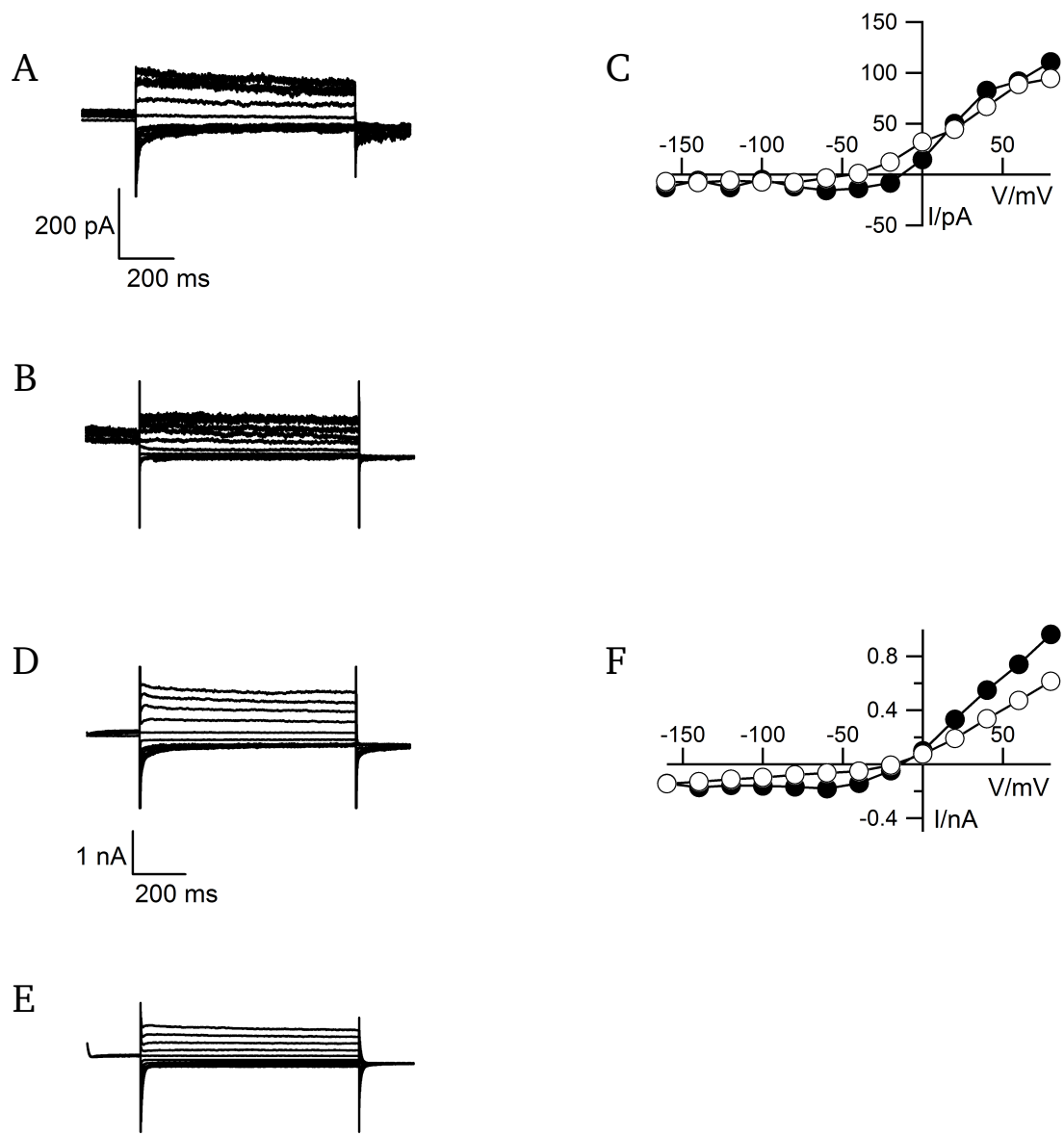


Fig. 27: Expression of Kolv₄:EGFP shows no specific conductance in HEK293 cells. Current responses of a HEK293 cell expressing Kolv₄:EGFP to voltage steps from holding voltage (0 mV) to test voltages between -160 mV and +80 mV. Currents were recorded in buffer with 50 mM K⁺ (A) and 50 mM Na⁺ (B). (C) Corresponding steady state I/V relations from measurements in (A) (closed symbols) and (B) (open symbols). Data in (D) and (E) were measured as in A with HEK293 cells expressing Kolv₄:EGFP. Currents were recorded in buffer with 50 mM K⁺ in the absence (D) and presence of 10 mM BaCl₂ (E). (F) Corresponding steady state I/V relations from measurements in (D) (closed symbols) and (E) (open symbols).

At a reference voltage of -100 mV, Kolv₄ expressing cells exhibited a geometrical mean current of -51.9 pA (-273 pA; +43.6 pA; n=11). At the same voltage, the untransfected control cells had a geometrical mean current of only -34 pA (-98 pA; +25 pA; n=9) (Fig. 13). The putative channel also does not conduct sodium (Fig. 27B). The little left shift of the reversal voltage by -19.3 mV (\pm 5.6 mV; n=3) is likely due to the endogenous potassium channels in HEK293 cells. Also the little reduction of -48,3% (\pm

29%; n=6) of the currents measured with Ba²⁺ in the buffer can be explained by an inhibition of endogenous potassium channels.

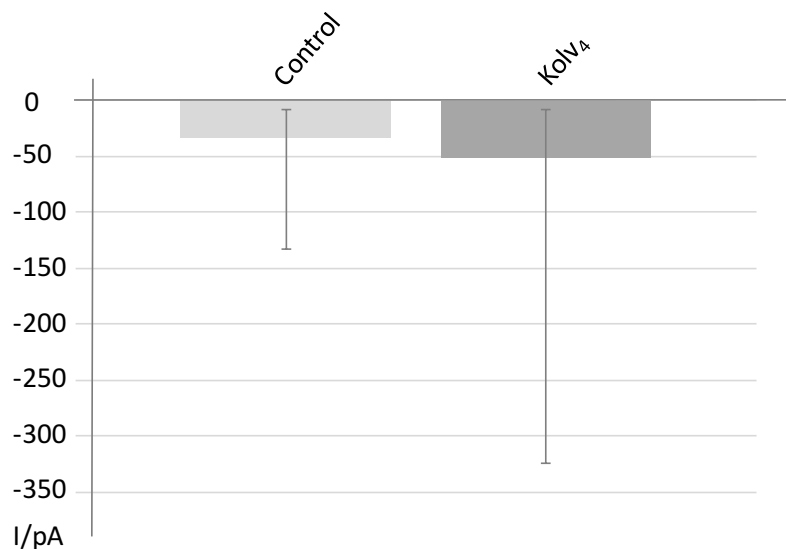


Fig. 28: Expression of KolV₄:EGFP shows no specific conductance in HEK293 cells. At a reference voltage of -100 mV, Kmpv_{PL1} expressing cells exhibit a geometrical mean current of -51.9 pA (-273 pA; +43.6 pA; n=11). At the same voltage the untransfected control cells have a geometrical mean current of only -34 pA (-98 pA; +25 pA; n=9). Cells transfected with Kmpv_{12T} rarely exhibited a conductance that was significantly different from non-transfected control cells.

7.3.11. Kotv_{RT} is a functional potassium channel which shows a fast and voltage depended barium and cesium block

Another putative channel protein, Kotv_{RT}, was found in the genome of an *Ostreococcus* virus. One special property of cells expressing the Kotv_{RT} protein was that we were not able to achieve the whole-cell configuration after reaching the giga-seal. All cells bursted, no matter how careful the suction was applied to the patch pipette. We reasoned that the Kotv_{RT}:EGFP protein might be well expressed in the cells and that a large conductance might stress the cells and promote instable membranes. To overcome this obstacle, cells were sealed in a buffer with 10 mM Ba²⁺. Under these circumstances it was possible to obtain good seals and to achieve the whole cell configuration. All measurements with cells expressing Kotv_{RT} were therefore first bathed in barium, before exchanging the external bath solution for subsequent experiments.

The recordings performed in the aforementioned manner showed that Kotv_{RT} generates a conductance in HEK293 cells, which is much larger than that of non-transfected control cells. At a reference voltage

of -100 mV, $Kotv_{RT}:EGFP$ expressing cells exhibited a geometrical mean current of -4.6 nA (-9.5 nA; +3.1 nA; n=9). At the same voltage, the untransfected control cells had a geometrical mean current of only -34 pA (-98 pA; +25 pA; n=9). To verify that the channel is selective for K^+ , we performed the same experiments as in Fig. 27 where the extracellular K^+ was replaced by Na^+ . But in a Na^+ containing buffer cells exhibited a lower inward current and a left shift of the reversal voltage by -48.4 mV (± 31 mV; n=7) (Fig. 29B and C). The mean reversal potential of $Kotv_{RT}$ with sodium buffer was 66.4 mV (± 27.8 mV; n=8). The results of these experiments imply that $Kotv_{RT}$ is more than 10 time more selective for K^+ than for Na^+ .

$Kotv_{RT}$ is blocked by Ba^{2+} in an unusual manner (Fig. 29 E). Addition of the blocker to the external solution elicits a steep voltage-dependent block of the $Kotv_{RT}$ conductance. A similar behavior was only known from Kcv_{NTS} with 10 mM Cs^+ in the buffer (Greiner, 2011). At 100 mV Ba^{2+} generated a mean reduction of the $Kotv_{RT}$ current by 95.1% ($\pm 4.5\%$; n=5). The steep voltage dependent block of $Kotv_{RT}$ currents was observed in 6 out of 13 measurements. In the remaining recordings, the channel was completely blocked at negative voltages.

Also the addition of 10 mM Cs^+ to the external K^+ buffer evoked a similar steep voltage-dependent block of the $Kotv_{RT}$ current (Fig. 29H). At 100 mV cesium causes a mean reduction of the $Kotv_{RT}$ current by 33.5% ($\pm 25.2\%$; n=8). The steep voltage-dependent block was observed in 50% (n=8) of the measurements.

The mechanism, which is underlying the steep block by Ba^{2+} or Cs^+ is not known. One possibility is that the voltage dependency of this process is indeed very steep. We can at this point however not exclude an artifact of the clamp amplifier as source of this phenomenon. It is possible that the amplifier starts to oscillate and shuts down the clamp under some extreme conditions when it is difficult to clamp the correct voltage.

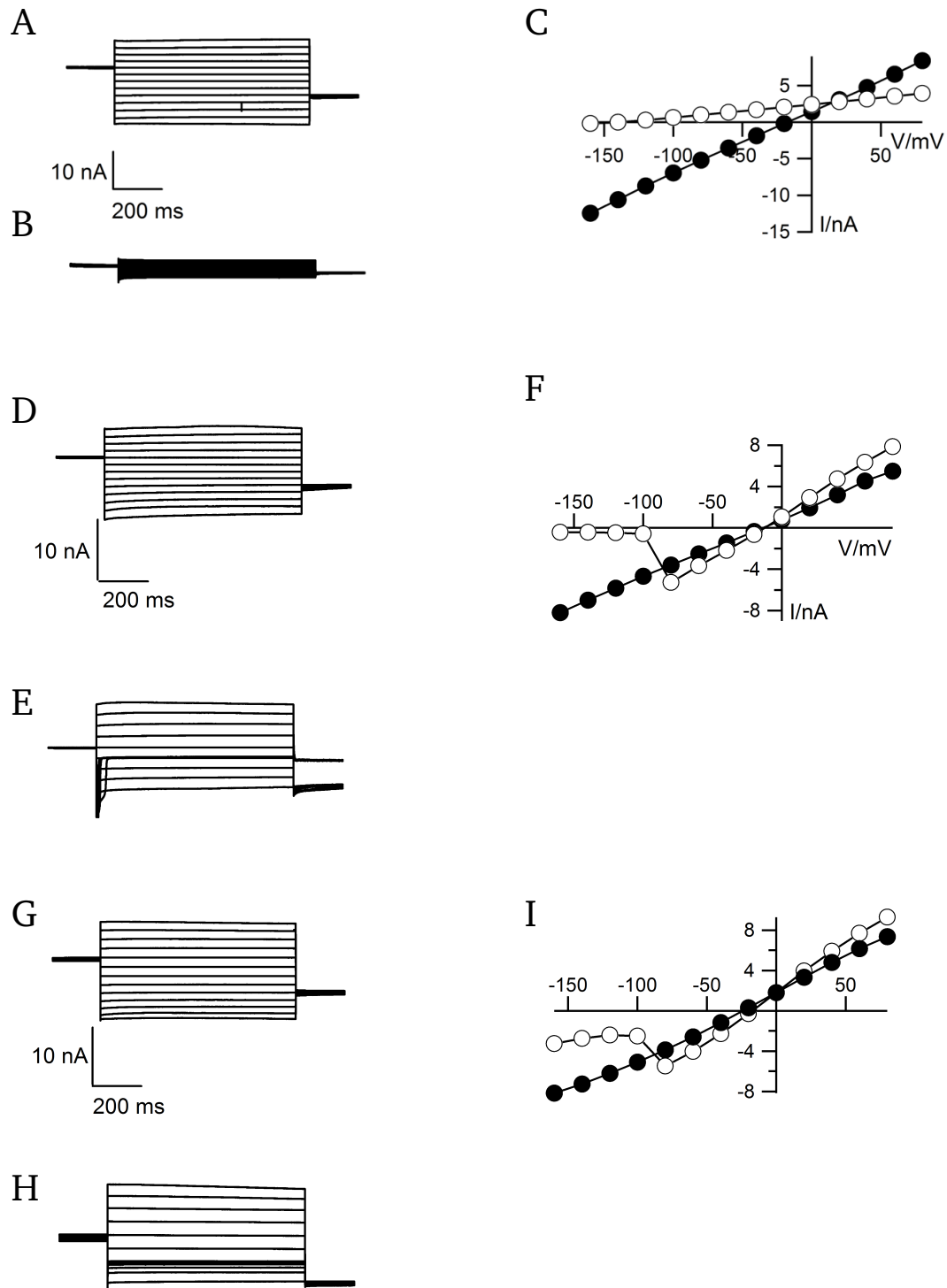


Fig. 29: Expression of $Kotv_{RT}$ -EGFP generates K^+ conductance in HEK293 cells. Current responses of a HEK293 cell expressing $Kotv_{RT}$ -EGFP to voltage steps from holding voltage (0 mV) to test voltages between -160 mV and +80 mV. Currents were recorded in buffer with 50 mM K^+ (A) and 50 mM Na^+ (B). (C) Corresponding steady state I/V relations from measurements in (A) (closed symbols) and (B) (open symbols). Data in (D) and (E) were measured as in (A) with HEK293 cells expressing $Kotv_{RT}$ -EGFP. Currents were recorded in buffer with 50 mM K^+ in the absence (D) and presence of 10 mM $BaCl_2$ (E). (F) Corresponding steady state I/V relations from measurements in (D) (closed symbols) and (E) (open symbols). Currents were recorded in buffer with 50 mM K^+ in the absence (G) and presence of 10 mM $CsCl$ (H). (I) Corresponding steady state I/V relations from measurements in (G) (closed symbols) and (H) (open symbols).

7.3.12. Kolpv₂ shows no characteristic conductance when expressed in HEK293 cells

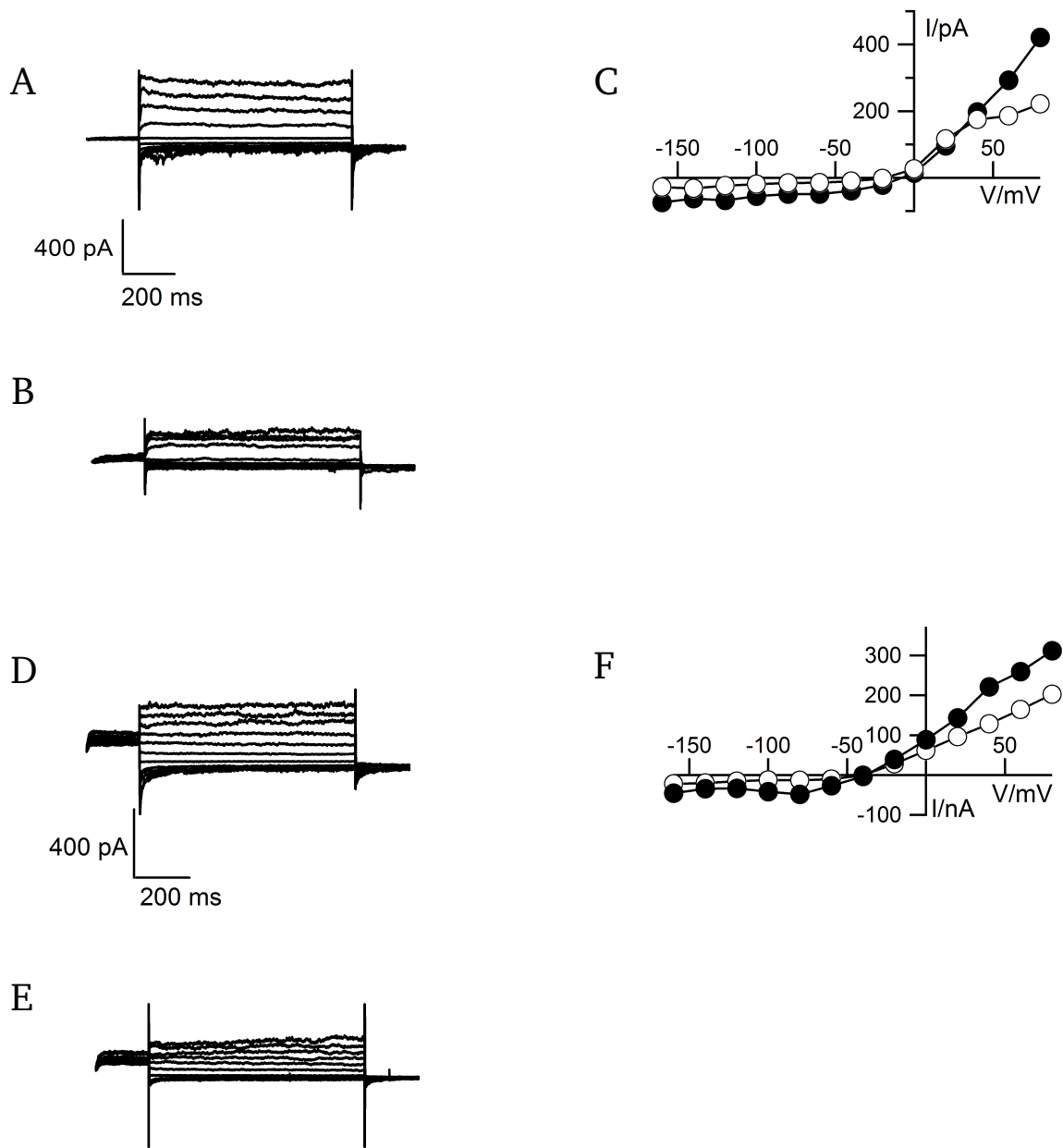


Fig. 30: Expression of Kolpv₂:EGFP shows no specific conductance in HEK293 cells. Current responses of a HEK293 cell expressing Kolpv₂:EGFP to voltage steps from holding voltage (0 mV) to test voltages between -160 mV and +80 mV. Currents were recorded in buffer with 50 mM K⁺ (A) and 50 mM Na⁺ (B). (C) Corresponding steady state I/V relations from measurements in (A) (closed symbols) and (B) (open symbols). Data in (D) and (E) measured as in (A) with HEK293 cells expressing Kolpv₂:EGFP. Currents were recorded in buffer with 50 mM K⁺ in the absence (D) and presence of 10 mM BaCl₂ (E). (F) Corresponding steady state I/V relations from measurements in (D) (closed symbols) and (E) (open symbols).

Cells expressing Kolpv₂ rarely showed a conductance, which exceeds that of untransfected HEK293 cells (Fig. 31). At a reference voltage of -100 mV, Kolpv₂ expressing cells exhibited a geometrical mean current

of -40.9 pA (-36.8 pA; +19.4 pA; n=10). At the same voltage the untransfected control cells had a geometrical mean current of -34 pA (-98 pA; +25 pA; n=9). It also did not conduct sodium (Fig. 30E). The little left shift of -34,4 mV (± 8.9 mV; n=6) is set of from the endogenous HEK293 cells potassium channels. Also the little reduction of the currents with Ba²⁺ in the buffer likely belongs to the endogenous potassium channels.

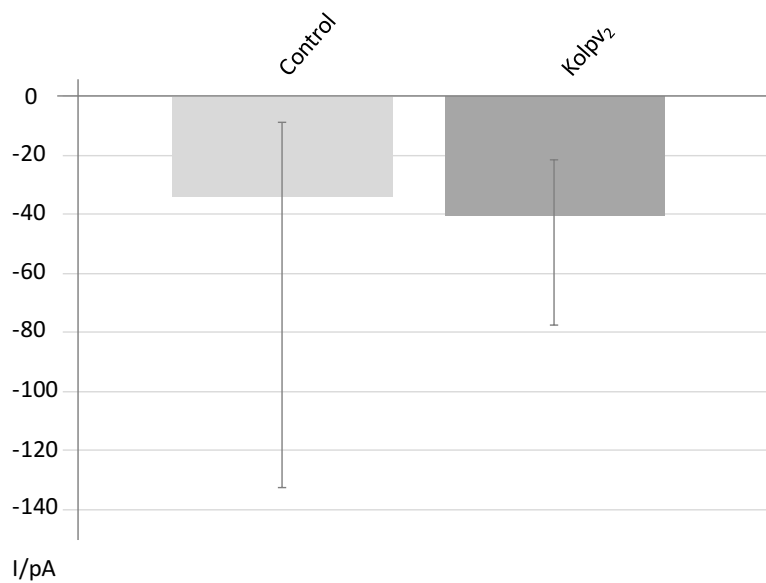


Fig. 31: Expression of Kolpv₂:EGFP shows no specific conductance in HEK293 cells. At a reference voltage of -100 mV, Kolpv₂ expressing cells exhibit a geometrical mean current of -40.9 pA (-36.8 pA; +19.4 pA; n=10). At the same voltage the untransfected control cells have a geometrical mean current of only -34 pA (-98 pA; +25 pA; n=9). Cells transfected with Kolpv₂ rarely exhibited a conductance that was significantly different from non-transfected control cells.

7.4. Results and Discussion - Channels from fresh water viruses

7.4.1. Kcv_{NH} is a functional potassium channel

The Kcv_{NH} channel protein was derived from a water sample of the New Hampshire Winnepesaukee lake. Kcv_{NH} generates a K⁺ conductance in HEK293 cells. At a reference voltage of -100 mV, Kcv_{NH} expressing cells showed a geometrical mean current of -0.2 nA (-0.5 nA; +0.2 nA; n=39). At the same voltage, the untransfected control cells had a geometrical mean current of -34 pA (-98 pA; +25 pA; n=9). In potassium buffer Kcv_{NH} also showed voltage dependent tail currents (Fig. 32A, D and G). At negative voltages Kcv_{NH} generated an intense flickering (Fig. 32A, D and G). A possible explanation could be that the single channel has a high unitary conductance. The stochastic fluctuation of a few channels with a high conductance could generate such a flickering phenotype of current.

Addition of 10 mM Ba²⁺ to the bath solution caused a full block of the Kcv_{NH} channel inward current. The mean current with 10 mM Ba²⁺ + 50 mM K⁺ buffer at -100 mV was -13 pA (-23 pA; +8.5 pA; n=10) (Fig. 32B). A peculiarity of the Kcv_{NH} channel is that Ba²⁺ also caused a block of the outward currents. This behavior seems to be unique for Kcv_{NH}, neither Kcv_{NTS}, Kcv_S nor Kcv_{ATCV-1} exhibit a reduced outward current in response to Ba²⁺ (Gazzarrini *et al.*, 2009; Greiner, 2011)

The channel did not conduct sodium. The geometrical mean current of Kcv_{NH} in a sodium buffer at -100 mV was -24 pA (-49.8 pA; +16 pA; n=9). The mean reversal potential in this sodium buffer was -41.8 mV (\pm 15 mV; n=9), which is a left shift compared to the reversal potential in a potassium buffer, which was at -8 mV (\pm 2.3 mV; n=39).

Because of the high degree of sequence identity between Kcv_{NH} and Kcv_{NTS} (Fig. 11) it was interesting to test sensitivity of Kcv_{NH} to cesium. Kcv_{NH} was blocked by cesium but did not show the same steep block (Fig. 32H) like Kcv_{NTS} (Greiner, 2011). It showed a voltage dependency of the block like the related channel Kcv_S (Greiner, 2011). The geometrical mean of the Kcv_{NH} current in a cesium buffer at -100 mV was -15 pA (-33 pA; +10 pA; n=10) (Fig. 32H).

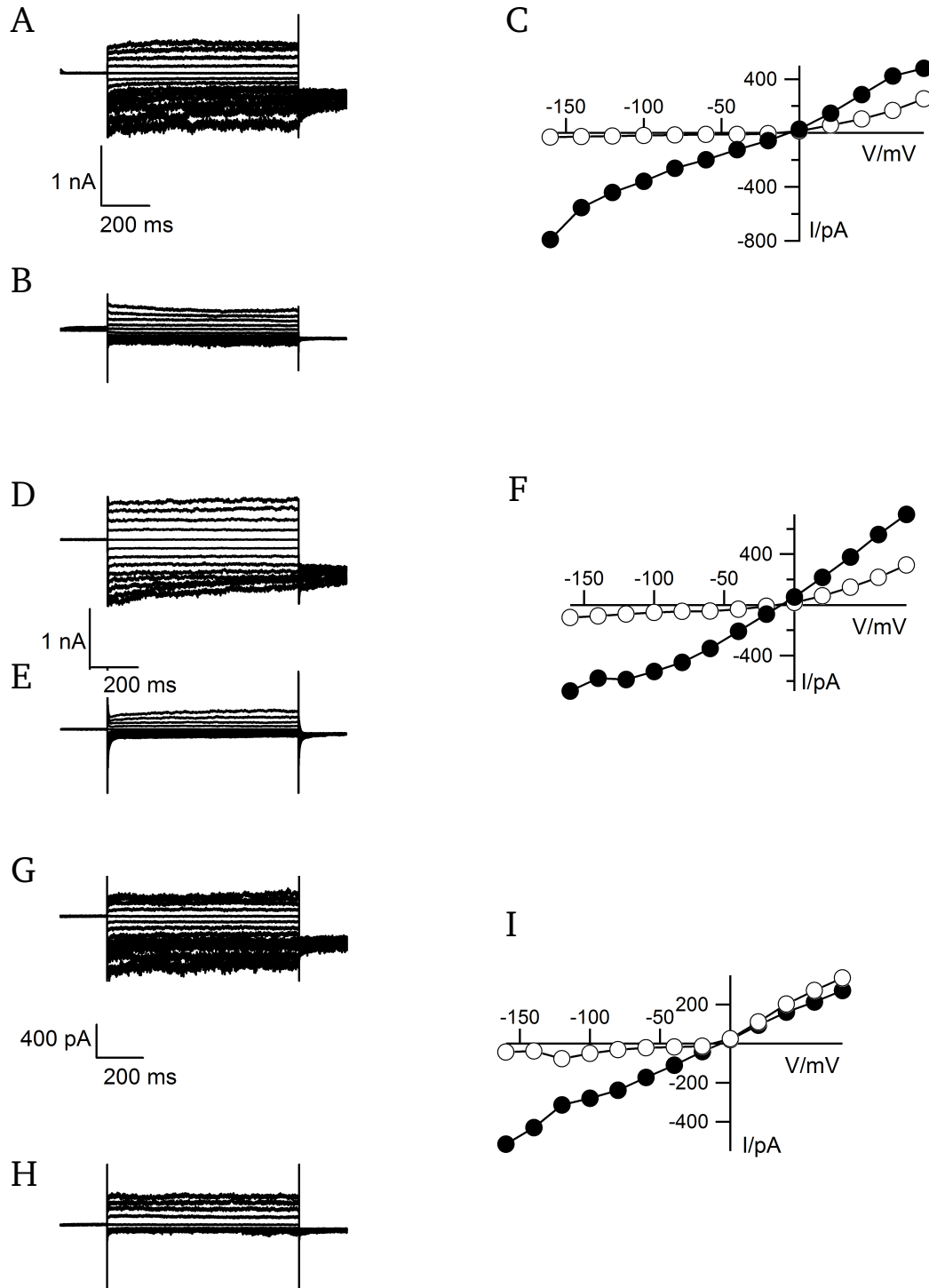


Fig. 32: Expression of Kcv_{NH}:EGFP generates K⁺ conductance in HEK293 cells. Current responses of a HEK293 cell expressing Kcv_{NH}:EGFP to voltage steps from holding voltage (0 mV) to test voltages between -160 mV and +80 mV. Currents were recorded in buffer with 50 mM K⁺ (A) and 50 mM Na⁺ (B). (C) Corresponding steady state I/V relations from measurements in (A) (closed symbols) and (B) (open symbols). (D) and (E) were measured as in (A) with HEK293 cells expressing Kcv_{NH}:EGFP. Currents were recorded in buffer with 50 mM K⁺ in the absence (D) and presence of 10 mM BaCl₂ (E). (F) Corresponding steady state I/V relations from measurements in (D) (closed symbols) and (E) (open symbols). Currents were recorded in buffer with 50 mM K⁺ in the absence (G) and presence of 10 mM CsCl (H). (I) Corresponding steady state I/V relations from measurements in (G) (closed symbols) and (H) (open symbols).

7.4.2. Kcv_{GNLD} is a functional potassium channel from a hybrid virus

The Kcv channel protein from a water sample from the Greenland's Sisimiut lake, which was termed Kcv_{GNLD} , generates a K^+ conductance in HEK293 cells. At a reference voltage of -100 mV, Kcv_{GNLD} expressing cells exhibited a geometrical mean current of -5.97 nA (-8.1 nA; $+3.4$ nA; $n=24$), which is a relatively high current amplitude. Some measurements showed a current response at -100 mV around 15 nA which is remarkable high.

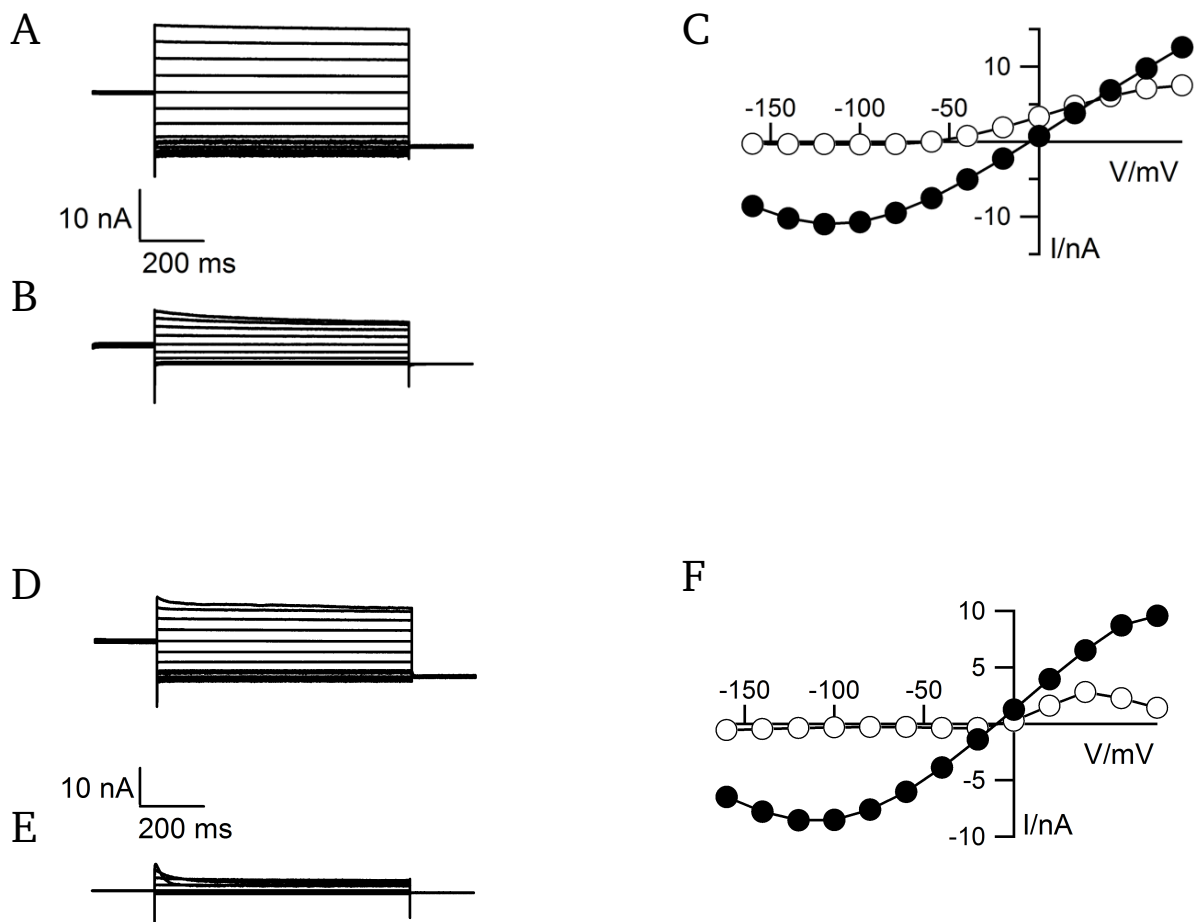


Fig. 33: Expression of Kcv_{GNLD} :EGFP generates a specific K^+ conductance in HEK293 cells. Current responses of a HEK293 cell expressing Kcv_{GNLD} :EGFP to voltage steps from holding voltage (0 mV) to test voltages between -160 mV and $+80$ mV. Currents were recorded in buffer with 50 mM K^+ (A) and 50 mM Na^+ (B). (C) Corresponding steady state I/V relations from measurements in (A) (closed symbols) and (B) (open symbols). (D) and (E) are obtained as in (A) with HEK293 cells expressing Kcv_{GNLD} :EGFP. Currents were recorded in buffer with 50 mM K^+ in the absence (D) and presence of 10 mM $BaCl_2$ (E). (F) Corresponding steady state I/V relations from measurements in (D) (closed symbols) and (E) (open symbols).

A special feature of the Kcv_{GNLD} current is a characteristic inactivation at high negative voltages (Fig. 33A and D). At the same voltage, the untransfected control cells had for comparison only a geometrical mean

current of only -34 pA (-98 pA; +25 pA; n=9) (Fig. 13) and no inactivation at negative voltages.

Experiments in which K^+ in the bath solution was exchanged for Na^+ showed that Kcv_{GNLD} is selective for potassium. It showed a mean left shift of the reversal potential of -63.4mV (± 28.5 mV; n=7) for changing the potassium buffer against sodium buffer. The final reversal potential in a sodium buffer was -70,93 mV (± 31.1 mV; n=12) (Fig. 33B). The results of these experiments showed that the channel is more than 10 times higher selective for K^+ than for Na^+ . As expected for a K^+ channel Kcv_{GNLD} was also blocked by Ba^{2+} ions (Fig. 33E). At a reference voltage of -100 mV and with 10 mM Ba^{2+} in the bath solution, Kcv_{GNLD} expressing cells exhibited a geometrical mean current of -0.6 nA (-0.9 nA; +0.4 nA; n=10). Hence 10 mM Ba^{2+} reduced the Kcv_{GNLD} current by about 92% ($\pm 4\%$; n=3).

7.4.3. Kcv_{MT325} generates K^+ conductance in HEK293 cells

Kcv_{MT325} has a high sequence similarity with Kcv_{GNLD} , the Kcv_{MT325} channel was already characterized in *Xenopus laevis* oocytes (Gazzarrini *et al.*, 2006), but not in HEK293 cells. To compare the two related channels, Kcv_{GNLD} and Kcv_{MT325} , we performed also whole-cell measurements with Kcv_{MT325} in HEK293 cells.

Kcv_{MT325} showed a current response in HEK293 cells which are similar to those reported from oocytes (Gazzarrini *et al.*, 2006) (Fig. 34A,D). At a reference voltage of -100 mV, Kcv_{MT325} expressing cells showed a geometrical mean current of -4.3 nA (-11 nA; +3.1 nA; n=11). At the same voltage, the untransfected control cells had a geometrical mean current of only -34 pA (-98 pA; +25 pA; n=9). Kcv_{MT325} generated also remarkable high currents like Kcv_{GNLD} in HEK293 cells; they were up to -15 nA at -100 mV. A explanation for the high currents could be either a high expression rate of the protein, a better transport into the membrane with the result of an higher amount of channels in the membrane. An alternative explanation could be a higher single channel conductance or a high open probability of the channels. Also a combination of these factors is possible.

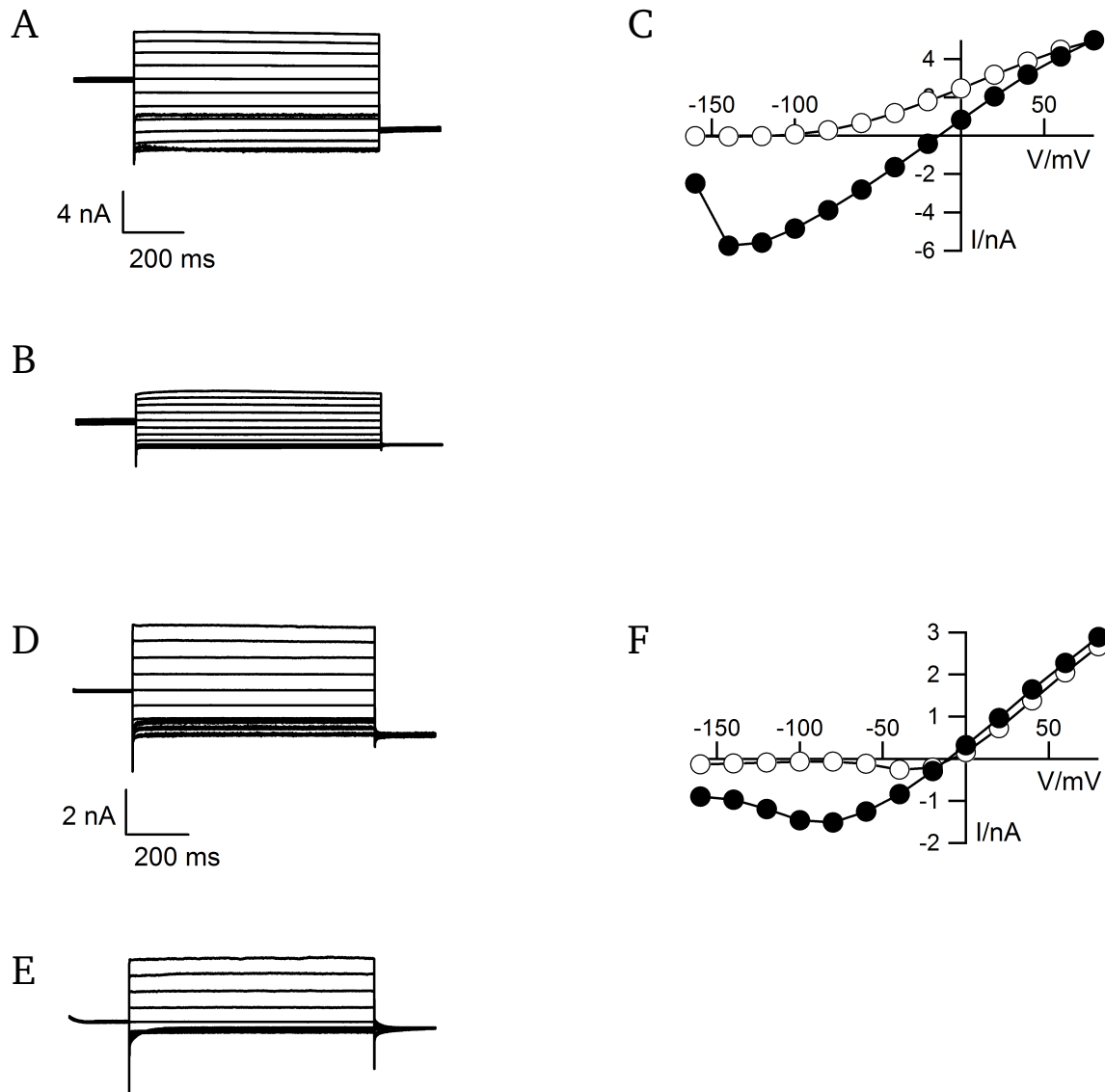


Fig. 34: Expression of Kcv_{MT325}:EGFP generates a specific K⁺ conductance in HEK293 cells. Current responses of a HEK293 cell expressing Kcv_{MT325}:EGFP to voltage steps from holding voltage (0 mV) to test voltages between -160 mV and +80 mV. Currents were recorded in buffer with 50 mM K⁺ (A) and 50 mM Na⁺ (B). (C) Corresponding steady state I/V relations from measurements in (A) (closed symbols) and (B) (open symbols). (D) and (E) are the same as in (A) from HEK293 cells expressing Kcv_{MT325}:EGFP. Currents were recorded in buffer with 50 mM K⁺ in the absence (D) and presence of 10 mM BaCl₂ (E). (F) Corresponding steady state I/V relations from measurements in (D) (closed symbols) and (E) (open symbols).

Kcv_{MT325} also showed the characteristic inactivation at high negative voltages like the Kcv_{GNLD} channel (Fig. 34A and D) and most other Kcv type channels. The apparent inactivation of Kcv_{MT325} as a result of fast gating were also confirmed by measurements of this channel in oocytes (Gazzarrini *et al.*, 2006). The similar behavior of the channel in different systems shows that the functional properties of the channel are robust and appear independent of the expressions system. Like Kcv_{GNLD} also Kcv_{MT325} is selective for potassium. It exhibited a mean left shift of the reversal potential of $-89.9 (\pm 17.9; n=4)$

upon changing the potassium buffer against sodium buffer. The mean reversal potential in a sodium buffer was -104.6 mV ($\pm 12.9 \text{ mV}$; $n=8$), which implies that this channel is even more K^+ selective than Kcv_{GNLD} (Fig. 33B).

$\text{Kcv}_{\text{MT325}}$ was blocked by Ba^{2+} ions (Fig. 34E). At a reference voltage of -100 mV and 10 mM Ba^{2+} in the bath solution, Kcv_{GNLD} expressing cells exhibited a geometrical mean current of -0.1 nA (-0.08 nA ; $+0.05 \text{ nA}$; $n=7$). 10 mM Ba^{2+} reduced the current by about 97% ($\pm 1\%$; $n=6$).

7.5. Channel sorting

To find an explanation for the observation that some channels could not be measured in HEK293 cells but after reconstitution of the isolated proteins in a planar lipid bilayer, we tagged the respective channels with EGFP and monitored their distribution in HEK293 cells in a CLSM. In the analysis of the following images we took a sorting of the GFP-tagged channel as indirect evidence for a positive trafficking of the channel to the plasmamembrane. The same approach was already used in a previous study to examine sorting of Kcv type channels (Balss *et al.*, 2008). A direct localization of the channels, which are synthesized in a cotranslational manner at the ER (Zhang *et al.*, 2016), in the plasmamembrane was not possible because of a low concentration. Fig. 35 shows an example for the cellular distribution of a channel protein from *Micromonas* sp. virus. The images show that $\text{Kmpv}_1\text{:EGFP}$ is in individual cells sorted into the mitochondria or the ER where they colocalize with either a mitochondria marker or an ER marker, respectively. This channel, which is at least in a fraction of cells sorted to the ER and presumably also to the plasma membrane can also be measured in HEK293 cells (Fig. 35A-F and Fig. 14). $\text{Kmpv}_{\text{sp1}}\text{:EGFP}$ also shows the characteristic reticulate distribution, which is typical for the ER. Accordingly it is also colocalizing with a fluorescent ER marker (Fig. 35G-I). A third channel, $\text{Kmpv}_{\text{pl1}}\text{:EGFP}$, which could not be measured in HEK293 cells, shows a different localization. The fluorescence is spread throughout the cell including the nucleus. A closer scrutiny of the images even implies that the fluorescence is absent from the mitochondria and the perinuclear ring (Fig. 35J-L). This suggests that this channel protein is not sorted to a target membrane, which explains why it was not measured in HEK293 cells. The global distribution of EGFP implies that the protein is destructed in the cell.

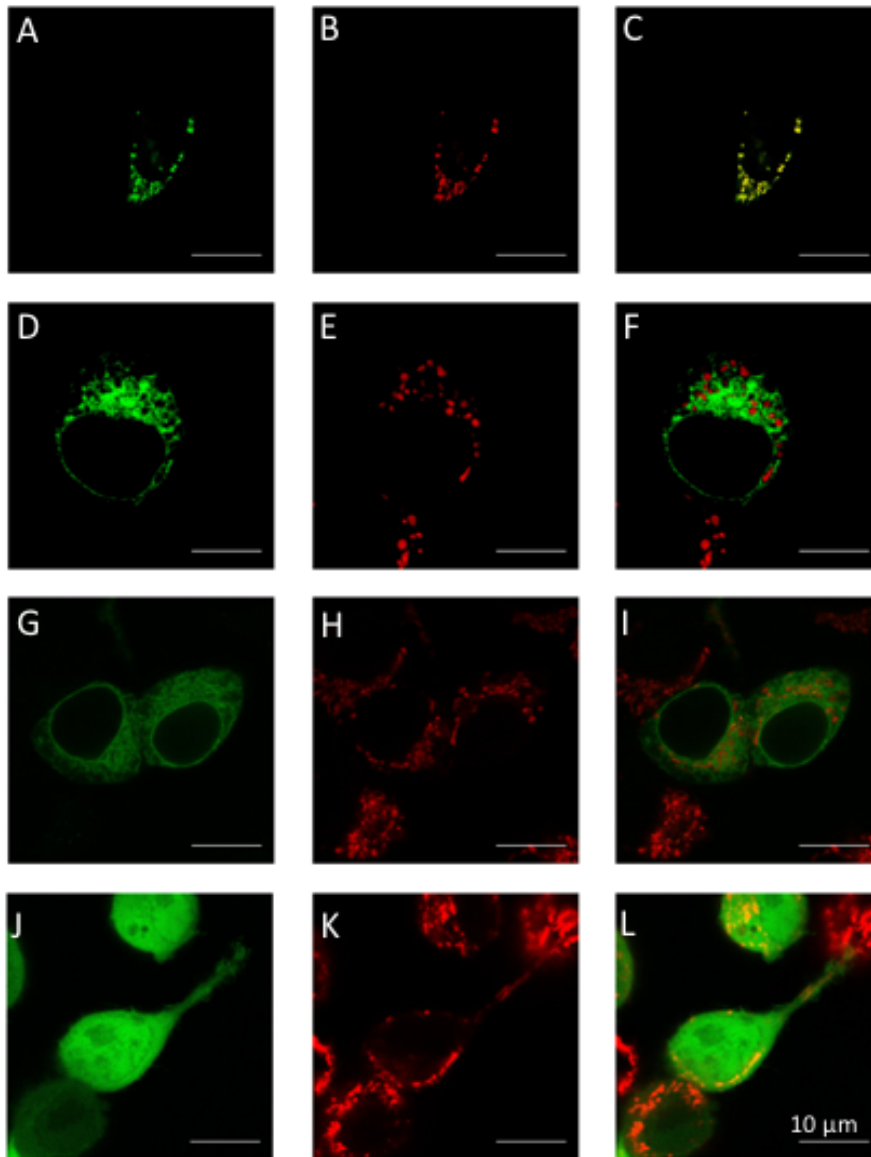


Fig. 35: Localization of $Kmpv_1$, $Kmpv_{SP1}$ and $Kmpv_{PL1}$ in HEK293 cells. (A) and (D) show a HEK293 cell expressing $Kmpv_1$:EGFP (B) and (E) show a Mito-Tracker labeling of same cells. (C) and (F) shows merged images from (A) and (B) such as (D) and (E). (G) shows a HEK293 cell expressing $Kmpv_{SP1}$:EGFP. (H) shows the Mito-Tracker labeling of same cell. (I) is merged image of (G) and (H). (J) shows a HEK293 cell expressing $Kmpv_{PL1}$:EGFP. (K) shows a Mito-Tracker labeling of same cell. (L) is merged image of (J) and (K). All scale bars are 10 μ m.

In Tab. 5 the functional data and the available information on the distribution of the channels are summarized. We clearly see that all channels, which we were able to measure in HEK293 cells, are sorted into the ER. Channels, which are sorted into the mitochondria or remain unsorted in the cytosol, are those, which did not generate a measurable current in HEK293 cells. Some of the latter channels however showed activity in bilayer measurements. The results of these data suggest that also channels, which were not generating a current in HEK293 cells, can still be functional channels. The reason behind the finding that some channels are and others are not active in HEK293 cells can be assigned to different sorting properties of these proteins. Some are trafficking via the ER into the plasma membrane while

others are sorted to the mitochondria. The data underscore that measurements of channel activity in bilayers are a good alternative option over heterologous expression in HEK293 cells because this method is independent on protein sorting in cells.

Tab. 5: Summary of basic properties of tested K⁺ channel candidate proteins. n.d.= not measured, mito=mitochondria, cyto=cytosol, ER= endoplasmatisches reticulum (some data are not shown in this work).

Name of protein	Functional in HEK293	Functional in bilayer	Reversal potential shift (mV) K ⁺ →Na ⁺	Ba ²⁺ block in %	Sorting
Kmpv ₁	✓	n.m.	59.6 (n=1)	25 ± 16 (n=9)	ER, mito
Kmpv _{12T}	✗	✓	-42 (n=1)	46 (n=1)	mito, cyto
Kmpv _{SP1}	✓	✓	-58.8 ± 22 (n=3)	93.4 ± 5 (n=3)	ER
Kmpv _{PL1}	✗	✓	-20 ± 12 (n=3)	57 ± 17 (n=3)	cyto
Kbpv ₁	✓	n.m.	-63.5 ± 20 (n=5)	82 ± 6 (n=3)	ER, mito
Kotv _{RT}	✓	n.m.	-48.4 ± 31 (n=7)	95.1 ± 4.5 (n=5)	n.m.
Kolv ₄	✗	n.m.	-19.3 ± 5,6 (n=3)	-48.3 ± 29 (n=6)	n.m.
Kolpv ₂	✗	n.m.	-34.4 ± 8.9 (n=6)	30 (n=1)	n.m.
Kcv _{NH}	✓	✓	-34.4 ± 8.9 (n=6)	82.8 ± 10 (n=7)	ER
Kcv _{GnLD}	✓	n.m.	-63.4 ± 28.5 (n=7)	92 ± 4 (n=3)	ER
Kcv _{MT325}	✓	n.m.	-89.9 ± 17.9 (n=4)	97 ± 1 (n=6)	ER

8. Main Discussion (Chapter 4)

Collectively the experimental results established that K⁺ channel-like gene products from marine viruses MpV1, MpV12T, BpV1, MPVSP1, OTVRT, as well as from the fresh water virus from lake Winnepesaukee and from Camping Ground Greenland are functional K⁺ channels (Tab. 5). The channels from viruses MpV1, MpV12T, BpV1, MPVSP1, OTVRT exhibit a K⁺ channel function even though prediction algorithms for TMDs failed to identify a proper structure for a K⁺ channel. It is reasonable to speculate that these proteins follow the general tendency of viruses to miniaturize the size of their genes and that they have evolved efficient TMDs, which are structurally different from those in cellular organisms. Consequently, the inability of the TMHHM algorithm to predict the second TMD in some of the viral channels might be because the algorithm was developed to identify canonical TMDs in prokaryotic and eukaryotic membrane proteins, the low hydrophobicity of many of the viral channels is very unusual for TMDs. Interestingly, three of the K⁺ channel proteins with very short sequences (Fig. 6A) have a cationic amino acid at the C-terminus. These amino acids are well known for a phenomenon termed “snorkeling” (Killian and von Heijne, 2000). Because of their long and flexible side chains, cationic amino acids can keep their hydrocarbon backbone inside the membrane while the positive charge reaches into the water-lipid interface (Segrest *et al.*, 1990; Strandberg and Killian, 2003). This property can keep proteins in a transmembrane orientation even when the structure of the protein seems not suitable as a TMD per se (Henkel *et al.*, 2010).

In order to judge the relationship between the viral channels a phylogenetic analysis was conducted for the K⁺ channels coded by viruses that infect algae from fresh water or marine water (Figs. 8, 36 and 37). The chloroviruses PBCV-1, MT325 and ATCV-1, which have different fresh water hosts, were chosen to represent viruses infecting 3 fresh water algae (Thiel *et al.*, 2011). Virus EsV-1 represents a virus, which infects a marine algae (Van Etten *et al.*, 2002). All of these viral encoded proteins were previously shown to function as K⁺ channels (Balss *et al.*, 2008; Gazzarrini *et al.*, 2009; Gazzarrini *et al.*, 2006). Previous studies on structure/function relations established that some amino acids are very important for Kcv channel activity (Gebhardt *et al.*, 2012; Gebhardt *et al.*, 2011). These significant amino acids are labeled with small letters (a–f) in Fig. 36. The aromatic amino acids a–c are required to anchor the first TMD in the lipid bilayer (Gebhardt *et al.*, 2011). The cationic amino acid (d) (Fig. 36) is a “snorkeling” amino acid and required for placing the TMD in the bilayer (Gebhardt *et al.*, 2012). Finally a pair of Phe or Met (e) form together with a His (f) in the second TMD, a π : π -stacking or C–H: π -interaction, this interaction attaches the inner TMD to the outer TMD (Gebhardt *et al.*, 2011). The listed amino acids are conserved among more than 80 Kcv type channels from viruses, which infect fresh water algae (Thiel and Van Etten, unpublished data). This high degree of conservation indicates that they are important for the

global architecture of the channel. Scrutiny of the new sequences reveals that the aromatic amino acids (b and c in Fig. 36) are highly conserved throughout most of the viral encoded K^+ channels, only the *Kolpv₂* protein differs from the rest. The result of this analysis indicates that the channels from fresh water viruses are more closely related to each other than to the other viral channels. The absence of amino acids in the new channel sequences, which are structurally important in the latter channels, implies that the newly discovered K^+ channel proteins use a different architecture for generating a functional K^+ channel. Further scrutiny of the alignment indicates that, collectively the channel sequences are quite diverse. Apart from the K^+ channel consensus sequence, which is moderately conserved among all the viral channels, only a few amino acids are highly conserved. The general picture is that the N-terminal part of the channels is more diverse than the C-terminal part downstream of the filter region (Fig. 8 and 36). It will be interesting to examine the functional significance of the few remaining conserved amino acids among the population of viral channels.

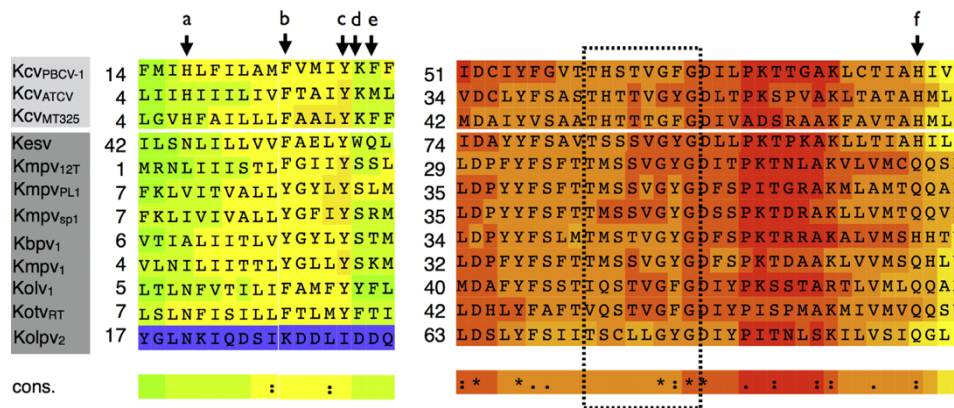
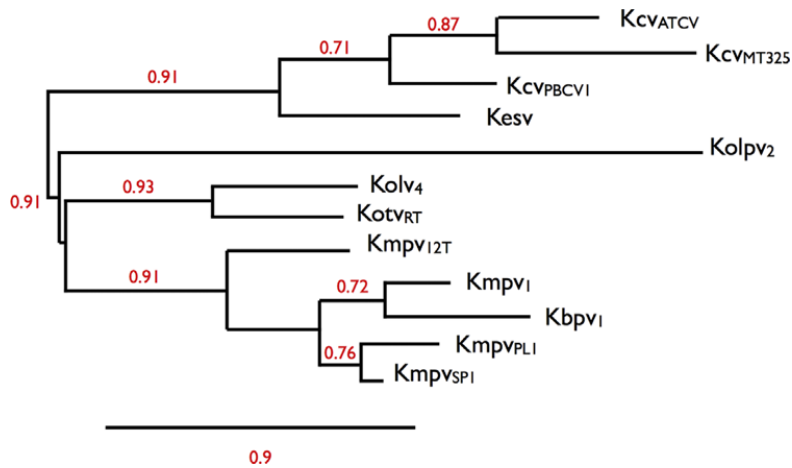


Fig. 36: Multiple alignments of K^+ channels from different viruses with focus on the first TMD and the selectivity filter domain. The alignment includes established K^+ channels from chloroviruses (*KcvPBCV1*, *KcvATCV-1*, *KcvMT325*) and from *Ectocarpus siliculosus* virus (*Kesv*). The remaining sequences are K^+ channels from viruses described in this work. The dotted box highlights the area of the consensus sequence of all K^+ channels; the arrows with letters a–f indicates amino acids that are highly conserved in K^+ channels from fresh water viruses and which were previously found essential for channel function. The channels from fresh water viruses are in light gray and those from sea or salt water in dark grey. Alignment was constructed with T-COFFEE version 6.85 software available at Phylogeny.fr (Dereeper *et al.*, 2008). The colors depict the degree of similarity from conserved (red) to not conserved (blue). * mark the amino acids which are identical in all sequences, : mark the conserved and . mark the semi-conserved amino acids.

A



B

Kolpv ₂	YGLNKIQDSI	KDDLIDDQNQ	RYLDSLYFSI	ITSCLLGYGD	IYPITNLSKI	LVSIQGLITL	SLILY
Kmpv ₁	VLNLIITTL	YGLLYSKMEK	SPLDPFYFSF	TMSSVGYGD	FSPKTDAAKL	VVMSQHLVMI	GELAK
Kmpv _{12T}	MRNLIIISTL	FGIIYSSLGK	SVLDPFYFSF	TMSSVGYGD	ITPKTNLAKV	LVMCQSSLF	NELMQ
Kmpv _{PL1}	FKLVIIVALL	YGLYSLMEK	TALDPYFYSF	TMSSVGYGD	FSPITGRAKM	LAMTQQAFIF	GELIK
Kmpv _{SP1}	FKLIVIVALL	YGFYSRMES	SPLDPYFYSF	TMSSVGYGD	SSPKTDRAKL	LVMTQQVFIF	GELIK
Kbpv ₁	VTIALIITLV	YGLYSTMES	DPLDPYFSL	MTMSTVGYGD	FSPKTRRAKA	LVMSHHTVIL	VELAT
Kolv ₄	LTNLFVITLI	FAMFYFLDV	SLMDAFYFSS	TIQSTVGFPGD	IYPKSSTART	LVMLQQAMLI	VGVDV
Kotv _{RT}	LSLNFISILL	FTLMYFTIES	GFLDHLYFAF	TVQSTVGFPGD	IYPISPMAM	IVMVQQSVLI	LGILE
KCV _{BVCV1}	FMIHLFILAM	FVMIYKFFNA	SWIDCIYFGV	TTHSTVGFPGD	ILPKTTGAKL	CTIAHIVTVF	FIVLT
Kesv	ILSNLILLV	FAELYWQLTS	SAIDAYYFSA	VTSSVGYGD	LLPKTPKAKL	LTIHAHLAMF	FVMLP
KCV _{ATCV}	LIHHIILLIV	FTAIYKMLSP	TWVDCLYFSA	STHTTVGYGD	LTPKSPVAKL	TATAHMLIVF	AIVIS
KCV _{MT325}	LGVHFAILLL	FAALYKFFNV	SWMDAIYVSA	ATHTTTGFPGD	IVADSRRAKF	AVTAHMLIVF	SIVVL

Fig. 37: Phylogenies of viral encoded K⁺ channel proteins. (A) The tree was constructed using PhyML (Guindon and Gascuel, 2003) available at Phylogeny.fr (Dereeper *et al.*, 2008) with WAG matrix and gamma distribution from gap free alignment. Branch labels indicate bootstrap percentages (40.7) after 100 replicates. The tree is an unrooted. (B) Alignment of channel sequences used for phylogenetic tree in (A).

The channel sequences in Fig. 37 were used to construct a phylogenetic tree (Fig. 38) with the maximum likelihood algorithm. The data show that the channel proteins can be separated with moderate statistical support between channels from fresh water viruses and marine or salt-water viruses. This result is consistent with previous suggestions that the viral K⁺ channels have a long evolutionary history (Hamacher *et al.*, 2012; Thiel *et al.*, 2013). However, the analysis does not indicate a strict separation of the channels on the basis of their viral hosts. The channels from virus BpV1/2 are on the same branch as those from virus MpV1. Also, the Kesv channel, which infects a brown alga, is not clearly separated from those infecting green algae. The latter finding is in good agreement with previous analyses that indicate the viral channels are not the product of molecular piracy (Hamacher *et al.*, 2012).

The present data show that K⁺ channel-like genes are abundant in viruses that infect either fresh water or sea/salt water algae. All viral channels have maintained the overall architecture of K⁺ channel proteins

with three α -helices, two form the required TMDs and the central one is adjacent to the canonical pore helix signature sequence. Apart from these common features the viral K^+ channels are quite diverse. A peculiarity of many of the channels coded by sea water viruses is their unusual TMDs, which are not detected by algorithms that predict protein structures. A further peculiarity of two of the newly discovered channel proteins is their small size. The present experimental verification of their function as K^+ selective channels makes them the smallest proteins known to form a functional K^+ channel. Sequence alignments and analysis of specific amino acids, which were identified in previous studies as functionally important (Gebhardt *et al.*, 2012; Gebhardt *et al.*, 2011), support a clear phylogenetic separation of channels from fresh water viruses versus salt/sea water viruses. The phylogenetic relationships, however, provide no evidence for a co-evolution between viruses and their hosts. This finding agrees with previous studies on the relationship between host and virus K^+ channels (Hamacher *et al.*, 2012; Thiel *et al.*, 2013). Altogether these data advocate a common origin of viral K^+ channels and indicate that they have a long evolutionary history.

9. References

- Abenavoli, A., DiFrancesco, M.L., Schroeder, I., Epimashko, S., Gazzarrini, S., Hansen, U.P., Thiel, G., Moroni, A., 2009. Fast and slow gating are inherent properties of the pore module of the K⁺ channel Kcv. *J Gen Physiol* 134, 219-229.
- Amico, M., Finelli, M., Rossi, I., Zauli, A., Elofsson, A., Viklund, H., von Heijne, G., Jones, D., Krogh, A., Fariselli, P., Luigi Martelli, P., Casadio, R., 2006. PONGO: a web server for multiple predictions of all-alpha transmembrane proteins. *Nucleic Acids Res* 34, W169-172.
- Angly, F.E., Felts, B., Breitbart, M., Salamon, P., Edwards, R.A., Carlson, C., Chan, A.M., Haynes, M., Kelley, S., Liu, H., Mahaffy, J.M., Mueller, J.E., Nulton, J., Olson, R., Parsons, R., Rayhawk, S., Suttle, C.A., Rohwer, F., 2006. The marine viromes of four oceanic regions. *PLoS Biol* 4, e368.
- Arrigoni, C., Schroeder, I., Romani, G., Van Etten, J.L., Thiel, G., Moroni, A., 2013. The voltage-sensing domain of a phosphatase gates the pore of a potassium channel. *J Gen Physiol* 141, 389-395.
- Aryal, P., Sansom, M.S., Tucker, S.J., 2015. Hydrophobic gating in ion channels. *J Mol Biol* 427, 121-130.
- Ashcroft, F.M., 2006. From molecule to malady. *Nature* 440, 440-447.
- Balss, J., Papatheodorou, P., Mehmel, M., Baumeister, D., Hertel, B., Delaroque, N., Chatelain, F.C., Minor, D.L., Jr., Van Etten, J.L., Rassow, J., Moroni, A., Thiel, G., 2008. Transmembrane domain length of viral K⁺ channels is a signal for mitochondria targeting. *Proc Natl Acad Sci U S A* 105, 12313-12318.
- Bellec, L., Grimsley, N., Moreau, H., Desdevises, Y., 2009. Phylogenetic analysis of new Prasinoviruses (Phycodnaviridae) that infect the green unicellular algae *Ostreococcus*, *Bathycoccus* and *Micromonas*. *Environ Microbiol Rep* 1, 114-123.
- Bergh, O., Borsheim, K.Y., Bratbak, G., Heldal, M., 1989. High abundance of viruses found in aquatic environments. *Nature* 340, 467-468.
- Bichet, D., Lin, Y.F., Ibarra, C.A., Huang, C.S., Yi, B.A., Jan, Y.N., Jan, L.Y., 2004. Evolving potassium channels by means of yeast selection reveals structural elements important for selectivity. *Proc Natl Acad Sci U S A* 101, 4441-4446.
- Braman, J., Papworth, C., Greener, A., 1996. Site-directed mutagenesis using double-stranded plasmid DNA templates. *Methods Mol Biol* 57, 31-44.
- Braun, C.J., Lachnit, C., Becker, P., Henkes, L.M., Arrigoni, C., Kast, S.M., Moroni, A., Thiel, G., Schroeder, I., 2014. Viral potassium channels as a robust model system for studies of membrane-protein interaction. *Biochim Biophys Acta* 1838, 1096-1103.
- Breitbart, M., Salamon, P., Andresen, B., Mahaffy, J.M., Segall, A.M., Mead, D., Azam, F., Rohwer, F., 2002. Genomic analysis of uncultured marine viral communities. *Proc Natl Acad Sci U S A* 99, 14250-14255.

-
- Cao, B., Porollo, A., Adamczak, R., Jarrell, M., Meller, J., 2006. Enhanced recognition of protein transmembrane domains with prediction-based structural profiles. *Bioinformatics* 22, 303-309.
- Chatelain, F.C., Gazzarrini, S., Fujiwara, Y., Arrigoni, C., Domigan, C., Ferrara, G., Pantoja, C., Thiel, G., Moroni, A., Minor, D.L., Jr., 2009. Selection of inhibitor-resistant viral potassium channels identifies a selectivity filter site that affects barium and amantadine block. *PLoS One* 4, e7496.
- Cole, C., Barber, J.D., Barton, G.J., 2008. The Jpred 3 secondary structure prediction server. *Nucleic Acids Res* 36, W197-201.
- Delaroque, N., Maier, I., Knippers, R., Muller, D.G., 1999. Persistent virus integration into the genome of its algal host, *Ectocarpus siliculosus* (Phaeophyceae). *J Gen Virol* 80 (Pt 6), 1367-1370.
- Dereeper, A., Guignon, V., Blanc, G., Audic, S., Buffet, S., Chevenet, F., Dufayard, J.F., Guindon, S., Lefort, V., Lescot, M., Claverie, J.M., Gascuel, O., 2008. Phylogeny.fr: robust phylogenetic analysis for the non-specialist. *Nucleic Acids Res* 36, W465-469.
- Derelle, E., Ferraz, C., Escande, M.L., Eychenie, S., Cooke, R., Piganeau, G., Desdevises, Y., Bellec, L., Moreau, H., Grimsley, N., 2008. Life-cycle and genome of OtV5, a large DNA virus of the pelagic marine unicellular green alga *Ostreococcus tauri*. *PLoS One* 3, e2250.
- Derelle, E., Ferraz, C., Rombauts, S., Rouze, P., Worden, A.Z., Robbens, S., Partensky, F., Degroeve, S., Echeynie, S., Cooke, R., Saeys, Y., Wuyts, J., Jabbari, K., Bowler, C., Panaud, O., Piegue, B., Ball, S.G., Ral, J.P., Bouget, F.Y., Piganeau, G., De Baets, B., Picard, A., Delseny, M., Demaille, J., Van de Peer, Y., Moreau, H., 2006. Genome analysis of the smallest free-living eukaryote *Ostreococcus tauri* unveils many unique features. *Proc Natl Acad Sci U S A* 103, 11647-11652.
- Doyle, D.A., Morais Cabral, J., Pfuetzner, R.A., Kuo, A., Gulbis, J.M., Cohen, S.L., Chait, B.T., MacKinnon, R., 1998. The structure of the potassium channel: molecular basis of K⁺ conduction and selectivity. *Science* 280, 69-77.
- Field, C.B., Behrenfeld, M.J., Randerson, J.T., Falkowski, P., 1998. Primary production of the biosphere: integrating terrestrial and oceanic components. *Science* 281, 237-240.
- Fischer, M.G., Kelly, I., Foster, L.J., Suttle, C.A., 2014. The virion of *Cafeteria roenbergensis* virus (CroV) contains a complex suite of proteins for transcription and DNA repair. *Virology* 466-467, 82-94.
- Fischer, W.B., Sansom, M.S., 2002. Viral ion channels: structure and function. *Biochim Biophys Acta* 1561, 27-45.
- Fitzgerald, L.A., Graves, M.V., Li, X., Feldblyum, T., Hartigan, J., Van Etten, J.L., 2007. Sequence and annotation of the 314-kb MT325 and the 321-kb FR483 viruses that infect *Chlorella Pbi*. *Virology* 358, 459-471.
- Frohns, F., Kasmann, A., Kramer, D., Schafer, B., Mehmel, M., Kang, M., Van Etten, J.L., Gazzarrini, S., Moroni, A., Thiel, G., 2006. Potassium ion channels of *Chlorella* viruses cause rapid depolarization of host cells during infection. *J Virol* 80, 2437-2444.
- Gazzarrini, S., Kang, M., Abenavoli, A., Romani, G., Olivari, C., Gaslini, D., Ferrara, G., van Etten, J.L., Kreim, M., Kast, S.M., Thiel, G., Moroni, A., 2009. *Chlorella* virus ATCV-1 encodes a functional potassium channel of 82 amino acids. *Biochem J* 420, 295-303.

-
- Gazzarrini, S., Kang, M., Epimashko, S., Van Etten, J.L., Dainty, J., Thiel, G., Moroni, A., 2006. Chlorella virus MT325 encodes water and potassium channels that interact synergistically. *Proc Natl Acad Sci U S A* 103, 5355-5360.
- Gebhardt, M., Henkes, L.M., Tayefeh, S., Hertel, B., Greiner, T., Van Etten, J.L., Baumeister, D., Cosentino, C., Moroni, A., Kast, S.M., Thiel, G., 2012. Relevance of lysine snorkeling in the outer transmembrane domain of small viral potassium ion channels. *Biochemistry* 51, 5571-5579.
- Gebhardt, M., Hoffgaard, F., Hamacher, K., Kast, S.M., Moroni, A., Thiel, G., 2011. Membrane anchoring and interaction between transmembrane domains are crucial for K⁺ channel function. *J Biol Chem* 286, 11299-11306.
- Graham, F.L., Smiley, J., Russell, W.C., Nairn, R., 1977. Characteristics of a human cell line transformed by DNA from human adenovirus type 5. *J Gen Virol* 36, 59-74.
- Greiner, T., 2011. Characterization of novel potassium transport proteins from Chlorella viruses. Technische Universität Darmstadt.
- Greiner, T., Frohns, F., Kang, M., Van Etten, J.L., Kasmann, A., Moroni, A., Hertel, B., Thiel, G., 2009. Chlorella viruses prevent multiple infections by depolarizing the host membrane. *J Gen Virol* 90, 2033-2039.
- Grunwald, I., Rischka, K., Kast, S.M., Scheibel, T., Bargel, H., 2009. Mimicking biopolymers on a molecular scale: nano(bio)technology based on engineered proteins. *Philos Trans A Math Phys Eng Sci* 367, 1727-1747.
- Guindon, S., Gascuel, O., 2003. A simple, fast, and accurate algorithm to estimate large phylogenies by maximum likelihood. *Syst Biol* 52, 696-704.
- Hamacher, K., Greiner, T., Ogata, H., Van Etten, J.L., Gebhardt, M., Villarreal, L.P., Cosentino, C., Moroni, A., Thiel, G., 2012. Phycodnavirus potassium ion channel proteins question the virus molecular piracy hypothesis. *PLoS One* 7, e38826.
- Heginbotham, L., Lu, Z., Abramson, T., MacKinnon, R., 1994. Mutations in the K⁺ channel signature sequence. *Biophys J* 66, 1061-1067.
- Henkel, M., Mitzner, D., Henklein, P., Meyer-Almes, F.J., Moroni, A., Difrancesco, M.L., Henkes, L.M., Kreim, M., Kast, S.M., Schubert, U., Thiel, G., 2010. The proapoptotic influenza A virus protein PB1-F2 forms a nonselective ion channel. *PLoS One* 5, e11112.
- Hille, B., 2001. *Ion Channels of Excitable Membranes*. Sinauer Associates, Inc., Massachusetts, USA.
- Hsu, K., Seharaseyon, J., Dong, P., Bour, S., Marban, E., 2004. Mutual functional destruction of HIV-1 Vpu and host TASK-1 channel. *Mol Cell* 14, 259-267.
- Jan, L.Y., Jan, Y.N., 1992. Structural elements involved in specific K⁺ channel functions. *Annu Rev Physiol* 54, 537-555.
- Jeanniard, A., Dunigan, D.D., Gurnon, J.R., Agarkova, I.V., Kang, M., Vitek, J., Duncan, G., McClung, O.W., Larsen, M., Claverie, J.M., Van Etten, J.L., Blanc, G., 2013. Towards defining the chloroviruses: a genomic journey through a genus of large DNA viruses. *BMC Genomics* 14, 158.

-
- Jiang, Y., Lee, A., Chen, J., Cadene, M., Chait, B.T., MacKinnon, R., 2002. Crystal structure and mechanism of a calcium-gated potassium channel. *Nature* 417, 515-522.
- Kang, M., Moroni, A., Gazzarrini, S., DiFrancesco, D., Thiel, G., Severino, M., Van Etten, J.L., 2004. Small potassium ion channel proteins encoded by chlorella viruses. *Proc Natl Acad Sci U S A* 101, 5318-5324.
- Killian, J.A., von Heijne, G., 2000. How proteins adapt to a membrane-water interface. *Trends Biochem Sci* 25, 429-434.
- Kiss, L., LoTurco, J., Korn, S.J., 1999. Contribution of the selectivity filter to inactivation in potassium channels. *Biophys J* 76, 253-263.
- MacKinnon, R., 1991. Determination of the subunit stoichiometry of a voltage-activated potassium channel. *Nature* 350, 232-235.
- MacKinnon, R., 2004. Potassium channels and the atomic basis of selective ion conduction (Nobel Lecture). *Angew Chem Int Ed Engl* 43, 4265-4277.
- Miller, C., 1992. Ion channel structure and function. *Science* 258, 240-241.
- Minor, D.L., Jr., 2007. The neurobiologist's guide to structural biology: a primer on why macromolecular structure matters and how to evaluate structural data. *Neuron* 54, 511-533.
- Minor, D.L., Jr., 2009. Searching for interesting channels: pairing selection and molecular evolution methods to study ion channel structure and function. *Mol Biosyst* 5, 802-810.
- Moniruzzaman, M., LeClerc, G.R., Brown, C.M., Gobler, C.J., Bidle, K.D., Wilson, W.H., Wilhelm, S.W., 2014. Genome of brown tide virus (AaV), the little giant of the Megaviridae, elucidates NCLDV genome expansion and host-virus coevolution. *Virology* 466-467, 60-70.
- Moreau, H., Piganeau, G., Desdevises, Y., Cooke, R., Derelle, E., Grimsley, N., 2010. Marine prasinovirus genomes show low evolutionary divergence and acquisition of protein metabolism genes by horizontal gene transfer. *J Virol* 84, 12555-12563.
- Moreau, H., Verhelst, B., Couloux, A., Derelle, E., Rombauts, S., Grimsley, N., Van Bel, M., Poulain, J., Katinka, M., Hohmann-Marriott, M.F., Piganeau, G., Rouze, P., Da Silva, C., Wincker, P., Van de Peer, Y., Vandepoele, K., 2012. Gene functionalities and genome structure in *Bathycoccus* prasinus reflect cellular specializations at the base of the green lineage. *Genome Biol* 13, R74.
- Moreira, D., Lopez-Garcia, P., 2009. Ten reasons to exclude viruses from the tree of life. *Nat Rev Microbiol* 7, 306-311.
- Moroni, A., Viscomi, C., Sangiorgio, V., Pagliuca, C., Meckel, T., Horvath, F., Gazzarrini, S., Valbuzzi, P., Van Etten, J.L., DiFrancesco, D., Thiel, G., 2002. The short N-terminus is required for functional expression of the virus-encoded miniature K(+) channel Kcv. *FEBS Lett* 530, 65-69.
- Neher, E., Sakmann, B., 1976. Single-channel currents recorded from membrane of denervated frog muscle fibres. *Nature* 260, 799-802.

-
- Neupartl, M., Meyer, C., Woll, I., Frohns, F., Kang, M., Van Etten, J.L., Kramer, D., Hertel, B., Moroni, A., Thiel, G., 2008. Chlorella viruses evoke a rapid release of K⁺ from host cells during the early phase of infection. *Virology* 372, 340-348.
- Nieva, J.L., Madan, V., Carrasco, L., 2012. Viroporins: structure and biological functions. *Nat Rev Microbiol* 10, 563-574.
- Nishida, M., Cadene, M., Chait, B.T., MacKinnon, R., 2007. Crystal structure of a Kir3.1-prokaryotic Kir channel chimera. *EMBO J* 26, 4005-4015.
- Pagliuca, C., Goetze, T.A., Wagner, R., Thiel, G., Moroni, A., Parcej, D., 2007. Molecular properties of Kcv, a virus encoded K⁺ channel. *Biochemistry* 46, 1079-1090.
- Perozo, E., Cortes, D.M., Cuello, L.G., 1999. Structural rearrangements underlying K⁺-channel activation gating. *Science* 285, 73-78.
- Plugge, B., Gazzarrini, S., Nelson, M., Cerana, R., Van Etten, J.L., Derst, C., DiFrancesco, D., Moroni, A., Thiel, G., 2000. A potassium channel protein encoded by chlorella virus PBCV-1. *Science* 287, 1641-1644.
- Romani, G., Piotrowski, A., Hillmer, S., Gurnon, J., Van Etten, J.L., Moroni, A., Thiel, G., Hertel, B., 2013. A virus-encoded potassium ion channel is a structural protein in the chlorovirus *Paramecium bursaria chlorella virus 1* virion. *J Gen Virol* 94, 2549-2556.
- Sansom, M.S., Shrivastava, I.H., Bright, J.N., Tate, J., Capener, C.E., Biggin, P.C., 2002. Potassium channels: structures, models, simulations. *Biochim Biophys Acta* 1565, 294-307.
- Schroeder, D.C., Oke, J., Hall, M., Malin, G., Wilson, W.H., 2003. Virus succession observed during an *Emiliana huxleyi* bloom. *Appl Environ Microbiol* 69, 2484-2490.
- Schroeder, I., Hansen, U.P., 2007. Saturation and microsecond gating of current indicate depletion-induced instability of the MaxiK selectivity filter. *J Gen Physiol* 130, 83-97.
- Segrest, J.P., De Loof, H., Dohlman, J.G., Brouillette, C.G., Anantharamaiah, G.M., 1990. Amphipathic helix motif: classes and properties. *Proteins* 8, 103-117.
- Shim, J.W., Yang, M., Gu, L.Q., 2007. In vitro synthesis, tetramerization and single channel characterization of virus-encoded potassium channel Kcv. *FEBS Lett* 581, 1027-1034.
- Siotto, F., Martin, C., Rauh, O., Van Etten, J.L., Schroeder, I., Moroni, A., Thiel, G., 2014. Viruses infecting marine picoplankton encode functional potassium ion channels. *Virology* 466-467, 103-111.
- Strandberg, E., Killian, J.A., 2003. Snorkeling of lysine side chains in transmembrane helices: how easy can it get? *FEBS Lett* 544, 69-73.
- Suttle, C.A., Chan, A.M., Cottrell, M.T., 1991. Use of ultrafiltration to isolate viruses from seawater which are pathogens of marine phytoplankton. *Appl Environ Microbiol* 57, 721-726.
- Tayefeh, S., Kloss, T., Kreim, M., Gebhardt, M., Baumeister, D., Hertel, B., Richter, C., Schwalbe, H., Moroni, A., Thiel, G., Kast, S.M., 2009. Model development for the viral Kcv potassium channel. *Biophys J* 96, 485-498.

-
- Thiel, G., Baumeister, D., Schroeder, I., Kast, S.M., Van Etten, J.L., Moroni, A., 2011. Minimal art: or why small viral K(+) channels are good tools for understanding basic structure and function relations. *Biochim Biophys Acta* 1808, 580-588.
- Thiel, G., Moroni, A., Blanc, G., Van Etten, J.L., 2013. Potassium ion channels: could they have evolved from viruses? *Plant Physiol* 162, 1215-1224.
- Thiel, G., Moroni, A., Dunigan, D., Van Etten, J.L., 2010. Initial Events Associated with Virus PBCV-1 Infection of *Chlorella* NC64A. *Prog Bot* 71, 169-183.
- Thompson, A.N., Posson, D.J., Parsa, P.V., Nimigeon, C.M., 2008. Molecular mechanism of pH sensing in KcsA potassium channels. *Proc Natl Acad Sci U S A* 105, 6900-6905.
- Van Etten, J.L., 2003. Unusual life style of giant chlorella viruses. *Annu Rev Genet* 37, 153-195.
- Van Etten, J.L., Burbank, D.E., Kuczmarski, D., Meints, R.H., 1983a. Virus infection of culturable chlorella-like algae and development of a plaque assay. *Science* 219, 994-996.
- Van Etten, J.L., Burbank, D.E., Xia, Y., Meints, R.H., 1983b. Growth cycle of a virus, PBCV-1, that infects *Chlorella*-like algae. *Virology* 126, 117-125.
- Van Etten, J.L., Dunigan, D.D., 2012. Chloroviruses: not your everyday plant virus. *Trends Plant Sci* 17, 1-8.
- Van Etten, J.L., Graves, M.V., Muller, D.G., Boland, W., Delaroque, N., 2002. Phycodnaviridae--large DNA algal viruses. *Arch Virol* 147, 1479-1516.
- von Charpuis, C., Meckel, T., Moroni, A., Thiel, G., 2015. The sorting of a small potassium channel in mammalian cells can be shifted between mitochondria and plasma membrane. *Cell Calcium* 58, 114-121.
- Wang, K., Xie, S., Sun, B., 2011. Viral proteins function as ion channels. *Biochim Biophys Acta* 1808, 510-515.
- Yamada, T., Onimatsu, H., Van Etten, J.L., 2006. *Chlorella* viruses. *Adv Virus Res* 66, 293-336.
- Yau, S., Lauro, F.M., DeMaere, M.Z., Brown, M.V., Thomas, T., Raftery, M.J., Andrews-Pfannkoch, C., Lewis, M., Hoffman, J.M., Gibson, J.A., Cavicchioli, R., 2011. Virophage control of antarctic algal host-virus dynamics. *Proc Natl Acad Sci U S A* 108, 6163-6168.
- Zhang, Y., Schaffer, T., Wolfle, T., Fitzke, E., Thiel, G., Rospert, S., 2016. Cotranslational Intersection between the SRP and GET Targeting Pathways to the Endoplasmic Reticulum of *Saccharomyces cerevisiae*. *Mol Cell Biol* 36, 2374-2383.
- Zhou, J., Zhang, W., Yan, S., Xiao, J., Zhang, Y., Li, B., Pan, Y., Wang, Y., 2013. Diversity of virophages in metagenomic data sets. *J Virol* 87, 4225-4236.

10. Appendix

These channel sequences of *Chlorella* viruses were used as template for the degenerated Primers which were used for the mining of new SAG- virus-channels in water samples:

```
Alkali52      -MLLL-----IIHVGILVFFTTVYKMLPGGMFSNT-----DP----SWVDCLY 38
Smith        -MLLL-----LIHVGILVFFTTVYKMLPGGMFSNT-----DP----SWVDCLY 38
10.1         MLLL-----LIHIAILTFFTVVYKMLPDGVFSNG-----DP----SWVDCLY 39
ATCV-1       -MLLL-----IIHIIILIVFTAIYKMLPGGMFSNT-----DP----TWVDCLY 38
9.1          -MLLL-----LIHIIILIVFTAIYKMLPGGMFSNT-----DP----TWVDCLY 38
AlkaliNPS    -MLLL-----LIHLSILVIFTAIYKMLPGGMFSNT-----DP----TWVDCLY 38
Next-to-Smith -MLLL-----IIHLSILVIFTAIYKMLPGGMFSNT-----DP----TWVDCLY 38
608          -MLLL-----IIHLSILVIFTTIYKMLPGGMFSNT-----DP----SWVDCLY 38
607.3        -MLLL-----LIHLSILVIFTTIYKMLPGGMFSNT-----DP----SWVDCLY 38
4.1          -MLLL-----IIHLSILVLFTTIYKMLPGGMFSNT-----DP----SWVDCLY 38
5.3          -MLLL-----LIHLSILVLFTTIYKMLPGGMFSNT-----DP----SWVDCLY 38
2.1          -MLLL-----LIHLCILIIFTTIYKMLPGGMFSNT-----DP----SWVDCLY 38
4.3          -MLLL-----IIHLCILIIFTTIYKMLPGGMFSNT-----DP----SWVDCLY 38
604          -MLLL-----LIHLCILIIFTTIYKMLPGGMFSNT-----DP----SWVDCLY 38
TN603        -MLLL-----LIHLCILIIFTTIYKMLPGGMFSNT-----DP----SWIDCLY 38
607.1        -MLLL-----IIHLCILIIFTTIYKMLPGGMFSNT-----DP----SWIDCLY 38
```

```
Alkali52      FSASTHTTVGYGDLTPKSPVAKLVATAHMMIVFAIVSSFTFPW----- 82
Smith        FSASTHTTVGYGDLTPKSPVAKLVATAHMMIVFAIVSSFTFPW----- 82
10.1         FSASTHTTVGYGDLTPKSPVAKLTATAHMMIVFAIVSSFTFPW----- 83
ATCV-1       FSASTHTTVGYGDLTPKSPVAKLTATAHMLIVFAIVISGFTFPW----- 82
9.1          FSASTHTTVGYGDLTPKSPVAKLTATAHMLIVFAIVISGFTFPW----- 82
AlkaliNPS    FSASTHTTVGYGDLTPKSPVAKLTATAHMLIVFAIVISGFTFPW----- 82
Next-to-Smith FSASTHTTVGYGDLTPKSPVAKLTATAHMLIVFAIVISGFTFPW----- 82
608          FSASTHTTVGYGDLTPKSPVAKLTATAHMLIVFAIVISGFTFPW----- 82
607.3        FSASTHTTVGYGDLTPKSPVAKLTATAHMLIVFAIVISGFTFPW----- 82
4.1          FSASTHTTVGYGDLTPKSPVAKLTATAHMLIVFAIVITGFTFPW----- 82
5.3          FSASTHTTVGYGDLTPKSPVAKLTATAHMLIVFAIVITGFTFPW----- 82
2.1          FAASTHTTVGYGDLTPKSPVAKLTATAHMLIVFAIVITGFTFPW----- 82
4.3          FAASTHTTVGYGDLTPKSPVAKLTATAHMLIVFAIVITGFTFPW----- 82
604          FSASTHTTVGYGDLTPKSPVAKLTATAHMLIVFAIVITGFTFPW----- 82
TN603        FSASTHTTVGYGDLTPKSPVAKLTATAHMLIVFAIVITGFTFPW----- 82
607.1        FSASTHTTVGYGDLTPKSPVAKLTATAHMLIVFAIVITGFTFPW----- 82
```

Fig. 1 appendix: Channel sequences of *Chlorella* viruses were used as template for the degenerated Primers.

Tab. 1: Appendix: Primer sequences for chimera PCR Kmpv_{SP1} /Kmpv₁.

Template: Kmpv _{SP1}	5' CCG <u>CTC GAG</u> ATG ACA CCC ATA GAT 3'	XhoI restriction site is underlined
Template: Kmpv _{SP1}	ATG TTC TGG TTT CAT TCT GCT ATA AAT AAA	
Template: Kmpv ₁	ATG AAA CCA GAA CAT TTC AAT	
Template: Kmpv ₁	CGG AAT TC AAA AAT <u>CTT</u> <u>TAA</u> AAT TTT	EcoRI restriction site is underlined

Beside the described channels during the project also the following channels were tested by whole-cell patch-clamp without a conductance that was significantly different from untransfected control cells (Tab. 2 Appendix).

Tab. 2 Appendix: Channels which were also tested during this work. All candidates show no clearly function in whole-cell measurements.

Virus	Hypothetical channelprotein	Reference	Amino acid sequence
<i>Aureococcus anophagefferens</i> virus	AaVIC	(Moniruzzaman <i>et al.</i> , 2014)	MKLLFGYNRFHLLIYQIIFFSILYMFLGSSHFSGINT LEDILKNEIVSKQVLDPIIEEKFTNASDPSKFISKDDI EVDKKEETEEIQEKAKEIKKEVKKELNLTDKDSFFDR FFLRFYFSFVTSTTIGYGDTPSSISTRTLAMIQACS TFYILMA
<i>Aureococcus anophagefferens</i> virus	AaVMscS	(Moniruzzaman <i>et al.</i> , 2014)	MRETFTDLYNSPNFIYRYSIIIVLLTFPISSILTQKL QDTDYKNEFDKFFQTGLSILLIRFATMFVLILIALK VANVNNLVIASAGILLIIVPAAMSTQISNYISGLL IAFDRITLNDYIIIDDFEGRIKLNLFSEVKDEFKTK TRFIPNADFWTKSFINVSKNTTAVAKIEITVASDND FDEIEDKILNIIDNNFEGIDASKTRIRYDHSIWGVKL SIAVEVPSKKYFEYKMLLLRVIRKKISEDEDINFVM
<i>Cafeteria roenbergensis</i> virus	CroVMscL	(Fischer <i>et al.</i> , 2014)	MSQIYVDFKDFLKDNDIIVTIIATIVSSNISMLSFSF MKNLVMPIINIDLNNDGIPDRQNLNWWVIHMKGV DLKIGQFLFTFIEFFLILIIYLINKLSKI
Unknown (Antarctic lakes genome project)	Kolpv _{2,1}	(Yau <i>et al.</i> , 2011)	MNPINFYGLNKIQDSIKDDLIDDQAKEPFYTPYNKE KVKEDVKNIVRNEEDKIYKPNYFQRYLDSLYFSIITS CLLGYGDIYPITNLSKILVSIQGLITLSLILY

11. Abbreviations

aa	amino acid
ATCV-1	<i>Acanthocystis turfacea Chlorella Virus Type 1</i>
Ba ²⁺	Barium ion
bp	base pairs
CLSM	Confocal Laser Scanning Microscopy
Cs ⁺	Caesium ion
DH5 α	e.coli strain
DNA	Desoxyribonucleic acid
dsDNA	double stranded Desoxyribonucleic acid
E. coli	<i>Escherichia coli</i>
EGFP	Enhanced Green Fluorescent Protein
EsV-1	<i>Ectocarpus siliculosus virus-1</i>
GFP	Green Fluorescent Protein
h	hour
HEK293	Human Embryonic Kidney 293 cell
I/V	Current-voltage relationship
K ⁺	Potassium ion
kb	Kilobase
kbp	Kilo base pair
Kbpv ₁	K ⁺ channel <i>Bathycoccus visus</i> 1
KcsA	K ⁺ crystallographically-sited activation channel
Kcv	K ⁺ channel <i>Chlorella Virus</i>
Kcv _{cmv-1}	K ⁺ channel <i>Chlorella virus cmv-1</i>
Kcv _{ATCV-1}	K ⁺ channel <i>Chlorella virus Acanthocystis turfacea Chlorella virus - 1</i>
Kcv _{GnLD}	K ⁺ channel <i>Chlorella virus Greenland</i>
Kcv _{MT325}	K ⁺ channel <i>Chlorella virus MT325</i>
Kcv _{NH}	K ⁺ channel <i>Chlorella virus New Hampshire</i>
Kcv _{NTS}	K ⁺ channel <i>Chlorella virus Next-to-Smith</i>
Kcv _{PBCV-1}	K ⁺ channel <i>Chlorella virus Paramecium bursaria Chlorella virus - 1</i>
Kcv _S	K ⁺ channel <i>Chlorella virus Smith</i>
Kir channel	Inwardly rectifying potassium channel
Kmpv ₁	K ⁺ channel <i>Micromonas pusilla virus 1</i>
Kmpv _{12T}	K ⁺ channel <i>Micromonas pusilla virus 12T</i>
Kmpv _{PL1}	K ⁺ channel <i>Micromonas pusilla virus PL1</i>
Kmpv _{SP1}	K ⁺ channel <i>Micromonas pusilla virus SP1</i>
Kolpv ₂	K ⁺ channel from <i>phycodnavirus</i> organic lakes project
Kolv ₄	K ⁺ channel <i>Ostreococcus lucimarinus virus OLV4</i>

Kotv _{RT}	K ⁺ channel <i>Ostreococcus tauri</i> virus OTVRT
ml	Millilitre
mM	Millimolar
mpv	<i>Micromonas pusilla</i> virus
MscL channel	Mechanosensitive channel of large conductance
MthK	Calcium and voltage dependent potassium channel
mV	Millivolt
Na ⁺	Sodium ion
NC64A	<i>Chlorella</i> strain NC64A
nm	Nanometre
PBCV-1	<i>Paramecium bursaria Chlorella</i> virus -1
PCR	Polymerase chain reaction
sp.	species
TMD	Transmembrane domain
U	Unit
wt	wildtype
μl	Microlitre

12. List of Figures

Fig. 1	Structure model of Kcv _{PBCV-1}	9
Fig. 2	Subunits of the different Potassium channel types	10
Fig. 3	Potassium channels are selective	11
Fig. 4	Small virus channels are a good model system	12
Fig. 5	Schematic work flow of channel mining in environmental samples	20
Fig. 6	Alignment of putative viral K ⁺ channel sequences from a salt water lake in Antarctica (Kolpv ₂) and marine water viruses	30
Fig. 7	Prediction algorithms fail to detect an expected K ⁺ channel TMD in some of the viral sequences	31
Fig. 8	Full multiple alignment of K ⁺ channels from viruses with different origins	33
Fig. 9	multiple alignment of conserved new K ⁺ channels from viruses	35
Fig. 10	Prediction algorithms detect expected K ⁺ channel TMD and α -helices	36
Fig. 11	Alignment of highly conserved new K ⁺ channels from SAG viruses	37
Fig. 12	Prediction algorithms detect expected K ⁺ channel TMDs and α -helices	37
Fig. 13	HEK293 endogenous potassium channels show very small currents	41
Fig. 14	Expression of Kmpv ₁ :EGFP generates K ⁺ conductance in HEK293 cells	42
Fig. 15	Kmpv ₁ S43T is not fully blocked by Ba ²⁺	43
Fig. 16	Kmpv ₁ :EGFP S43/44T is fully blocked by Ba ²⁺	44
Fig. 17	Expression of Kbpv ₁ :EGFP creates a specific conductance in HEK293 cells	46
Fig. 18	Expression of Kmpv _{12T} :EGFP show no specific conductance in HEK293 cells	48
Fig. 19	Expression of Kmpv _{12T} :EGFP show no specific conductance in HEK293 cells	49
Fig. 20	Kmpv _{12T} protein is a canonical K ⁺ channel	50
Fig. 21	Expression of Kmpv _{PL1} :EGFP show no specific conductance in HEK293 cells	51
Fig. 22	Expression of Kmpv _{PL1} :EGFP show no specific conductance in HEK293 cells	52
Fig. 23	Expression of Kmpv _{SP1} :EGFP generates K ⁺ conductance in HEK293 cells	53
Fig. 24	Kmpv _{SP1} protein is a canonical K ⁺ channel	55
Fig. 25	Expression of Kmpv _{SP1} :EGFP S53F show the same specific conductance in HEK293 cells like the wildtype	56
Fig. 26	Expression of the Kmpv _{SP1} :EGFP chimere show the same specific conductance in HEK293 cells like the wildtype	57
Fig. 27	Expression of Kotv ₄ :EGFP show no specific conductance in HEK293 cells	59
Fig. 28	Expression of Kolv ₄ :EGFP show no specific conductance in HEK293 cells	60

Fig. 29	Expression of K _{otv_{RT}} :EGFP generates K ⁺ conductance in HEK293 cells	62
Fig. 30	Expression of K _{olpv₂} :EGFP show no specific conductance in HEK293 cells	63
Fig. 31	Expression of K _{olpv₂} :EGFP show no specific conductance in HEK293 cells	64
Fig. 32	Expression of K _{cv_{NH}} :EGFP generates K ⁺ conductance in HEK293 cells	66
Fig. 33	Expression of K _{cv_{G_NL_D}} :EGFP generates a specific K ⁺ conductance in HEK293 cells	67
Fig. 34	Expression of K _{cv_{MT325}} :EGFP generates a specific K ⁺ conductance in HEK293 cells	69
Fig. 35	Localization-study of K _{mpv₁} , K _{mpv_{SP1}} and K _{mpv_{PL1}}	71
Fig. 36	Multiple alignments of K ⁺ channels from different viruses with a focus on the first TMD and the selectivity filter domain	74
Fig. 37	Phylogenies of viral encoded K ⁺ channel proteins	75

13. List of Tables

Tab. 1	Overview of Cholrella viruses and their hosts	14
Tab. 2	List of tested water samples	16-17
Tab. 3	Gene accession numbers, viral source of genes, nomenclature of putative K ⁺ channels, protein accession numbers and protein sizes	18
Tab. 4	Used patch-clamp solutions	21-22
Tab. 5	Summary of the behavior from the tested proteins	72

14. Ehrenwörtliche Erklärung

Ich erkläre hiermit ehrenwörtlich, dass ich die vorliegende Arbeit entsprechend den Regeln guter wissenschaftlicher Praxis selbstständig und ohne unzulässige Hilfe Dritter angefertigt habe.

Sämtliche aus fremden Quellen direkt oder indirekt übernommenen Gedanken sowie sämtliche von Anderen direkt oder indirekt übernommenen Daten, Techniken und Materialien sind als solche kenntlich gemacht. Die Arbeit wurde bisher bei keiner anderen Hochschule zu Prüfungszwecken eingereicht.

Darmstadt, den 20.10.2017

Dipl. Biol. Fenja Siotto

15. Own work

Parts of **Chapter 2** “Viruses encode for new hypothetical K⁺ channels” (“Abstract”, “Introduction”, “Discussion”, “Methodes” and “Results- Virus channels from Internet mining”), parts of **Chapter 3** “New functional channels” (“Methodes”, “Results and Discussion-Channels from salt water” and “Conclusion”), parts of **Chapter 4** “Main Discussion” were already published in a similar form in (Siotto et al., 2014). Also, the Fig. 6, Fig. 7, Fig. 8, Fig. 14, Fig. 17, Fig. 20, Fig. 36, Fig. 37 and Tab. 3 were already published in the same or similar way in (Siotto *et al.*, 2014).

DNA isolation and sequence of Kcv_{G_NL_D} was provided from van Etten Lab (Nebraska/USA).

All Experiments, data analysis and writing of the present thesis were performed by myself with the following exceptions:

Chapter 2: Prof. Dr.Gerhard Thiel helped with the data analysis and writing of the manuscript (for (Siotto *et al.*, 2014).

Chapter 3: The Kmpv_{12T} Bilayer measurements were performed by Corinna Martin (Master student, TU Darmstadt/Germany) and Oliver Rauh (Master Student, TU Darmstadt/Germany) under my supervision.

Also Some statistical patch-clamp measurements of Kmpv_{12T} were made from Corinna Martin (Master student, TU Darmstadt/Germany) under my supervision.

Some statistical patch-clamp measurements of Kmpv_{PL1} were made from Marina Kithil (Master student, TU Darmstadt/Germany) under my supervision.

Denise Eckert (Master student, TU Darmstadt/Germany) performed the patch-clamp and bilayer experiments of Kmpv_{SP1} for Fig. 23A-C and 24. and statistical measurements under my supervision.

Tobias Schulze (Bachelor student, TU Darmstadt/Germany) performed the patch-clamp experiments of Kcv_{NH}, Kcv_{G_NL_D} and Kcv_{MT325} for Fig. 32 A-C and G-F, 33 and 34 under my supervision.

Corinna Martin (Master student, TU Darmstadt/Germany) produced the Kmpv₁ mutations S43T and S43/44T under my supervision.

Denise Eckert (Master student, TU Darmstadt/Germany) produced the Kmpv_{SP1} F53S mutation, and the Chimera Kmpv_{SP1}/loop Kmpv₁, contributed to the patch-clamp measurements of Fig. 25 and 26 under my supervision.

Marina Kithil (Master student, TU Darmstadt/Germany) contributed to data in Fig. 35 under my supervision.

Chapter 4: Prof. Dr. Gerhard Thiel helped with the data analysis and writing of the manuscript (for (Siotto *et al.*, 2014).

16. Curriculum vitae

Personal data

Date and place of birth June 24th 1985, Frankfurt (Main)
Nationality German
Marital status not married

Career and Education

Since 10/2016 **Product Consultant patch-clamp** at Harvard Bioscience Inc.

10/2011-9/2016 **Research for my dissertation** in Prof. Thiel's lab at the *Technische Universität Darmstadt*.

03/2015-05/2015 **Internship at Merck KGaA. In the Inhouse Consulting.**

12/2010-08/2011 **Diploma thesis** *Technische Universität Darmstadt (1,0)*. „Struktur-Funktions-Beziehung in dem viralen Kalium-Kanal K_{CV}Next-to-Smith“.

10/2005-08/2011 **Study of biology** at the *Technische Universität Darmstadt*
Focused on plant physiology, biochemistry, cell-, radiation- and developmental biology.

07/1996-06/2005 **Abitur** at *Bertha-von-Suttner-Schule, Mörfelden-Walldorf, Integrierte Gesamtschule mit Gymnasialer-Oberstufe (2,2)*.

Publications

05/2014 F. Siotto, C. Martin, O. Rauh, J. L. Van Etten, I. Schroeder, A. Moroni, G. Thiel, Viruses Infecting Marine Picoplankton Encode Functional Potassium Ion Channels, *ELSVirology*. (2014) Oct;466-467:103-11. DOI: 10.1016/j.virol.2014.05.002.

07/2013 F. Siotto, T. Greiner, I. Schroeder, J. van Etten, A. Moroni, G. Thiel, Channel mining: Searching for virus channels in environmental probes, *Eur Biophys J* (2013) Volume 42 (Suppl 1):S1–S236, DOI 10.1007/s00249-013-0917-x

- 05/2014 **Talk and Poster:** Patch-clamp analysis of new viral potassium channel-proteins from marine picoplankton and *chlorella* viruses F.Siotto, I. Schroeder, J. Van Etten, A. Moroni, G. Thiel 42th Course of International School of Biophysics-Channels and Transporters. (Erice, Italy)
- 07/2013 **Poster:** Metal ion block in viral potassium channels: more than a simple pore block. I. Schroeder, P. Becker, C. J. Braun, F. Siotto, T. Greiner, M. Schönrock, C. Arrigoni, L. M. Henkes, A. Moroni, S. M. Kast, G. Thiel. 541. WE-Heraeus-Seminar. Transport through Nanopores: From Understanding to Engineering. (Bremen, Germany)
- 07/2013 **Poster:** Channel mining: Searching for new virus Channels in environmental samples. F. Siotto, T. Greiner, I. Schroeder, J. Van Etten, A. Moroni, G. Thiel. 9th European Biophysics Congress. (Lisbon, Portugal)
- 09/2012 **Poster:** Unusually steep Cs⁺ block in miniature viral K⁺ channel: Importance of outer transmembrane domain. F. Siotto, T. Greiner, C. Lachnit, I. Schroeder, L. Henkes, S. M. Kast, A. Moroni, G. Thiel. 3rd International Workshop on Expression, Structure and Function of Membrane Proteins. (Florence, Italy)
- 5/2011 **Poster:** Unusual steep voltage dependency for caesium block in miniature viral potassium channels. T. Greiner, F. Siotto, J. Van Etten, A. Moroni, G. Thiel. 41th Course of International School of Biophysics-Channels and Transporters. (Erice, Italy)

17. Danksagung

Zum Ende meiner Arbeit möchte ich mich noch bei Einigen bedanken die zum Gelingen beigetragen haben.

Mein besonderer Dank gilt natürlich **Prof. Dr. Gerhard Thiel** für die Betreuung dieser sehr spannenden Arbeit. Für seine Begeisterung für mein Thema, die fortwährende Unterstützung und für die Möglichkeit auf tolle Konferenzen fahren zu dürfen. Nicht zu vergessen für jede Menge Freitagbrötchen.

Prof. Dr. Bertl für die Übernahme des Koreferats.

Dr. Timo Greiner fürs seine Freundschaft, die Übergabe seines ehemaligen Themas, die tolle Zusammenarbeit und das Korrekturlesen meiner Arbeit.

Meinen Studenten **Corinna Martin, Denise Eckert, Marina Kithil** und **Tobias Schulze** für die gute Zusammenarbeit und viele Messungen.

Dr. Indra Schröder für ihre Begabung physikalische Sachverhalte anschaulich zu erklären, für ihre Hilfsbereitschaft beim Suchen von Rausch-Ursachen, finden von nicht eingesteckten Steckern ;), lösen von Löt-Problemen und beantworten von tausend anderen kleinen Fragen.

Dr. Brigitte Hertel für Ihre freundliche Art und die tolle Zusammenarbeit beim Gestalten von Praktikas und betreuen von Studenten.

Oliver Rauh für die Einführung in die Bilayermessungen und gute wissenschaftliche und nicht wissenschaftliche Unterhaltungen.

Mirja Manthey für schöne Zellen, **Silvia Haase** für etliche Bestellungen, **Silvia Lenz** für schöne Algen und **Barbara Reinhardt** für ihre freundliche Hilfe bei allerlei organisatorischen.

PD Dr. Ulrike Homann und **Anne Einheupl** für die gute Zusammenarbeit und schöne Zeit beim Schülerlabor, TUDay und Hessentag.

Dem alten Kinderzimmer, für die vielen lustigen Arbeitstage: **Dr. Timo Greiner, Dr. Manuela Gebhard, Alice Krüger, Dr. Charlotte von Charpuis, Dr. Christian Braun, Dr. Bastian Roth** und **Dr. Timo Wulfmeyer**. Und dem neuen Kinderzimmer für ebenfalls steht's gute Unterhaltung: **Marina Kithil, Denise Eckert, Laura Schlee, Patrick Voos, Oliver Rauh, Sebastian Fuck** und **Tobias Winterstein**.

Allen lieben Menschen die mir aus ihrem Urlaub Wasserproben zum Screening mitgebracht haben!

Der gesamten **AG Thiel** für die gute Arbeitsatmosphäre, die wunderschöne Zeit mit lustigen Grillabenden, Feuerzangenbowle, Kegeln, Freitagsfrühstücken und vielem mehr.

Mein Dank gilt auch meinen großartigen Freundinnen, die immer da sind, wenn man sie braucht und mit denen man jeden stressigen Tag problemlos vergessen kann: **Kira Kugelstadt, Marie Freisinger, Judith Enke, Natascha Riedhammer, Marina Kithil, Aileen Barz** und **Dr. Carolin Sellmann**.

Dem **Chor der TU Darmstadt** für immer schöne Konzerte und Chorfahrten mit tollen Menschen.

Meinen Eltern **Renate** und **Marco Siotto** und meiner Schwester **Felicia**, die an mich geglaubt haben und mir die Freiheit gegeben haben, meinen Weg zu gehen.

Mein besonderer Dank gilt meinem Freund **Tim Köhler**, für seine Liebe und Freundschaft, aber auch für wertvolle wissenschaftliche Diskussionen und eine schöne gemeinsame Studien- und Promotionszeit.